An exported protein of the human malaria parasite *Plasmodium falciparum* plays a role in modifications of the erythrocyte membrane and parasite survival in the host

Submitted by
Uyen To Nguyen, M.Sc.

A thesis submitted in total fulfilment
of the requirements for the degree of Doctor of Philosophy

School of Molecular Sciences
Faculty of Science, Technology and Engineering

La Trobe University
Bundoora, Victoria 3086
Australia

August 2014

Table of contents

List of Figures and Tables

Chapter 1:

Chapter 2:

Chapter 3:

Chapter 4:

Chapter 5:

Abbreviations

Δ	knock-out
Ω	ohm
µF	microfarad
µg	microgram(s)
µJ	microjoule(s)
µL	microliter(s)
µM	micromolar
µm	micrometre(s)
ºC	degrees Celcius
aa	amino acids
amp	ampere(s)
bp	base pair(s)
BN-PAGE	blue native – polyacrylamide gel electrophoresis
BSA	bovine serum albumin
CAM5'	camodulin 5' UTR
CD36	leukocyte differentiation antigen
cDNA	complementary deoxyribonucleic acid
CHAPS	3-[(3-cholamidopropyl) dimethylammonio]-1-propanesulfonate
ConA	concanavalin A
CRT	chloroquine resistance transporter
CSA	Chondroitin sulphate A
DAPI	4,6-diamidino-2-phenylindole
DIG	digoxigenin
DMSO	dimethyl sulfoxide
DNA	deoxyribonucleic acid
dNTP	deoxynucleotide triphosphate
DOC	deoxycholic acid
ECL	enhanced chemiluminescence
E. coli	*Escherichia coli*
EDTA	ethylene-diamine-tetra-acetic acid
ER	endoplasmic reticulum
EtBr	ethidium bromide
EXP1	exported protein 1

FACS	fluorescent-activated cell sorting
FITC	fluorescein isothiocyanate
g	gram(s)
g	gravitational accerlation
GFP	green fluorescent protein
GST	glutathione S-transferase
GYT	media containing glucose, yeast and tryptone
HA	hemagglutinin
h*dhfr*	human *dihydrofolate reductase*
HEPES	N-2-hydroxyethylpiperazine-N'-2-ethanesulfonic acid
HIS	hexahistidine
IOVs	inside-out vesicles
IFA	immunofluorescence assay
IP	immunoprecipitation
IP spleen	isolated-perfused spleen
IPTG	isopropylthio-beta-D-galactoside
iRBCs	infected red blood cells
KAHRP	knob-associated histidine-rich protein
kb	kilobase(s)
kDa	kilodalton(s)
KO	knock-out
kV	kilovolt(s)
L	litre(s)
LB	Luria-Bertani
M	molar
mA	milliampere(s)
mg	milligram(s)
min	minute(s)
mL	millilitre(s)
mm	millimetre(s)
mM	millimolar
mRNA	messenger RNA
ms	millisecond
MAHRP1	membrane-associated histidine-rich protein 1

MEC	MESA erythrocyte cytoskeleton-binding domain
MESA	mature parasite-infected erythrocyte surface antigen
MCs	Maurer's clefts
MS	mass spectrometry
MW	molecular weight
nm	nanometre(s)
nM	nanomolar
NP-40	Tergitol-type NP-40
OD	optical density
OGP	n-Octyl-β-D-glucopyranoside
ORF	open reading frame
OTGP	n-Octyl-β-D-thioglucopyranoside
PAGE	polyacrylamide gel electrophoresis
PBS	phosphate buffered saline
PCR	polymerase chain reaction
PEXEL	*Plasmodium* export element
P. falciparum	*Plasmodium falciparum*
PFD	PFD1170c protein
PfEMP1	*P. falciparum* erythrocyte membrane protein 1
PfEMP2	*P. falciparum* erythrocyte membrane protein 2
PfEMP3	*P. falciparum* erythrocyte membrane protein 3
PfHSP70	*P. falciparum* heat shock protein 70 kDa
PHIST	*Plasmodium* helical interspersed subtelomeric
PV	parasitophorous vacuole
PVM	parasitophorous vacuole membrane
RBCs	red blood cells
REX1	ring exported protein 1
RESA	ring parasite-infected erythrocyte surface antigen
RNA	ribonucleic acid
rpm	revolutions per minute
RPMI	Roswell Park Memorial Institute
RT	room temperature
q-PCR	quantitative polymerase chain reaction
s	seconds

SBP1	skeleton binding protein 1
SEM	scanning electron microscopy
SDS	sodium dodecyl sulfate
SOC	SOB (super-optimal broth) with the B changed to C for "catabolite repression", indicative of the presence of glucose
SSC	side-scattered light
SSC solution	sodium chloride and sodium citrate solution
STREP	streptavidin
TBE	Tris-borate EDTA (buffer)
TCA	trichloroacetic acid
TE	Tris-EDTA
TEM	transmission electron microscopy
TEMED	N,N,N,'N' – tetramethylethylenediamine
TMD	transmembrane domain
Tris	tris(hydroxymethyl)aminomethane
TX	triton
TVN	tubulovesicular network
U	unit(s)
uRBC	uninfected red blood cell(s)
UV	ultraviolet
SAXS	Small Angle X-ray Scattering
SS	signal sequence
V	volt(s)
v/v	volume per volume
w/v	weight per volume
WHO	World Health Organisation
W	white cells
WT	wild-type

Abstract

Human malaria caused by *Plasmodium falciparum* is one of the most serious infectious diseases. Parasites with knob-like protrusion in the erythrocyte membrane enable to adhere to the host endothelium cells in human capillaries and organs, which allows them to avoid clearance by macrophages of the spleen. A number of exported *P. falciparum* proteins are associated with the infected erythrocyte membrane and cytoskeleton, which modifies the physical properties of the infected erythrocytes in terms of rigidity, deformability and cytoadherence. However, molecular mechanisms responsible for this remain largely unknown. In the present study, a novel parasite exported molecule called PFD (encoded by *PFD1170c* gene) was found to influence filterability of infected red blood cells. GFP-tagged PFD parasites and antibodies against PFD were generated to investigate its localisation, solubility and interacting partners. Co-immunoprecipitation assays and blue native gel electrophoresis showed PFD is associated with ring infected-erythrocyte surface antigen (RESA) to form a ~ 400 kDa complex. Furthermore, PFD deleted parasites show a lower retention rate compared to wild-type via both *in vitro* microsphiltration and *ex-vivo* perfusion of human spleen assays, which subsequently results in increased phagocytosis of the wild-type cells. We also found that PFD deletion influences parasite growth. In studying membrane stability, the knock-out parasites exhibit a higher level of osmotic fragility compared to wild-type at low salt concentrations. Together, the PFD could play a role in reducing parasite loads when fever occurs due to the parasite clearance by the spleen, while the molecule is also important for the parasite growth at normal body temperature. This study opens new avenues for the investigation of mechanisms that the parasites might use to regulate their proliferation to adapt with temperature changes in human body in order to facilitate their transmission to insect vector. Research on the aspect might help to interfere with the *P. falciparum* survival.

Statement of Authorship

Except where reference is made in the text of the thesis, this thesis contains no material published elsewhere or extracted in whole or in part from a thesis submitted for the award of any other degree or diploma.

No other person's work has been used without due acknowledgment in the main text of the thesis.

This thesis has not been submitted for the award of any degree or diploma in any other tertiary institution.

I am grateful to Dr. Pierre A. Buffet and Dr. Papa Alioune Ndour (Department of Parasitology, Pitié Salpétrière Hospital, Paris, France) for performing the *ex vivo* human spleen experiments and supporting the data analysis. I would also like to acknowledge Dr. Phuong Tran (The Australian National University) for helping to generate the second PFD knock-out and complementation cell lines; Dr. Pierre Faou and Dr. Ira Cooke (La Trobe University) for performing the mass spectrometry and supporting me with the proteomic data analysis; Dr Philippe Boeuf (University of Melbourne) for helping me to perform the adhesion assays; Dr. Eric Hanssen (University of Melbourne) for performing the immunoelectron microscopy, which resulted in data shown in this thesis.

Uyen To Nguyen — Assoc. Prof. Alexander G. Maier

Date: 28/08/2014 — Principle supervisor

Acknowledgements

Firstly and foremost I would like to thank my husband Phuong who was also my lab mate for all of his love, patience and support throughout the past four years. I am grateful to his knowledge and contribution in teaching me performing experiments and analysing data in a logical and scientific way. Secondly, I would like to thank my little girl Trinh, husband's and my family for their love, especially my lovely mum who is always thinking of, encouraging and supporting me in all kinds of life.

A big thank to my principle supervisor Associate Professor Alexander G. Maier for giving me the opportunity to undertake my PhD. His outstanding mentoring and constant support greatly contributed to the outcome of my PhD project. Regular meetings with Alex during my PhD candidature have allowed me to improve my scientific thinking and to keep the project on track.

Big thanks to Dr. Pierre A. Buffet and Dr. Papa Alioune Ndour (Department of Parasitology, Pitié Salpétrière Hospital, Paris, France), Dr. Phuong Tran (The Australian National University), Dr. Pierre Faou and Dr. Ira Cooke (La Trobe University), Dr Philippe Boeuf and Dr. Eric Hanssen (University of Melbourne) for their contributions to the data which were shown in the thesis.

Thanks to Professor Odile Mercereau-Puijalon, Pasteur Institute, Paris for providing me the opportunity to visit her lab and Dr. Pierre A. Buffet's lab via OzEMalaR researcher exchange program.

Thanks to Associate Professor Matthew Perugini and Associate Professor Christine Hawkins (La Trobe University) and Dr. Diana Stojanovski (University of Melbourne) who have acted as my primary supervisor and mentors respectively, for paperwork associated with research services at La Trobe University for the past two and a half years after Maier lab moved to The Australian National University.

Thanks to Associate Professor Alexander G. Maier, Dr. Phuong Tran and Mr. Vinson Tran for proofreading my thesis.

Thanks to all the past and current members, especially Phuong, Nick, Andy, Tilo and Dion, of the Maier lab for their help and friendship over the past four years.

Thanks to all members participating in the ANU parasitology meeting who have given me valuable advice and friendship. My knowledge of malaria has been nurtured every time I attended the weekly meeting.

Thanks to La Trobe University for providing me with the PhD scholarships, supporting me with research services and facility; The Australian National University for supporting me with research services and facility over the past two and a half years, The Australian Society for Parasitology (OzEMalaR program) for travel funding.

Chapter 1

Introduction

Malaria is a life-threatening disease that causes enormous human suffering and hundreds of thousands of deaths globally. Worldwide, an estimated 207 million malaria cases and 627,000 malaria deaths have been reported in 2012 (WHO, 2013). Most of the people at risk of contacting malaria in poor countries do not have access to malaria prevention and treatment interventions. About 90 per cent of the deaths are estimated to be in children in sub-Saharan Africa (WHO, 2013). Many antimalarial drugs such as artemisinin-based combination therapies have been developed. However, drug-resistant *Plasmodium* variants are emerging in many parts of the world (WHO, 2013), which challenges human immune detection and has hindered the development of vaccines to date. In order to identify effective malaria drug and/or vaccine candidates, an understanding of the biological mechanism of malaria pathogenesis is important. One of the main factors for the pathogenesis is parasite proteins that are exported and deposited on the surface of the infected red blood cells (iRBCs). In this chapter, a general background of malaria with a focus on erythrocyte membrane modification by RBC cytoskeleton-binding *Plasmodium falciparum* (*P. falciparum*) proteins will be discussed.

1.1 The global burden of malaria

This highest burden of malaria is borne by some of the world's poorest countries

(Figure 1.1) (Murray et al, 2012). Countries in tropical Africa bear the brunt of malaria, accounting for more than 90 per cent of the 200 million annual cases of malaria. Malaria was estimated to cost the African economy alone more than US$12 billion annually (Antoine, 2004).

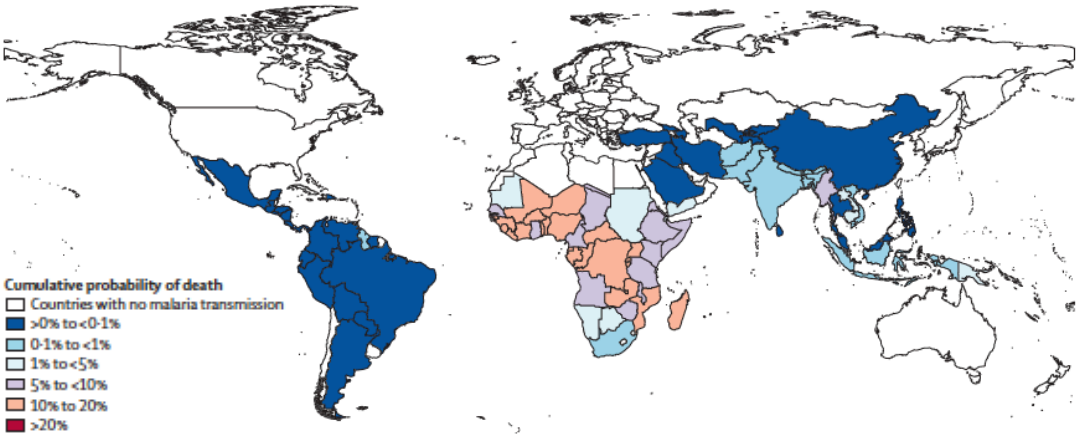

Figure 1.1. Cumulative probability of dying from malaria in 2010 (Murray et al, 2012).

1.2 The disease

Malaria is caused by obligate intraerythrocytic protozoa of the genus *Plasmodium*. Humans could be infected with one (or more) of the following five species of *Plasmodium* parasites: *Plasmodium falciparum*, *Plasmodium vivax*, *Plasmodium ovale, Plasmodium malariae* and *Plasmodium knowlesi*. *Plasmodium* parasites are transmitted by the bite of an infected female *Anopheles* mosquito, but infections could also occur through exposure to infected blood products and by congenital transmission (Trampuz et al, 2003). The signs and symptoms of malaria in human are caused by the asexual blood stages of the malaria parasite and are quite diverse with a wide range of outcomes and pathologies (Weatherall, 2002). Clinical manifestations of malaria occur between 8 and 25 days after the bite of an infected mosquito (Fairhurst RM, 2010), depending on the *Plasmodium* species, and could range from an imperceptible illness to a rapidly life-threatening disease or even death (Miller et

al, 2002). The consequence of an infection is dependent on a combination of host and parasite factors including the parasite species, the host age and prior exposure to the disease. In general, malaria is a curable disease if diagnosed and treated promptly and correctly.

Initial manifestations of the disease generally begin with non-specific flu-like symptoms that may include fever, chills, headache, sweats, fatigue, nausea and vomiting (Bartoloni A, 2012). The classic cyclical symptom of malaria occurs everyday with *P. knowlesi* (Collins, 2012; White, 2008) or every two days with *P. falciparum*, *P. vivax* and *P. ovale* or every three days with *P. malariae* (Ferri, 2009). *P. falciparum* is the deadliest of the five species, and responsible for most of the severe complications (Prudêncio et al, 2006). From here onwards, the parasite mentioned in this thesis is *P. falciparum*. The *P. falciparum* parasites modify the surface of the infected red blood cells so that they could adhere to the endothelia or placenta in order to avoid spleen-dependent killing mechanism, thereby leading to the pathology (Luse & Miller, 1971; Miller et al, 2002).

In most cases, severe malaria occurs as a result of delay in treatment and its features begin 3 – 7 days after the onset of illness. The rupture of mature parasite infected RBCs could cause acute anaemia (Jakeman GN, 1999). Adherence of mature parasites to certain host receptors on endothelia of venular blood vessel walls through electron-dense knobs on the iRBC surface could also generate clumps (Macpherson et al, 1985), blocking blood flow and damaging internal organs (Beeson et al, 2002; Silamut et al, 1999). The adherence protects the parasites from destruction in the spleen (Langreth & Peterson, 1985) and may cause problems in certain tissues such as the lung (Gachot et al, 1995), kidney (Barsoum, 2000; Kanodia et al, 2010) and brain

(Macpherson et al, 1985; Pongponratn E et al, 1991). When the sequestration of infected erythrocytes occurs in the blood vessels of the brain, it causes cerebral malaria. This is considered a major complication of *P. falciparum* and might lead to transient or permanent neurological effects, coma and death (Idro R, 2005).

People with a weak immune system have the highest morbidity and mortality with malaria (Julianna Schantz-Dunn, 2009). In the patients, multiplication of *P. falciparum* parasites is relatively efficient, which may associate with severe malaria (Gravenor MB, 1998). Children may additionally suffer from rapid breathing, a cough and fitting (Miller et al, 2002). Pregnant women infected with malaria usually have more severe symptoms and outcomes including higher rates of miscarriage, intrauterine demise, premature delivery, low-birth-weight neonates, and neonatal death. They are also at a higher risk of severe anaemia and maternal death (Julianna Schantz-Dunn, 2009).

Today, malaria is preventable by using insecticides and bed nets and treatable by using effective anti-malaria drugs in an appropriate dose (WHO, 2013). However, mosquito resistance to insecticides and malaria parasite resistance to anti-malaria drugs have now been detected in some countries (WHO, 2013). Therefore effective anti-malaria drugs and/or vaccines are crucial for a sustainable plan to decrease the mortality cases by malaria. Since most symptoms are caused by the asexual blood stages of parasites, a successful development of cures to the malaria disease is principally dependent upon our understanding of molecular mechanism of the asexual parasites.

1.3 Life cycle and pathogenesis of *P. falciparum*

The malaria parasites possess a complicated life cycle, including an asexual stage in

mammalian tissues and bloodstream and a sexual stage in the female *Anopheles* mosquito vector (Figure 1.2). The asexual cycle starts when an infected female *Anopheles* mosquito injects sporozoites into a human host during a blood meal. The sporozoites leave the blood vascular system within 30 to 40 minutes (min) and enter the liver (Aly et al, 2009). Within hepatocytes the sporozoites undergo many nuclear and cellular divisions to become a large hepatic schizont. This occurs over a period of 6 to 15 days, after which the schizonts burst and release thousands of merozoites into the circulation (Knell, 1991).

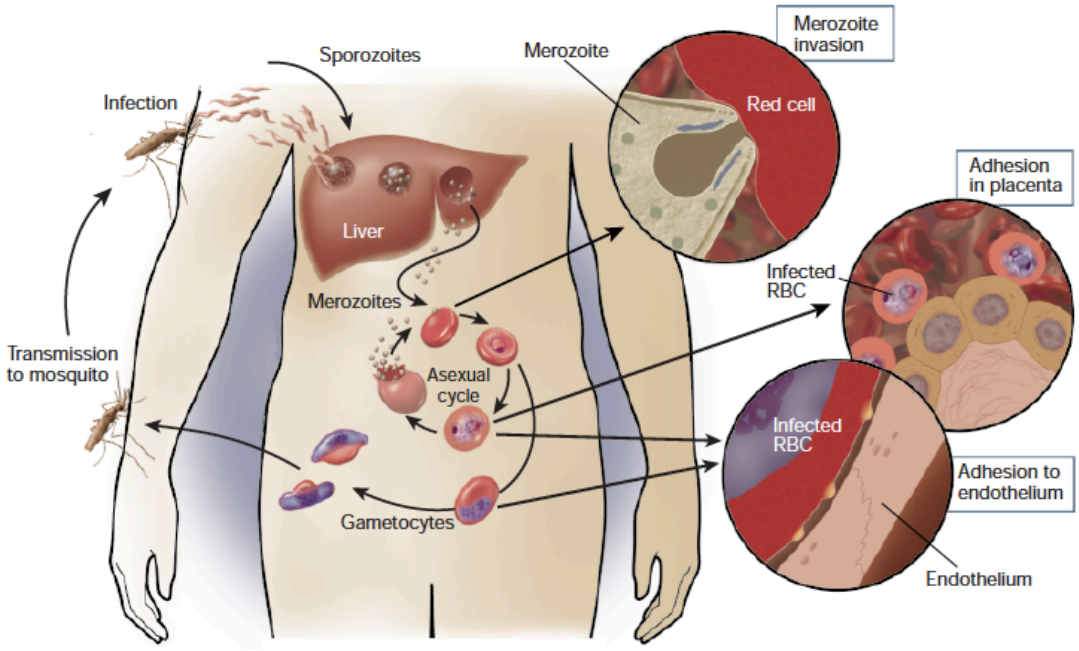

Figure 1.2. **Life cycle of *P. falciparum* malaria parasite** (Miller et al, 2002). During a blood meal, a parasite-infected female *Anopheles* mosquito inoculates sporozoites into the human host. Sporozoites infect liver cells and mature into schizonts, which rupture and release merozoites. From the exo-erythrocytic schizogony stage, merozoites undergo asexual multiplication in the erythrocytes. The released merozoites infect RBCs, mature into asexual rings, trophozoites and schizonts, which rupture releasing merozoites again. A majority of these merozoites continue the cycle of asexual multiplication while a subset of these cells develops into sexual erythrocytic stages (gametocytes). The sexual stages of parasite are essential for malaria transmission. In the asexual blood stage, *P. falciparum* RBCs can adhere to endothelium and thus avoid spleen clearance.

After the initial replication in the liver, the parasites undergo asexual multiplication in

the erythrocytes. Once in the blood, merozoites rapidly adhere to and invade erythrocytes, replicate and generate further infectious merozoites (Cowman & Crabb, 2006). After merozoites invasion into mature human RBCs, the intraerythrocytic parasite develops inside a parasitophorous vacuole (PV) into a ring stage (0-24 hours). It develops to the trophozoite stage after 24 - 36 hours of invasion, in which the parasite enlarges in size and initiates DNA replication. The schizont is formed at 36 - 48 hours followed by a rupture of the infected RBC, releasing 16 – 32 daughter merozoites (Bannister et al, 2000; Garcia et al, 2008). At this stage, merozoites could either infect new RBCs to start the asexual erythrocytic cycle again, or develop into sexual parasites (gametocytes) in iRBCs for further transmission to mosquito vector (Dixon et al, 2008b). Cell rupture is responsible for the clinical symptoms of malaria by inducing periodic waves of fever in patients (Miller et al, 2002).

The *P. falciparum* life cycle continues when the sexual gametocytes are taken up by mosquitoes during subsequent blood meals (Dixon et al, 2008b). The gametocytes undergo fertilization and maturation in the mosquito midgut, forming an infective ookinete form, which migrates through the mosquito midgut, developing into an oocyst. When fully matured, the oocysts burst and release sporozoites, which migrate into the mosquito's salivary glands, ready for the next transmission (Prudêncio et al, 2006; Simonetti, 1996).

1.4 RBC modifications after invasion of the *P. falciparum* parasites

The existence of *P. falciparum* parasite in the RBC after the invasion of merozoite alters the physical properties of the host cell membrane due to the delivery of its proteins to the RBC cytosol and membrane. The parasite is surrounded by a parasitophorous vacuole and is visible as ring-like structure within the RBC. The ring-

stage parasite induces membranous extensions of the parasitophorous vacuole membrane (PVM) into the host cell, which forms a tubulovesicular network (TVN) and RBC membrane–tethered Maurer's clefts (MCs) (Hanssen et al, 2008; Lanzer et al, 2005; Wickert & Krohne, 2007). These membranous structures play an important role in the trafficking of the parasite proteins to the red blood cell membrane (Lanzer et al, 2005). In order to access to the erythrocyte cytosol, the parasite proteins have to traverse the parasite plasma membrane (PM) and the PVM. The exported proteins usually have a signal sequence in the N-terminus of the proteins that facilitates their insertion to the parasite endoplasmic reticulum (ER) (Hortsch & Meyer, 1986; Walter & Lingappa, 1986). To transport from the PV to the PVM, most of the proteins need an extra sequence (following the hydrophobic sequence) called the *P. falciparum* Export Element (PEXEL) (Marti et al, 2004) or the Vacuolar Transport Signal (VTS) (Hiller et al, 2004). The PEXEL motif is cleaved by the parasite ER-resident protease Plasmepsin V and the processed proteins can enter the secretory pathway for trafficking to the PV (Boddey et al, 2010; Russo et al, 2010). To across the PVM, the proteins can travel through a *Plasmodium* translocon of exported proteins (PTEX) (see (de Koning-Ward et al, 2009) for review) or via separate trafficking pathways (for example, vesicular-mediated shuttling from the PM to the PVM (see (Haase & de Koning-Ward, 2010) for review) for other exported proteins without the PEXEL motif. After crossing the PVM, the proteins can be soluble in the RBC cytosol or associated with MC or other vesicles to reach their final destination (see (Haase & de Koning-Ward, 2010) for review).

The RBC properties are dramatically modified when the parasite reaches mature trophozoite stages. At the stages, the parasite increases in its volume considerably and induces knob structure on the iRBC surface that plays a critical role in cytoadhesion

of iRBCs (Crabb et al, 1997). Hundreds of parasite proteins are synthesized during this stage and some of them are exported to the RBC plasma membrane, where they interact with the RBC cytoskeleton (see (Cooke et al, 2004; Marti et al, 2004) for review). The changes in the host cell membrane lead to the greatly reduced deformability of the iRBCs (Cranston et al, 1984), as such, affects the circulation of blood flow in human.

1.5 Deformabilty of iRBCs

The deformability of parasitized RBC progressively decreases as *P. falciparum* matures in its host RBC, from ring (Cranston et al, 1984; Parker et al, 2004) to trophozoite and then to schizont (Deplaine et al, 2011; Miller et al, 1994). The less deformable ring iRBCs can be retained in the spleen (Figure 1.3 A) (Safeukui et al, 2008) while the rest of the ring iRBCs are found in the peripheral blood circulation (White et al, 1992) and do not adhere to endothelial cells (Pouvelle et al, 2000). The retained parasitized-RBCs are destroyed by macrophages or other immune cells from the spleen (Buffet et al, 2011). The phenomenon is thought to diminish a subset of further mature parasites that can adhere to endothelial cells (Figure 1.3B) via its virulence factors (see (Maier et al, 2009) for review) and sequester in vital organs leading to the risk of severe complications such as cerebral malaria or multi-organ failure (Safeukui et al, 2008).

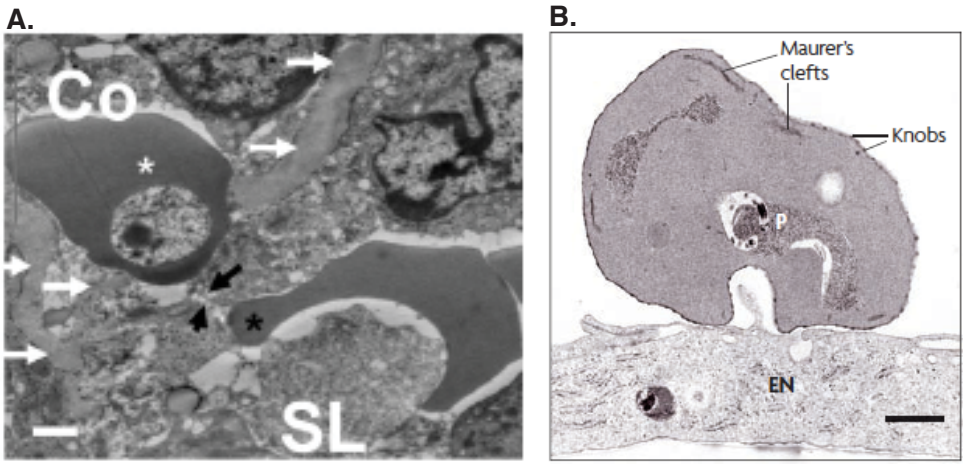

Figure 1.3. Transmission electron micrograph of retention of ring-iRBCs in the spleen and adhesion of mature parasite-iRBCs to endothelial cells (adapted from (Horrocks et al, 2005; Maier et al, 2009; Safeukui et al, 2008)). **A**. A ring-iRBC (white star) and an uninfected RBC (black star) at upstream and downstream of an interendothelial slit (black arrows) of a human isolated-perfused spleen sample. Co: the cord of the spleen; SL: sinus lumen circulation of RBC in the spleen red pulp. The knobless membrane of the ring-iRBC is very close to the sinus wall basal membrane (white arrows). Scale bar is 50 µm. **B.** A knob positive parasite (P)-infected red blood cell adhering to the surface of a microvascular endothelial cell (EN). Scale bar is 1 µm.

The molecular mechanisms involved in the host cell remodelling leading to parasite's retention and adherence have received much attention in recent years. Several parasite molecules responsible for the adhesion, knob formation (Maier et al, 2008) or interacting with the RBC cytoskeleton (Cooke et al, 2004; Silva et al, 2005) have been identified.

1.6 Exported proteins associated with the RBC membrane

Once parasites enter the RBCs, they produce their novel membranes and machinery to export their proteins to the host cytoplasm. Parasite proteins accumulated on the erythrocyte membrane and cytoskeleton have been shown to contribute to the alteration of physical properties of RBC membrane and thus influence the adhesion of the iRBCs (Glenister et al, 2002). Many of them (Figure 1.4) such as *P. falciparum* erythrocyte membrane protein 1 (PfEMP1), knob-associated histidine-rich protein

(KAHRP) (Biggs et al, 1989; Crabb et al, 1997), *P. falciparum* erythrocyte membrane protein 3 (PfEMP3) (Glenister et al, 2002), ring parasite-infected erythrocyte surface antigen (RESA) (Mills et al, 2007) and mature parasite-infected erythrocyte surface antigen (MESA) (Black et al, 2008) have been well-studied. Most of these exported proteins contain a hydrophobic signal sequence and a conserved pentameric motif (PEXEL), which is responsible for transportation of the proteins across the PVM to erythrocyte cytoplasm (Hiller et al, 2004; Marti et al, 2004). Although PfEMP1 lacks a signal sequence at the N terminus, the virulence protein is exported via a PEXEL-like motif (Marti et al, 2004) that is not cleaved by Plasmepsin V in the parasite endoplasmic reticulum (Boddey et al, 2013). Furthermore, these exported proteins show an overall mRNA level peaking in late schizonts and ring stages and these proteins are likely to be involved in remodelling of the host erythrocyte after parasite invasion (Marti et al, 2004). The following sections summarize recent studies about the functions of these proteins and a *P. falciparum* exported protein PFD1170c named as PFD that is studied in this thesis.

KAHRP. The knob structure on the surface of iRBCs contains the knob-associated histidine-rich protein (KAHRP) (Kilejian, 1979). KAHRP is essential for knob formation (Crabb et al, 1997) and for efficient adhesion of infected RBCs to endothelia under physiological flow conditions (Crabb et al, 1997; Rug, 2006). The knobs act as platforms for the presentation of PfEMP1 to mediate the cytoadherence between the iRBCs and the endothelial cells (see (Maier et al, 2009) for review). KAHRP is interacting with spectrin and actin of the RBC (Chishti et al, 1992; Kilejian et al, 1991; Oh et al, 2000). KAHRP also contains binding sites for the cytoplasmic domain of PfEMP1 at both N- and C-terminal regions (Oh et al, 2000; Waller et al, 1999). KAHRP deficient parasites do not cytoadhere effectively under

physical flow conditions (Biggs et al, 1989; Crabb et al, 1997; Udomsangpetch et al, 1989) and produce less dramatic changes in erythrocyte membrane deformability (Crabb et al, 1997; Glenister et al, 2002). Thus, KAHRP is likely to be an important virulence factor involved in knob formation.

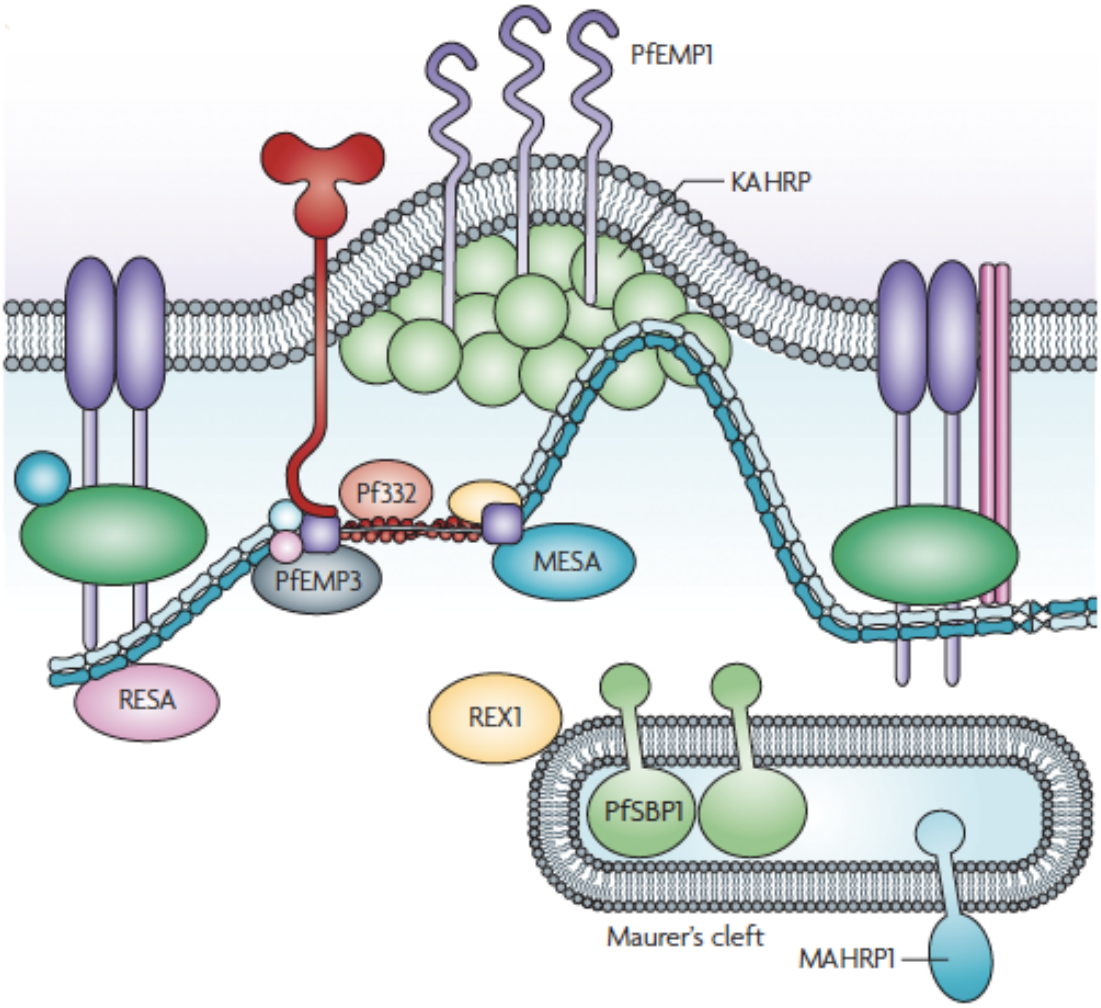

Figure 1.4. Schematic representation of infected RBC membrane (Maier et al, 2009). The model describes the cytoskeleton binding proteins underneath of infected RBCs and proteins associated with Maurer's clefts. Cytoskeleton binding proteins such as the knob-associated histidine-rich protein (KAHRP), the *P. falciparum* erythrocyte membrane protein 3 (PfEMP3), the mature parasite-infected erythrocyte surface antigen (MESA), and the ring parasite-infected erythrocyte surface antigen (RESA) contribute to the decreased deformability of iRBC, whereas the virulence and surface associated *P. falciparum* erythrocyte membrane protein 1 (PfEMP1) is a mediator of the adhesive phenotype. Parasite-derived, membrane-bound Maurer's clefts are involved in PfEMP1 trafficking. The formation and architecture of the organelles are controlled by resident proteins such as the ring exported protein 1 (REX1), membrane-associated histidine-rich protein 1 (MAHRP1) and *P. falciparum* skeleton binding protein 1 (PfSBP1), and they are attached to the RBC membrane by tether-like structures (not shown).

PfEMP1. *P. falciparum* erythrocyte membrane protein 1 (PfEMP1) is encoded by approximately 60 *var* genes. Only one *var* gene is expressed at a time in each individual parasite in order to support parasite adherence within the microvasculature to certain host vascular receptors, resulting in severe disease (Scherf et al, 2008). The expression can be switched on to other *var* genes to avoid recognition by the existing antibody response (Scherf et al, 2008). The variant antigens of PfEMP1 have a central role in the malaria pathogenesis (Miller et al, 2002). The protein is exported to the RBC surface and connected to the cytoskeleton and KAHRP via its cytoplasmic domain (Oh et al, 2000; Waller et al, 1999). The extracellular domains of PfEMP1 bind to receptors on endothelial cells such as ICAM1 (in the brain) (Newbold, 1999), CD31, CD36 (located on microvascular endothelial cells, monocytes and platelets) (Cooke, 1994), CSA (located on the placental synchytiotrophoblast epithelium) (Buffet, 1999) and glucosaminoglycans (in every cell surface of human body (Kjellen & Lindahl, 1991; Lensen et al, 2005)) (Baruch et al, 1996; Magowan et al, 1988; Rogerson et al, 1995). In the absence of knobs, PfEMP1 cannot form sufficient strength for adhesive interactions under the forces of blood flow (Crabb et al, 1997).

PfEMP3. *P. falciparum* erythrocyte membrane protein 3 (PfEMP3) is predominantly synthesized during ring and trophozoite stages of *P. falciparum*. The protein is transported into the RBC cytoplasm where it associates with Maurer's clefts, before relocating to the cytoplasmic surface of the RBC membrane. PfEMP3 can be detected in knob structures but is more broadly distributed under the parasite-infected RBC membrane (Waterkeyn et al, 2000). Unlike KAHRP, PfEMP3 is not essential for knob formation, but truncation of the protein has been shown to block the trafficking of PfEMP1 to the outside of the infected-erythrocyte cells (Waterkeyn et al, 2000). Both KAHRP and PfEMP3 contribute to the increased rigidity of iRBCs, however the

contribution of the former is significantly greater (Glenister et al, 2002).

RESA. The ring-infected erythrocyte surface antigen (RESA) plays a role in decreasing deformability of ring-iRBCs (Mills et al, 2007) and in increasing retention that might lead to accelerating parasite clearance, particularly at febrile temperature (Diez-Silva et al, 2012). RESA is located in the dense granules that presents in the anterior part of *P. falciparum* merozoites (Aikawa et al, 1990), releases shortly after invasion into the PV and rapidly translocates to the internal face of the parasitized RBC membrane (Culvenor et al, 1991). RESA is then phosphorylated (Foley et al, 1990) and remains associated with spectrin (Foley et al, 1991) for the first 24 h of the asexual intra-erythrocytic development. This interaction appears to favor the tetrameric state of spectrin, resulting in membrane mechanical stabilization and increased membrane thermal stability (Pei et al, 2007). RESA is also a protein possessing a conserved C-terminal in different *P. falciparum* strains (Perlmann et al, 1987) that had been suggested as a major candidate for the malaria vaccine (Kabilan et al, 1988).

MESA. The mature-parasite-infected erythrocyte surface antigen (MESA, also known as PfEMP2) was originally discovered as a surface antigen in infected RBCs, but was subsequently shown rather to be associated with the RBC cytoskeleton (Coppel et al, 1986; Coppel, 1988; Lustigman et al, 1990). MESA is not required for knob formation or cytoadherence (Petersen et al, 1989). MESA interacts with protein 4.1R (Lustigman et al, 1990) and competes with erythrocyte membrane protein p55 for binding to 4.1R, a major structural element of the erythrocyte membrane skeleton (Takakuwa, 2000). The binding of MESA to 4.1R is essential for the parasite to modulate the protein interactions that form the RBC membrane skeleton and facilitate

parasite survival *in vivo* (Black et al, 2008; Waller, 2003).

PFD. A protein encoded by *PFD1170c* gene contains a predicted hydrophobic signal sequence (SS), a PEXEL motif at the N terminal region (Figure 1.5) and a PHISTb (*Plasmodium* helical interspersed subtelomeric) domain near the C-terminus, one of the subgroups in the PHIST family. The PHIST family is divided into three distinct subgroups PHISTa, PHISTb and PHISTc based on the presence and position of several conserved tryptophan residues (Sargeant et al, 2006). The function of the domains is largely unknown. The signal peptide is responsible for the transportation of the protein from the ER to the PV while the PEXEL motif is responsible for its translocation across the PVM into the RBC cytoplasm (Ansorge et al, 1996; Crabb et al, 2010). PFD does not contain a transmembrane domain (Appendix 3, supplementary Figure S9) (as analyzed by using the TMHMM program (Sonnhammer et al, 1998)). mRNA expression of PFD is more abundant in merozoite and ring stage (Le Roch et al, 2004).

Figure 1.5. Structural representation of PFD protein. SS, signal sequence (blue box). PEXEL, *Plasmodium* export element (yellow box). PHIST, *Plasmodium* helical interspersed subtelomeric domain (red box).

Preliminary functional screening of PFD was performed by Maier et al, 2008. The authors showed that disruption of PFD does not affect PfEMP1 transportation to erythrocyte surface and deformability of iRBCs, but results in the reduced adhesion to CSA and alters knob formation (Maier et al, 2008). However, its molecular mechanism in the iRBCs is largely unknown. Characterization of this protein will be

discussed in the following chapters.

1.7 Splenic clearance of *P. falciparum*-altered RBCs

The spleen is the main organ involved in the development of the immune response and in destroying the *Plasmodium*-parasitized RBCs (Buffet et al, 2009; Engwerda et al, 2005) during the erythrocytic stages of malaria infection. iRBCs are removed by the spleen via the clearance of less deformable cells. This section summarizes the structure and function of the spleen in filtering RBCs.

The spleen is a complex organ composing of splenic artery (red), white pulp (white), perifollicular zone (PFZ) (around the white pulp), red pulp (red-orange), venous sinuses (blue) and splenic vein (blue) (Figure 1.6) (Buffet et al, 2011; del Portillo et al, 2012). Erythrocytes and immune cells enter splenic artery and engage in fast and slow circulations (Groom et al, 1991; Schmidt et al, 1993). Approximately 90% of the splenic blood from artery (red) enter to the fast circulation in which the cells flows through the central artery, then passes through the venous sinuses (blue) and the splenic vein at the hilus (Cesta, 2006). The other 10% of the splenic blood cells pass through the red pulp (red-orange), which is called slow circulation. Here, RBCs have to squeeze through the endothelial slits of the spleen sinuses to return to the blood stream (Buffet, 2006; Safeukui et al, 2008).

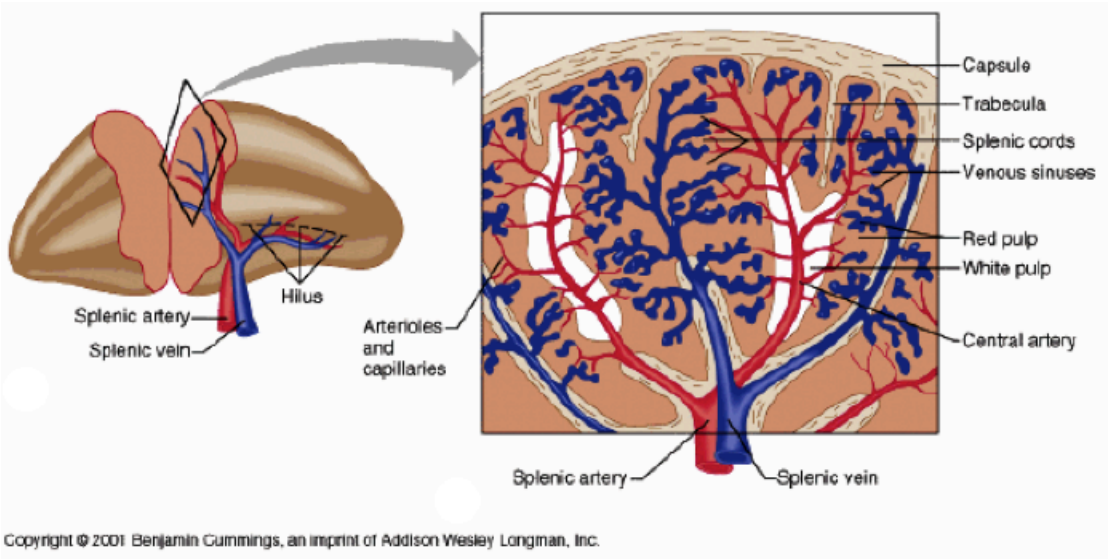

Figure 1.6. Model of spleen structure. The model describes inside structures of the spleen. Red, splenic artery; blue, splenic vein; orange, red pulp; white, white pulp**.**

Squeezing splenic interendothelial slits is the most stringent challenge on RBC deformability in the body (Mohandas & Gallagher, 2008) and hence, results in the retention of less deformable RBCs (due to aging or infection) in the red pulp (Figure 1.7). Red pulp macrophages and other immune cells can destroy the retained RBCs via recognizing antigens on the surface of infected cells (del Portillo et al, 2012; Groom et al, 1991).

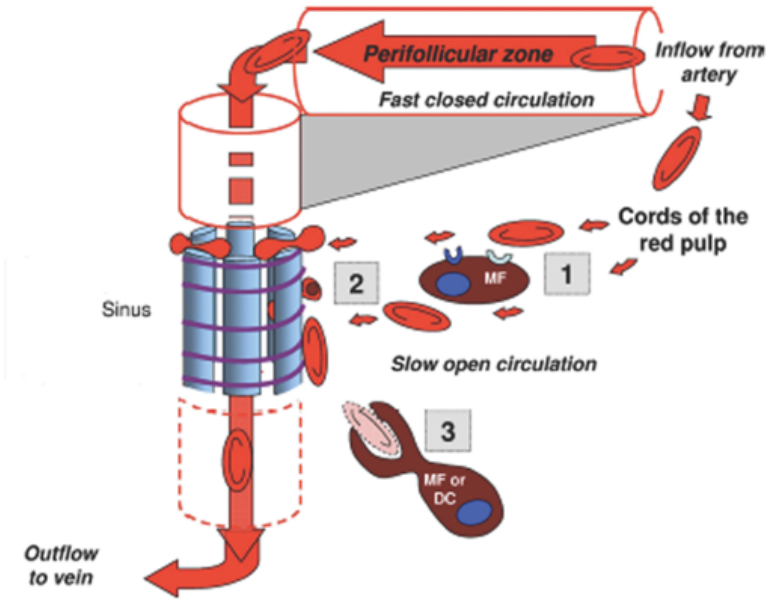

Figure 1.7. **Circulation of blood flow in the spleen and its capacity in removing less deformable RBCs in red pulp (adapted from (Buffet et al, 2011)).** Approximately 90% RBCs pass through the fast closed circulation from the perifollicular zone to the vein. The other 10% RBCs squeeze between interendothelial slits of the spleen in a slow opened circulation (red pulp), which occurs the filtering process of the altered RBCs, either through ligand-receptor interactions or by sensing their abnormal mechanical properties. The spleen plays a key process during infection by *P. falciparum* since the macrophages could recognize the antigen ligand in infected RBCs (iRBCs) surface since the parasites retained in red pulp. The functional filtering of the spleen includes 3 steps (Buffet et al, 2011). The "prefiltration step" [1] is macrophages recognition of the RBC surface via ligand – receptor interactions in the cords. The "filtration" step [2] is the RBC crossing of interendothelial slits. Mechanically modified RBCs are retained here. The "postfiltration" step [3] is the modifications and processing of retained RBCs. Both the prefiltration and postfiltration steps potentially result in the phagocytosis of abnormal, decorated, or opsonized RBCs. Phagocytosis of parasitized RBCs is an initial step of antigen presentation to immune cells, thereby connecting filtration to the antigen-specific response.

In the case of malaria, *P. falciparum* reduces the deformable RBC membrane by linking its proteins with the host membrane. Mature parasitized-RBCs with the virulence antigen exposed on the host cell surface sequester in many organs in the human body in order to avoid the clearance by the spleen (David et al, 1983). Indeed, the mature forms are unable to cross interendothelial slits of the spleen and hence are removed by the splenic macrophages recognition (Cranston et al, 1984). Thus, the

spleen is thought to modulate the amount of parasitized cells to the vascular endothelium and remove less deformable iRBCs (Cranston et al, 1984). A proportion of ring stage iRBCs are also retained and destroyed in the spleen due to their altered surface deformability (Buffet et al, 2011; Safeukui et al, 2008). Since this retention process correlates with the clearance of parasitized-RBCs in circulation, it likely reduces parasite density in the human body and sequestered parasites at later stages (Buffet et al, 2011; Buffet et al, 2009). Thus, the early-retained parasites appear to be important in reducing the risk of severe malaria. However, the molecular biological mechanism of the phenomenon is largely unknown, which leads to a huge demand in studying the retention process of the *P. falciparum* parasites in the human spleen.

In order to explore the clearance mechanism of the spleen, Buffet et al. had established an *ex-vivo* experiment in isolated-perfused (IP) human spleen (Buffet, 2006). Spleens were collected from patients with left pancreas tumors since they have been suffered vascular-related constraints (Fagniez & Munoz-Bongrand., 1999). By controlling O_2, CO_2, glucose, pressure, temperature, hematocrits, K^+ and Na^+ during the perfusion, the IP-spleen can function at physiologic levels for at least 4 hours (Figure 1.8). The *ex-vivo* perfusion of human spleen, therefore, is a powerful tool to study the mechanism of removal of pathogen infected RBCs or clearance of aged or abnormal RBCs (Buffet, 2006). For example, the authors have found that an approximately 10% of ring stage *P. falciparum*-iRBCs are retained and destroyed by the spleen (Safeukui et al, 2008). Studying in the IP-human spleen will reveal more relevant insights into the mechanism of the iRBCs removal.

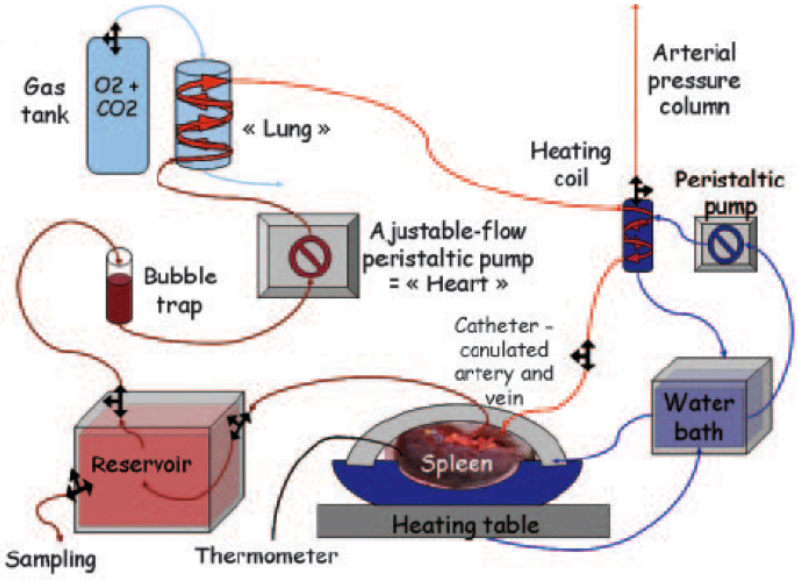

Figure 1.8. Schematic diagram of the experimental set-up of the isolated-perfused human spleen (Buffet, 2006). A peristaltic pump provides flow into polypropylene tubing. The perfusate is aspirated from the reservoir through a bubble-trap and then pushed into 2 m of silicone gas-permeable tubing around which a 3% CO2/100% O2 atmosphere is maintained through a constant 1 L/min gas flow. Prior to entry into the spleen through a glass catheter, the perfusate is warmed using a 37.5°C-equilibrated heating coil. Cells, reagents, and samples for analysis are introduced into or removed from the reservoir.

It is difficult to experimentally replicate the spleen experiments due to the unpredictable availability of the tissue. Buffet's group had generated a microsphiltration system (Figure 1.9) (Deplaine et al, 2011) that imitates one aspect of the spleen - the filtering mechanism of the spleen in a slow circulation. The device contains a mixture of 5 – 25 μm diameter micro-beads mimicking the geometrical dimension (Deplaine et al, 2011) and mechanical sensing of RBCs of inter-endothelial slits in the human spleen. Retention of ring iRBCs in the micro-beads was similar to that observed in the isolated human spleen (Deplaine et al, 2011). Thus, this system allows us to monitor the filterability of iRBCs *in vitro* with lower cost and less time-consuming although it cannot completely replace the spleen model.

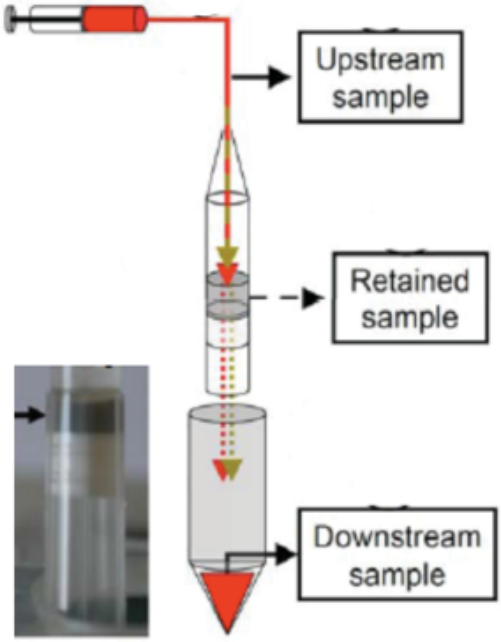

Figure 1.9. Microsphiltration system. (Buffet et al, 2011). The device is mimicking the diameter of splenic interendothelial slits. The less deformable iRBCs are retained at the beads by imitating the sensing mechanical process that happens at a slow opened circulation of the spleen. Micro-beads are added into an inverted 1000 µl-tip, leading to the formation of a 5 mm-thick bead layer (black arrow) above the anti-aerosol filter (left image). iRBCs from a *P. falciparum* culture are re-suspended at 2% hematocrit in medium (PBS/1% albumin), then introduced on top of the micro-bead layer (upstream sample). The suspended RBCs are gently flowed through the micro-bead layer by the action of an electric pump containing medium. The downstream sample is retrieved after washing the micro-bead layer with 7 ml of medium. The proportion of infected RBCs in "upstream", "downstream", and "retained" RBC samples is determined by flow cytometry and Giemsa-staining.

1.8 Aims of this study

Despite the fact that many molecules of the malaria parasites have been identified, their molecular interactions and functions contributing to the pathology are known for very few. The study aims to tackle this gap.

In this thesis, one of *P. falciparum* exported proteins called PFD encoded by *PFD1170c* gene is elucidated. C**hapter 3** demonstrates the **molecular characterization of PFD**. We determined the localization and interacting partners of PFD via gene tagging. GFP and HA tagged PFD cell lines were subjected to localization studies, solubility, pull-down, co-immunoprecipitation and blue-native electrophoresis assays. **The physiological role of PFD *in vivo*** is investigated in **chapter 4**. Experiments on the retention ability of wild-type and PFD knock-out cell lines were performed by using microsphiltration device and *ex-vivo* isolated-perfused human spleen. Parasite growth was examined via growth competition experiment. Membrane stability was accessed via osmotic fragility assays. A deeper understanding of molecular mechanism of the parasite protein, in a long-term, could lead to the development of novel therapeutic approaches to prevent severe symptoms of malaria.

Chapter 2

Materials and Methods

The below methods were adapted from the standard operation procedures of Maier lab (the Australian National University) and Tran's PhD thesis (Tran, 2014).

2.1 Cell culture methods for the human malaria parasite *P. falciparum*

2.1.1 Preparation of human blood for use in culture

Human O^+ RBC were supplied by the Australian Red Cross, Melbourne and Canberra. The blood was aseptically aliquoted into sterile 50 mL tubes, labelled with the expire date and stored at 4ºC until used.

2.1.2 Thawing of *P. falciparum* stabilates and parasite culture

The vial was removed from liquid nitrogen and thawed immediately in a 37ºC water bath for 5 minutes (min). The stabilate was then transferred to a sterile 50 mL tube and 0.2 mL 12% (w/v) NaCl in PBS was added slowly while constantly swirling the tube. After incubation of the tube at room temperature (RT) for 5 min, 10 mL 1.6% (w/v) NaCl in PBS was slowly added. After completion of the incubation, 10 mL 0.9% (w/v) NaCl with 0.2% (w/v) glucose in PBS was slowly added. The resulting solution was then centrifuged at 644 × *g* for 5 min and the supernatant was discarded. The cells were resuspended in 10 mL complete RPMI culture medium and transferred to a 25 cm^2 tissue culture dish. *P. falciparum* CS2 and 3D7 parasites were cultured using standard methods (Trager & Jensen, 1976) with slight modifications (Maier &

Rug, 2013). Parasites were maintained in O^+ red blood cells (RBCs) at 4% haematocrit resuspended in RPMI medium supplemented with 10 mM glucose, 480 μM hypoxanthine, 20 μg/mL gentamycin, 2.5% (v/v) human serum and 0.75% (w/v) Albumax II (appendix 1). Cultures were maintained at 37°C under microaerophilic conditions (1% O_2, 5% CO_2, 94% N_2).

2.1.3 Cryopreservation of parasite lines

Cultures containing more than 5% ring-infected parasites were spun down at 644 × *g* for 5 min and supernatant was removed. Two pellet volumes of freezing solution (appendix 1) were slowly added to RBC pellet while constantly swirling tube. Parasites were gently mixed using a sterile transfer pipette and allowed to stand for 5 min. One mL of solution containing parasites was transferred to each freezing vial, which was then plunged into the liquid nitrogen. Frozen tubes were placed into a storage box that was immediately stored in the liquid nitrogen tank.

2.1.4 Assessment of culture parasitemia

A small drop (~3 μL) of blood was placed on a labelled microscope slide, smeared, and air-dried. The smear was then fixed with 100% methanol for 1 min and stained with 10% Giemsa stain (in water) for 5 min. The slide was rinsed with tap water, blotted dry gently with tissue paper and then allowed to air dry. Culture parasitemia was determined by microscopic examination of the smear. Where required, the proportion of rings, trophozoites and schizonts were also determined. The parasite culture was maintained at 4% haematocrit and less than 3% parasitemia by dilution and fed with fresh media and blood every 2 days.

2.1.5 Sorbitol synchronisation

Ring stage parasites were synchronised by sorbitol treatment (Lambros & Vanderberg, 1979). Briefly, cultures containing at least 1% ring-stage infected RBCs were centrifuged at 644 × *g* for 5 min and the supernatant was discarded. Five to ten pellet volumes of 5% sorbitol (~2 mL for a pellet of a 10 mL culture) were added to the pellet, mixed gently and incubated at 37ºC for 10 min. The solution was then centrifuged at 644 × *g* for 5 min and the supernatant was discarded. The cell pellet was resuspended in fresh, pre-warmed media, transferred to a new dish, gassed and incubated at 37ºC.

2.1.6 Permeabilising cellular membrane of uninfected RBCs by tetanolysin

The cells from 10 mL culture were pelleted centrifuging at 644 × *g* for 5 min and the supernatant was discarded. The pellet was gently mixed in a solution containing 100 U/mL tetanolysin (Biological laboratories, Inc) and 1 x complete protease inhibitor cocktail (Roche) in PBS and incubated at 37ºC for 20 min. After completion of the incubation, the iRBCs cells were centrifuged at 1,300 x *g* for 10 min and the supernatant was discarded. The cells were washed twice with ice-cold PBS. The pellets can be stored at -80ºC for later analysis.

2.1.7 Automated synchronization in a temperature-cycling incubator

Mimicking *in vitro* conditions, parasites were incubated in a custom temperature-cycling incubator (TCI), which was programmed to periodical change between two different temperatures, 2 hours at 41ºC and 46 hours at 37^{o}C. During incubation at 41ºC for 2 hours, most trophozoites and schizonts died; only the ring-stage parasites

could survive, therefore the parasite culture was synchronously maintained (Kwiatkowski, 1989).

2.1.8 Gelatin flotation synchronisation

RBCs infected with knob-positive mature *P. falciparum* were purified using 4% Succinylated Gelatin Solution (Gelofusine®, B. Braun) as previously described (Goodyer et al, 1994). Parasites was grown in 30 mL dish to obtain > 3% trophozoites. Twenty mL of the culture supernatant was removed and the cells in the remaining 10 mL media was resuspended and then transferred to a 15 mL tube. The cells were then centrifuged at 644 x *g* for 4 min, Supernatant was discarded and the cells were gently resuspended in 7.5 mL Gelofusine and 4.5 mL incomplete RPMI. The tube was allowed to stand with loosed lid in a gassed box at 37ºC for 30 – 45 min until a separation of knob-negative RBCs and gelatin supernatant phase containing knob-positive RBCs was observed. The supernatant containing the knob-positive parasites was carefully collected. The supernatant was centrifuged at 644 x *g* for 4 min to pellet the parasitized RBCs. The cells were transferred back into culture supplemented with fresh blood and media.

2.1.9 Saponin lysis

To collect all the intact parasites and membranes derived from the infected and uninfected RBCs, saponin was used to lyse all the erythrocyte membranes. The cells were pelleted centrifuging at 644 × *g* for 5 min and the supernatant was discarded. Three pellet volumes of pre-chilled 0.15% saponin (1.2 mL for a 10 mL dish) (Benting et al, 1994) were used to resuspend the cell pellet and the cells were incubated on ice for 15 min with gentle mixing every few minutes. After completion of the incubation, the cells were centrifuged at 4,000 x *g* for 1 min and the supernatant

was discarded. The cells were washed with ice-cold PBS containing 1 x protease inhibitor (Roche) until the supernatant was clear. The pellets were stored at -20ºC until use.

2.1.10 Transfection of *P. falciparum*

Transfection of *P. falciparum* method was established as described previously with slight modifications (Fidock & Wellems, 1997). One hundred µg plasmid DNA resuspended in 15 µL TE buffer was pre-warmed to 37ºC and 385 µL pre-warmed cytomix (appendix 1) was added into the DNA solution and mixed. Two hundreds µL of parasite pellet containing at least 5% rings was electroporated with the DNA solution at 0.31 kV, 950 µF and immediately resuspended in 10 mL complete media containing 300 µL fresh RBCs and incubated at 37ºC. After 4-6 hours, 7 mL media was removed and replaced with fresh media and appropriate antibiotic for selection (2 nM WR99210 or 100 ng/mL puromycin) was added. The transfected cells were fed with fresh complete media supplemented with selection drug every day in the first 5 days and then, every two days until viable parasites could be observed.

2.1.11 Drug selection cycling

For integration of the plasmid into the genome the selection drug was removed from the culture for 3 weeks, once a healthy culture had been established after transfection. After 21 days of culturing without drug, the selection drug was added back to a culture of 2-3% parasitemia. Death of parasites was monitored by blood smears and feeding every day. Once ring stages were observed again, the culture was expanded and cryopreserved. This marked the end of cycle 1. This on/off drug cycling steps were repeated until integration of plasmid into expected genome locus (Crabb & Cowman, 1996) was obtained and validated by Southern blot.

2.1.12 Negative selection

To exclude episomal plasmid in the transfected cells, negative selection was performed. After the 2nd cycle off-drug was established, the culture was grown in the presence of Ganciclovir at a final concentration of 20 nM (Maier et al, 2006). The culture was fed and parasitemia was assessed daily. When growth of transfectant parasites was re-established, they were cryopreserved as soon as the parasitemia reached 2-5% ring stage parasites.

2.1.13 Isolation of *P. falciparum* genomic DNA

The parasites were grown up to > 5% trophozoite or schizont stages and saponin lysed. The parasite genomic DNA (gDNA) was isolated with a DNeasy Blood & Tissue Kit (Qiagen) following manufacture's instruction.

2.2 Molecular biology methods

2.2.1 Preparation of bacteriological media

All media and reagents used for bacteria transformation were prepared as previously described (Ausubel et al, 2004; Sambrook et al, 1989).

Luria-Bertani (LB) media

LB media were prepared by dissolving ready-to-use LB power (Amresco) into 1 L distilled water and autoclaved at 121ºC for 20 min. The broth was allowed to cool and stored at 4ºC until use.

Luria-Bertani (LB) agar

LB agar powder (Amresco) was dissolved in 500 mL distilled water and autoclaved at 121ºC for 20 min. The broth was allowed to cool to ~55ºC and supplemented with appropriate antibiotics. It was then poured into petri dishes and allowed to set and dry at RT for overnight. The agar plates were then stored at 4ºC until use.

SOC Recovery media

SOC media was prepared according to the compositions mentioned in appendix 1. After autoclaving, the media was allowed to cool and Mg^{2+} and glucose solutions were added accordingly. The media was then stored at 4ºC until use.

2.2.2 DNA extraction and purification methods

The colony of interest was picked and inoculated into 10 mL of LB broth with appropriate antibiotic. The broth was incubated with shaking at 180 rpm at 37°C overnight. The culture was then ready to harvest for use in small scale DNA plasmid extraction (Miniprep). Alternatively, 10 mL culture was transferred to flask containing 500 mL of LB broth and incubated with shaking at 180 x rpm at 37°C overnight. The following day, the culture was ready to harvest for use in large scale DNA plasmid extraction (Maxiprep).

2.2.2.1 Miniprep plasmid DNA extraction

The extraction was performed using a Miniprep DNA extraction kit (Invitrogen) according to manufacturer's instruction.

2.2.2.2 Maxiprep plasmid DNA extraction

The extraction was performed using a Maxiprep DNA extraction kit (Invitrogen) according to manufacturer's instruction.

2.2.3 Enrichment of DNA by precipitation

For 100 µL DNA sample to be precipitated, 10 µL of 3 M sodium acetate (10% v/v) and 250 µL 100% ethanol (2.5 times v/v) were added into the sample. The tube was inverted several times and incubated at -20°C for at least 30 min. The precipitated DNA was pelleted by centrifugation at 16,200 × *g* for 20 min. The supernatant was then discarded without disturbing the pellet. The pelleted DNA was washed by adding 1 mL of 70% (v/v) ethanol and centrifuged at 16,200 × *g* for 5 min. The supernatant was discarded, the DNA pellet was allowed to air-dry at RT and resuspended in an appropriate volume of distilled water.

2.2.4 Estimation of nucleic acid concentration by Nanodrop ND-1000 spectrophotometer

The nucleic acid concentration of a solution was calculated using a Nanodrop ND-1000 based on the absorbance at 260 nm. An $OD_{260\ nm}$ results of 1 equates to 50 ng/µL double stranded DNA or 40 ng/µL single stranded RNA. The sample purity was assessed based on $OD_{260\ nm}$ / $OD_{280\ nm}$ ratio. Pure preparation of sample should have the ratio close to 1.8 for DNA or 2.0 for RNA.

2.2.5 Resolution of DNA by agarose gel electrophoresis

0.8% (w/v) agarose (Bioline) was used to resolve high molecular weight DNA fragments (greater than 1 kb) and high agarose concentration (1.3%) was used to

resolve low molecular weight DNA fragments (less than 1 kb), respectively. 0.8% or 1.3% agarose gel made in 0.5 x TBE (appendix 1) supplemented with 100 ng/mL ethidium bromide (Amresco) was poured into a gel caster to a depth of approximately 5 mm. The gel was allowed to set for 30 - 60 min. The gel was submerged into an electrophoresis tank and covered with 0.5 x TBE Buffer. The DNA sample was mixed with 6 x DNA Loading Buffer (appendix 1) and loaded into the agarose gel. The 100 bp or 1 kb DNA molecular weight markers (NEB) were also loaded as required. 120 V / 400 amp were applied for 1 hour, or until the blue Gel Loading Buffer front was close to the end of the gel. The result was visualised and photographed using a Bio-Rad Gel Doc^{TM} XR+ system.

2.2.6 Purification of DNA from agarose gels

The extraction was performed using a gel extraction kit (Qiagen) according to manufacturer's instruction. Briefly, the digested plasmid DNA or PCR amplification products were resolved on an agarose gel. Using a sterile scalpel blade, the DNA of interest was excised from the agarose gel. The agarose block was placed into a pre-weighed sterile 1.5 mL polypropylene tube, and the weight of the block was determined. Buffer QG equivalent to 3 times the weight of the agarose block was added and incubated at 50°C for 10 min, or until the agarose block has completely melted and dissolved into the buffer. One gel volume of isopropanol was added and mixed thoroughly. The sample was applied to the QIAquick column and centrifuged at 16,200 × *g* for 1 min. The flow-through was discarded and 500 µL of Buffer QG was added to the column and centrifuged at 16,200 × *g* for 1 min. The flow-through was discarded and the column was centrifuged at 16,200 × *g* for additional 1 min. The column was placed into a sterile 1.5 mL microfuge tube and DNA was eluted by

adding 50 µL of TE Buffer to the column that was then centrifuged at 16,200 × *g* for 1 min.

2.2.7 Restriction endonuclease digestion of DNA

The reactions were made up to 10 or 20 µL volume by mixing distilled water, DNA sample (up to 1 µg), 1 x NEB digestion buffer, 5 unit of enzyme(s) and 1 x BSA if required. The reaction was incubated for 15 - 60 min at 37°C. Depending on the experiment, the reaction was stopped by heat inactivation, ethanol precipitation or the addition of 6 x DNA Loading Buffer.

2.2.8 Modification and ligation of DNA

To prevent self-ligation of the vector following digestion reaction, 5' phosphates of digested plasmid vector fragments were removed using an Antarctic Phosphatase (NEB). Following restriction digestion, the reaction was supplemented with 1 unit of Antarctic Phosphatase enzyme and corresponding buffer; and incubated at 37°C for 60 min. The reaction was inactivated by heating to 65°C for 5 min.

The ligation reactions were performed in 20 µL total volume by mixing distilled water, vector fragment DNA, insert fragment DNA, 2 units of T4 DNA ligase (NEB) and 1 x ligation buffer. The reaction was incubated at 4°C for overnight. After completion of the incubation, the ligation products were ethanol precipitated and resuspended in 10 µL of distilled water. The ligates were ready for bacteria transformation.

2.2.9 Blunt II-TOPO cloning (Invitrogen)

The TOPO® Cloning reaction was performed with Blunt II-TOPO kit (Invitrogen) according to manufacturer's instruction (Invitrogen).

2.2.10 Preparation of electro-competent *Escherichia coli* cells

A single colony of PMC103 *E. coli (Doherty et al, 1993)* was inoculated from a fresh agar plate into a flask containing 50 mL of LB medium and incubated with vigorous aeration at 100 x *g* at 37°C overnight. On the following day, each 25 mL of the overnight bacterial culture was inoculated into two aliquots of 500 mL each of pre-warmed LB medium in 2 L flasks and incubated with agitation at 180 rpm at 37°C. The OD_{600} of the growing bacterial cultures were measured every 20 min. Once the OD_{600} of the cultures reached 0.4, the flasks were rapidly transferred to an ice-water bath for 15-30 min. The cultures were occasionally swirled to ensure that cooling occurred evenly. The cultures were then transferred to ice-cold centrifuge bottles and the cells were harvested by centrifugation at 1,000 x *g* at 4°C for 15 min. The supernatant was decanted and the cells were resuspended in 500 mL of ice-cold distilled water. The cells were again harvested by centrifugation at 1,000 x *g* at 4°C for 20 min. The supernatant was decanted and the cells were washed in 250 mL of ice-cold 10% (v/v) glycerol. The cells were again harvested by centrifugation at 1,000 x *g* at 4°C for 20 min. The supernatant was decanted and the cells were resuspended in 10 mL of ice-cold 10% glycerol. The cells were again harvested by centrifugation at 1,000 x *g* at 4°C for 20 min. The supernatant was carefully decanted and any remaining drops of buffer were removed completely. The cells were resuspended in 1 mL of ice-cold GYT medium (appendix 1). The OD_{600} of a 1:100 dilution of the cell suspension was measured and the cell suspension was then diluted to a concentration

of 2 x 10^{10} cells/mL (1 OD_{600} = 2.5 x 10^{8} cells/mL) with ice-cold GYT medium. 40 µL aliquots of the cell suspension were dispensed into sterile ice-cold 1.5 mL tubes, dropped into liquid nitrogen and stored at -80°C until use.

2.2.11 Transformation of electro-competent *Escherichia coli* cells

One aliquot of electrocompetent cells (40 µL) for each transformation to be carried out was thawed on ice. Five µL of DNA or ligation production was added to the cells and mixed by gently pipetting. The mixture was then transferred into a 0.2 cm gap electroporation cuvette (Bio-Rad) that has been chilled on ice for at least 5 min, and the cuvette was tapped to remove any bubles from the cuvette. An electroporator (Bio-Rad Gene Pulser II) was set to deliver a pulse of 2.5 kV, 25 µF, 200 Ω. The cuvette was placed into the sample chamber and the charge was applied by pressing the pulse button. The time constant was approximately 4.6 – 5.2 ms. The cuvette was removed and 1 mL of pre-warmed SOC recovery medium (appendix 1) was immediately added. The cells were resuspended, transferred to a sterile 1.5 mL tube and incubated at 37°C for 1 hour. After the completion of incubation, the cells were pelleted by centrifugation at 4,000 x *g* at RT for 5 min and spread on LB agar plates containing appropriate antibiotic if required. The plates were incubated at 37°C overnight.

2.2.12 Polymerase chain reaction (PCR) amplification of DNA

The PCR reactions were prepared in 50 µL total volume containing 1 x Phusion HF Buffer (NEB), 200 µM dNTPs (Invitrogen), 0.5 µM of each forward and reverse primers, 3% DMSO, 50 ng of parasite gDNA, 1 unit of Phusion HF DNA Polymerase (NEB) and distilled water. Amplification was performed with a 96-well thermocycler (ABI) with the following temperature condition: denaturation at 96°C for 5 min,

amplification for 35 cycles (denaturation at 96°C for 30 s, annealing at 55°C for 30 s, extension at 65°C for 2 min), and final extension at 68°C for 10 min. The PCR products were resolved by agarose gel electrophoresis.

2.2.13 PCR amplification from *Escherichia coli* colonies

The PCR reactions were prepared in 20 µL total volume containing 1 x ThermoPol Reaction Buffer (NEB), 200 µM dNTPs, 0.5 µM of each forward and reverse primers, 3% DMSO, 1 unit of *Taq* DNA Polymerase (NEB) and distilled water. An single colony was picked using pipette tip, streaked onto a fresh agar plate, and the tip was then dipped into the PCR mix. The plate was incubated at 37°C overnight and the PCR amplification was performed with the following temperature condition: denaturation at 96°C for 5 min, amplification for 35 cycles (denaturation at 96°C for 30 s, annealing at 55°C for 30 s, extension at 65°C for 1 min), and final extension at 68°C for 10 min. The PCR products were resolved by agarose gel electrophoresis and then visualised under UV light. The PCR positive clones were propagated by inoculating LB broth and the plasmid was then extracted using a Miniprep kit.

2.2.14 Cryopreservation of *Escherichia coli* strains

The strain to be stored was inoculated into a fresh 10 mL LB broth supplemented with appropriate antibiotic and grown with agitation at 37°C overnight. The cells were pelleted by centrifugation at 1,500 × *g* for 5 min before resuspended in 1.5 mL of glycerol Broth (appendix 1). The strain was stored at -80°C.

2.2.15 DNA sequencing

The plasmids containing DNA fragments of interest were prepared using Maxiprep kit and sent for sequencing. The sequencing data was visualised by FinchTV version

1.4.0 (Geospiza Inc.) and aligned with annotated sequence (downloaded from www.PlasmoDB.com) using Serial Cloner v 2.6.0 (Franck Perez).

2.2.16 Digoxigenin-labelled hybridization probe synthesis

The probe was synthesized following the instructions of the PCR DIG Probe Synthesis Kit (Roche). The 20 µL PCR reaction contained 1 x Roche PCR Buffer, 0.3 x PCR DIG labelling mix, 0.7 x dNTP solution, 1 µM of each forward and reverse primers, 1 µg of plasmid DNA, 3.5 units of enzyme mix and distilled water. Amplification was performed with a 96-well thermocycler (Veriti) under the following temperature condition: denaturation at 96°C for 5 min, amplification for 35 cycles (denaturation at 96°C for 30 s, annealing at 52°C for 30 s, extension at 65°C for 2 min), and final extension at 68°C for 10 min. The PCR products were resolved by agarose gel electrophoresis and purified with a gel extraction kit (Qiagen).

2.2.17 Southern hybridisation

Southern blotting was performed according to (Rug & Maier, 2013). Two µg of parasite gDNA was digested by appropriate enzymes at 37°C for 4 hours before it was resolved on a 0.8% agarose gel with 0.5 x TBE at 25 V overnight. The following day, the gel was documented and depurinated in 0.125 M HCl for 20 min followed by denaturing in 0.5 M NaOH, 1.5 M NaCl solution for 30 min. The gel was then neutralised in 0.5 M Tris, 1.5 M NaCl solution pH 8.0 for 30 min. The digested DNA was then transferred onto a Hybond-N+ membrane (GE Healthcare) by blotting the gel with a 2 x SSC solution (appendix 1) by capillary transfer overnight. The membrane was then UV crosslinked at 1200 µJ/cm^2 before being blocked with a pre-hybridization solution (appendix 1) supplemented with 25 µg/mL heat-denatured Herring Sperm DNA in a hybridisation pouch at 45°C for 4 hours. After the

incubation, the pre-hybridization solution was removed and the pre-hybridization solution supplemented with the heat-denatured digoxigenin-labelled hybridization probe (hybridization solution) was added to the plastic bag. The membrane was hybridized at 45°C overnight. The hybridized probe was detected with a DIG Chemiluminescent Detection Kit (Roche) following the manufacturer's instruction. If required, the membrane was stripped and re-probed by rinsing it in distilled water for 1 min before incubated in 0.2 M NaOH containing 0.1% SDS at 37°C for 30 min. The membrane was then washed in 2 x SSC at RT for 5 min and stored in 2 x SSC at 4°C until re-probing.

2.3 Protein methods (Coligan et al, 2009)

2.3.1 Expression of recombinant protein

The pGEX-4T-1 GST (Amersham) recombinant protein system was used for the expression of recombinant fusion proteins. The DNA fragment of interest was cloned into the vector and then transformed into electro competent BL21 *E. coli* cells for protein expression.

2.3.2 Growth and induction of *Escherichia coli* cultures

The *E. coli* culture of interest was streaked onto a LB agar plate supplemented with appropriate antibiotic and incubated at 37°C overnight. The next day, a single colony was inoculated into 50 mL LB broth supplemented with the required antibiotic and grown on a shaker at 37°C overnight. The following day, 10 mL of overnight culture was inoculated into 500 mL of pre-warmed LB broth supplemented with appropriate antibiotic and incubated on a shaker at 37°C, 180 rpm until the $OD_{(600\ nm)}$ reached 0.5. At this stage, recombinant protein expression was induced by adding IPTG

(Biovecta) to 1 mM final concentration (Bio Vectra) and the culture was incubated on a shaker at 37°C for an additional 3 - 4 hours. The cells were collected by centrifugation at 6,000 × *g* at 4°C for 15 min. The cell pellet could be stored at -80°C until proceeding with the lysis step.

2.3.3 Cell disruption for purification of soluble proteins

In order to limit protein degradation following cell lysis, all steps were carried out on ice or at 4°C. The *E. coli* cell pellet was resuspended in 50 mL ice-cold PBS containing 1 x Protease Inhibitor (Roche) and transferred to a glass beaker. The cells were disrupted by sonication with 30 cycles of alternating 5 s pulse and 10 s rest. After cell disruption, the cell extract was centrifuged at 16,200 x *g* at 4°C for 30 min to pellet any insoluble material. The lysate's supernatant was removed and used for chromatographic purification.

2.3.4 Purification of GST-tagged recombinant proteins

The lysate's supernatant was added into PBS washed Glutathione Sepharose 4B resin to make a 10% slurry suspension and incubated at 4°C overnight. The beads were centrifuged at 500 × *g* for 5 min. The supernatant was removed and kept as the unbound control. The beads were then washed 3 times with ice-cold PBS containing 1 x Protease Inhibitor (Roche). The GST fusion protein was eluted adding 1 x bed volume of elution buffer (50 mM Tris-HCl, 10 mM reduced glutathione, pH 8.0) and incubated at RT for 10 min. The eluted protein in the supernatant was collected after centrifugation at 500 × *g* for 5 min. The elution step was repeated to collect totally 3 elutes. To analyse the protein purity, 10 µL of each fraction (unbounded, beads and elutes) was heated for 5 min and loaded on a SDS-PAGE gel.

2.3.5 Bio-Rad (Bradford) protein assay

The protein concentration was determined based on a Bradford assay following manufacturer's instruction with known amount of BSA as a protein standard.

2.3.6 Polyacrylamide gel electrophoresis (SDS-PAGE) for the fusion protein analysis

The protein samples were mixed with LDS sample buffer (Invitrogen, Life Technologies) supplemented with 10% 2-mercaptoethanol (Sigma) and boiled for 5 min. Any aggregates were pelleted by centrifugation at 16,200 x *g* for 5 min before the supernatant was loaded on a 4-12% Bis-Tris NuPAGE precast gel (Invitrogen, Life Technologies). The denatured proteins were separated by electrophoresis running at 200 V for 45 min.

2.3.7 TCA protein precipitation

The protocol was established as described previously (Link & LaBaer, 2011) with slight modifications. One per hundred volume of 2% sodium deoxycholate (DOC) was added to the protein solution. The mixture was vortexed and incubated on ice for 30 min. One per ten volume of 100% (w/v) trichloroacetic acid (TCA) was added to the protein solution, which was then incubated at -20°C for 30 min. The solution was centrifuged at 20,000 x *g* at 4°C for 10 min. The supernatant was carefully removed. One mL ice-cold acetone was added to rinse the pellet. The solution was again centrifuged at 20,000 x *g* at 4°C for 10 min and the supernatant was carefully removed. The protein pellet was then dried at RT for 10 min. The protein sample was resuspended in reducing loading buffer and heated at 70°C for 3 min before loaded onto a SDS-PAGE gel.

2.3.8 Polyacrylamide gel electrophoresis (SDS-PAGE) for the analysis of parasite proteins

Synchronous parasites were enriched using magnetic cell separating columns (CS and D columns; MACS Cell Separation, Miltenyi Biotec). The membranes of iRBCs were lysed by incubating the parasites in a 0.15% saponin solution (in water) on ice for 15 min. Parasites were then pelleted at 4,000 x *g* for 1 min and washed in PBS containing 1 x Protease Inhibitor (Roche) until the supernatant was clear. The parasite pellets were either stored at -80°C or treated immediately with benzonase nuclease (Novagen) and taken up in LDS sample buffer (Invitrogen, Life Technologies) supplemented with 10% 2-mercaptoethanol (Sigma). Denatured proteins were separated on a 4-12% Bis-Tris NuPAGE gel (Invitrogen, Life Technologies) at 200 V for 45 min.

2.3.9 Coomassie staining of polyacrylamide gels

The gel was removed from the casting plates, placed in a container containing 50 mL of Coomassie Blue Stain Solution (appendix 1) and incubated with gentle rocking at RT for 30 min. The stain was removed and the gel was destained by incubating on a rocker in 50 mL of Coomassie Blue Destain Solution (appendix 1). The Coomassie Blue Destain Solution in the container was replaced with fresh solution until the background of the gel was clear. The gel was then re-hydrated in 50 mL of distilled water at RT.

2.3.10 Silver staining of polyacrylamide gels

Once proteins were resolved on a SDS-PAGE gel, silver stainning was performed using a SilverQuest^{TM} Silver Staining Kit (Life Technologies) according to manufacturer's instructions.

2.3.11 Antibody production

A coding sequence (amino acid 91-190) of *PFD1170c* was PCR amplified and cloned into the expression vector pGEX-4T at the BamHI/XhoI sites to express the protein in *E. coli* with a GST tag at the N-terminus position (see section 2.3.4). The recombinant protein was purified via glutathione sepharose beads. The lyophilised GST-tagged PFD recombinant protein was sent to GenScript USA Inc. for generating rabbit polyclonal antibodies against the PFD fragment.

2.3.12 Immunoblotting (Western blotting)

Proteins were transferred from a SDS-PAGE gel onto a nitrocellulose membrane using an iBlot system (Invitrogen, Life Technologies) according to manufacturer's instructions. Following the transfer, the membrane was blocked with PBS solution containing 10% milk for 30 min and then incubated with a primary antibody solution at RT for at least 2 hours. The membrane was then washed 3 times with PBS/1% Tween-20 and incubated with a secondary antibody solution at RT for at least 1 hour. Both primary and secondary antibodies were made up in PBS containing 1% milk powders. Primary antibodies used included: rabbit anti-PFD (1:1000; U. Nguyen), rabbit anti-GFP (1:1000; Roche), mouse anti-HA (1:1000; Roche), rabbit anti-STREP tag II (1:500; Roche), mouse anti-PfHSP70 (1:1000; A. Maier), rabbit anti-EXP1 (1:500, A. Maier), rabbit anti-MESA (1:1000; A. Maier), rabbit anti-KAHRP (1:1000,

M. Rug), and mouse anti-RESA (1:1000, a gift from R. Anders). Horseradish peroxidase-coupled goat anti-mouse IgG (1:2000; Southern Biotech) or donkey anti-rabbit IgG (1:5000; GE Healthcare) were used as secondary antibodies. After incubation with the secondary antibodies solution, the membrane was then washed 3 times with PBS and incubated with ECL solution (Roche) for 1 min before exposed on an X-ray film (Fuji medical X-ray film, Super RX), which was developed in a film processor.

2.3.13 Stripping Western blots for re-probing

The membrane was incubated under shaking with pre-heated Western Stripping Buffer (appendix 1) supplemented with 100 mM 2-mercaptoethanol at 70°C for 10 min. The incubation was then repeated with fresh buffer. After completion of the incubation, the membrane was washed with PBS at RT until the smell of 2-mercaptoethanol disappeared (~ 10-time changes). The membrane could be blocked again and pre-probed with new antisera.

2.3.14 Determining insoluble proteins in infected erythrocyte's cytosol

The parasitized RBCs were harvested using magnetic cell sorting columns (CS columns; MACS Cell Separation, MiltenyiBiotec) and RBC membranes were lysed by incubating the cells with 0.15% saponin solution (in water) on ice for 15 min (see section 2.1.9). The pellet and supernatant were separately collected after centrifugation at 644 × *g* for 5 min. Proteins in supernatant were precipitated by TCA (see section 2.3.7) while the pellet was washed with ice-cold PBS for 3 times. Both fractions were resuspended in the same volume of reducing loading buffer. The protein samples were loaded equally onto a 12% SDS-PAGE. Upon completion of the

gel electrophoresis, the proteins were transferred to nitrocellulose membrane for Western blot analysis. Primary anti-antibodies used: mouse anti-GFP antibodies (1:1000; Roche) to detect PFD-GFP protein, mouse anti-PfHSP70 antibodies (1:1000; A. Maier) to detect PfHSP70, a parasite soluble protein located within parasite's cytosol (Shonhai et al, 2007) and rabbit anti-EXP1 antibodies (1:500; A. Maier) to detect EXP1, a trans-membrane protein located at the PVM (Günther et al, 1991).

2.3.15 Determining membrane association of proteins (Triton X-114)

Triton X-114 phase separation was performed as described previously (Spielmann et al, 2006) with some modifications. Briefly, 12% equilibrated Triton X-114 was prepared as following: 5 g Triton X-114 was dissolved in 245 ml of a cold solution containing 10 mM Tris-HCl pH 7.4, 150 mM NaCl, 0.0016% bromophenol-blue at 4°C with stirring for 8 hours. The solution was then incubated at 37°C for 20 hours to form 2 layers. The upper (clear) phase was removed and replaced with equal volume of a cold solution 10 mM Tris-HCl pH 7.4, 150 mM NaCl. The solution was then stirred at 4°C for 30 min and incubated at 37°C for another 20 hours. Clear supernatant was removed completely and the lower phase containing equilibrated ~12% Triton X-114 was stored at -20°C until use.

CS2-PFD-GFP parasites harvested from 30 ml of culture (~ 5% parasitemia at trophozoite stage) were treated with saponin (see section 2.1.9). The parasite pellet was then washed and resuspended in 50 µL of 1 x PBS. A fifth of the solution (containing ~ 1 mg protein / mL) was mixed into 200 µL of 12% equilibrated Triton X-114. The subsequent solution was layered over a 300 µL of sucrose buffer [6% (w/v) sucrose, 10 mM Tris-Cl, pH 7.4, 150 mM NaCl, 0.06% (w/v) Triton X-114], incubated at 37°C for 20 min, and then centrifuged at 300 x *g* at RT (not below 25°C)

for 3 min. The aqueous (upper) phase and the hydrophobic (lower) phase were separately collected. Equilibrated Triton X-114 was added to the hydrophilic (upper) phase to a final concentration of 0.5% (w/v). The solution was cooled on ice for 30 min to re-establish a single phase and warmed to 37°C again. When the solution became turbid, the centrifugation at 300 x *g* at RT for 3 min was repeated. The aqueous phase and hydrophobic phase were then collected. The lower phase was combined with the previous lower phase solution and kept on ice. The upper phase was TCA precipitated (see section 2.3.7). The protein samples from both phases were taken up into 4 x reducing loading buffer to make a 100 µL total volume each, then, resolved on a SDS-PAGE gel, transferred to nitrocellulose membrane for Western blot analysis (see section 2.3.12). Mouse anti-GFP, mouse anti-PfHSP70 and rabbit anti-EXP1 antibodies were used as primary antibodies.

2.3.16 Carbonate extraction

Alkaline sodium carbonate was used to extract peripheral membrane proteins as described previous (Fujiki et al, 1982). CS2-PFD-GFP parasites harvested from 90 mL culture were treated with saponin. One mL of 100 µM sodium carbonate pH 11.5 was added to the cell pellet and then incubated on ice for 1 hour with vortex pulse every 10 min. The solution was then centrifuged at 70,000 x *g* at 4^{o}C for 1 hour (TLA 55 rotor, Beckman Coulter Optima). The supernatant was collected and proteins were TCA precipitated (see section 2.3.7). The protein samples from the supernatant and pellet were taken up each in 4 x reducing loading buffer to a final volume of 100 µL total. Equal volumes of both fractions were loaded on a 4-12% SDS-PAGE and analysed by Western blot (see section 2.3.13). Antibodies used included mouse anti-GFP and rabbit anti-EXP1.

2.3.17 Determining protein solubility for immunoprecipitation assay

To remove haemoglobin the parasites were magnet purified and then saponin lysed (see section 2.1.9). The parasite pellet was re-suspended in solubilisation buffer (20 mM Tris pH 7.4, 0.25 M NaCl, 10% glycerol, 1 mM DTT, 1 mM EDTA) containing 1% (v/v if liquid or w/v if powder) detergent and incubated on ice for 1 hour with gentle vortexing every 10 min. The detergents used to screen the solubility of PFD were 3-[(3-cholamidopropyl) dimethylammonio]-1-propanesulfonate (CHAPS), Deoxycholic acid (DOC), n-Octyl-β-D-glucopyranoside (OGP), n-Octyl-β-D-thioglucopyranoside (OTGP), Zwittergent 3-14, Triton X-100, Digitonin and Tergitol-type NP-40 (NP-40) (all Calbiochem). Upon completion of the incubation the suspension was centrifuged at 100,000 x *g* at 4°C for 1 hour, the supernatant was separated. The pellet and supernatant were mixed with reducing loading buffer and loaded on 4-12% Bis-Tris NuPAGE gels (Invitrogen, Life Technologies). The Western blot was performed as previously described (see section 2.3.12) to detect the relative amounts of PFD in the supernatant and pellet in order to assess its solubility. Antibodies against GFP were used to detect PFD-GFP protein.

2.3.18 Co-immunoprecipitation

Co-immunoprecipitation method was used to precipitate protein complexes using specific antibodies against one of the known proteins in the complex. This protocol was performed as described previously (Li et al, 2004) with some modifications. CS2-wildtype parasites from 60 mL of culture were purified by using magnetic cell sorting columns (CS columns; MACS Cell Separation, Miltenyi Biotec). The parasite pellet was then treated with ten pellet volume of lysis buffer containing 75 mM Tris pH 8.0, 225 mM NaCl, 1 x protease inhibitor, 0.5% Zwittergent 3-14 and 1 mM EDTA. The

mixture was incubated on ice for 3 hours with gentle mixing every 30 min. The solution was then centrifuged at 17,000 x *g* at 4°C for 15 min. Two hundred µL of 50% slurry of protein G sepharose was washed 3 times and used to pre-cleared the supernatant after the previous centrifugation. The tube was gently rotated at 4°C for 1 hour. The pre-cleared sample was centrifuged at 1,500 x *g* at 4°C for 4 min. This step was included to reduce the non-specific binding of the cell lysate. The supernatant was collected and divided into 2 eppendorf tubes. Five µL of prebleed rabbit serum was added to one tube. Five µL of rabbit antibodies against PFD (or mouse antibodies against RESA in a complement immunoprecipitation assay) was added to the other tube. Both tubes were gently rotated at 4°C for 16 hours. Then, 50 µL of a 50% protein G sepharose was added into each solution, gently rotated at 4°C for 1 hour. The solutions were then centrifuged at 1,500 x *g* at 4°C for 4 min. The supernatants were discarded and the pellets were washed 6 times with 0.1% Zwittergent 3-14 in lysis buffer. The immune complex polypeptides associated beads were heated to 70°C for 3 min, then analysed on SDS-PAGE gels followed by Western blotting. The primary antibodies used included rabbit anti-KAHRP (1:1000; M. Rug), mouse anti-PfEMP3 (1:1000, A. Maier), mouse anti-MESA (1:1000, A. Maier), mouse anti-RESA (1:1000, R. Anderson) and rabbit anti-PFD (1:1000, U. Nguyen). The precleared sample was loaded as a (negative) control for the non-specific binding between beads and non-specific proteins. The rabbit preimmune sera were used to control for non-specific binding.

2.3.19 Blue Native - Polyacrylamide gel electrophoresis (BN-PAGE)

Blue-Native PAGE was performed based on the method described by Schägger and von Jagow (Schägger & von Jagow, 1991) with minor modifications (Dunning et al,

2007). Synchronous parasites were harvested by magnet purification and saponin lysed. An approximately 200-600 μg protein was solubilised in 90 μl of 20 mM Tris pH 7.4, 0.25 M NaCl, 10% Glycerol, 1 mM DTT, 1 mM EDTA and 0.5% (w/v) Zwittergent 3-14 (Calbiochem) on ice for 1 hour. Insoluble materials were precipitated by centrifugation at 16,200 x *g* at 4°C for 5 min and the supernatant was combined with 10 μL blue native-PAGE loading dye (5% [w/v] Coomassie Blue G [MP biomedicals], 500 mM ε-amino n-caproic acid [Calbiochem], 100 mM Bis-Tris [pH 7.0]). Solubilised parasite material was separated on a 4-16% acrylamide-bisacrylamide blue native-PAGE gel (66.7 mM ε-amino n-caproic acid, 50 mM Bis-Tris [pH 7.0]) using an SE-600 Chroma standard vertical electrophoresis unit (Hoefer). Native complexes were separated at 100 V / 7 mA at 4°C for 14 hours. Cathode buffer [15 mM Bis-Tris [unbuffered] and 50 mM tricine (Amresco)] containing 0.02% Coomassie Blue G was used until the dye front reached a quarter of the way through the gel and was then exchanged for cathode buffer devoid of Coomassie. The anode buffer consisted of 50 mM Bis-Tris (pH 7.0). Nativemark unstained protein standards (Invitrogen) were used to estimate the size of the protein complexes. The electrophoresis was stopped when the blue dye reaching to the bottom of the gel. The gel was then gently removed and soaked in 1 x transfer buffer prior to electro-blotting on PVDF membranes with a iBLOT system (Invitrogen). The membrane was stained with coomassie staining solution for 1 – 2 min to indicate the protein markers. Then, the membrane was quickly rinsed with distilled water and placed in a destain solution (50% methanol, 7% acetic acid) for 20 min and in complete destain solution (90% methanol, 10% acetic acid) for 15 min. After destaining step, the membrane was washed in 1 x PBS several times for 30 min until

the smell of acetic acid disappeared. The membrane was then blocked and analysed by Western blot (see section 2.3.12).

2.4 Microscopic imaging techniques

2.4.1 Live cell immunofluorescence assay

Five hundred of the parasite culture were washed 3 times with RPMI and 3 μL of it was loaded onto a microscopy slide. The cells were covered with a coverslip and examined with a deconvolution microscope (DeltaVision Elite, Applied Precision). All images were recorded at the same setting and exposure time. Images were deconvolved using the softWoRx acquisition software (version 5.0) and then analysed with ImageJ 1.43u software (NIH, USA).

2.4.2 Indirect immunofluorescence assay (IFA)

Microscopy slides were coated with 50 μL of 0.5 mg/mL concanavalin A (ConA) in water at 37°C for 15 min in a humid chamber and then washed three times in PBS. Parasites were allowed to adhere to the ConA coated slides for 15 min then fixed in 2% paraformaldehyde / 0.008% glutaraldehyde for 20 min, washed three times with PBS, before being permeabilised in 0.1% (v/v) Triton X-100 (Sigma) in PBS for 10 min. After incubated in diluted primary antibody solution in 3% BSA/PBS for at least 2 hours, the cells were then washed three times in PBS, incubated with secondary antibodies conjugated with Alexa Fluor 488 (green) and Alexa Fluor 594 (red) dyes respectively (Invitrogen) for at least 1 hour, then mounted in Vectashield containing 4,6-diamidino-2-phenylindole (DAPI) (Vectashield, Vector laboratories) and examined with a deconvolution microscope (DeltaVision Elite, Applied Precision). Primary antibodies used include: mouse anti-GFP (1:1000, Roche), rabbit anti-GFP

(1:1000; a gift from M. Ryan, Latrobe University), rabbit antibodies anti-KAHRP (1:1000; M. Rug), mouse anti-PfEMP3 (1:1000, A. Maier), mouse anti-MESA (1:1000, A. Maier), mouse anti-RESA (1:1000, R. Anderson). All images were recorded at the same setting and exposure time. Images were deconvolved using the softWoRx acquisition software (version 5.0) and then processed with ImageJ 1.43u software (NIH, USA).

2.5 Osmotic fragility

The cellular osmotic fragility was determined according to previously described protocols (Parpart et al, 1947; Veale et al, 2011; Zehnder et al, 2008). A stock solution of 10 x buffered saline solution containing 18 g NaCl, 2.73 g Na_2HPO_4 and 0.374 g NaH_2PO_4 in 200 mL distilled water, osmotically equivalent to 10% NaCl (pH 7.4), was prepared. Distilled water was used for further dilutions. 50 mL solutions containing NaCl-PO_4 with concentrations of 0.1%, 0.2%, 0.3%, 0.4%, 0.45%, 0.5%, 0.6%, 0.7%, 0.8% and 0.9% (w/v) were prepared. The osmotic resistance series were established by adding 300 µL of each NaCl-PO_4 concentration or water (100% lysis control) to 1 x 10^8 RBCs or infected RBCs in CS2-wildtype or CS2-ΔPFD parasites. The reactions were incubated at RT for 45 min followed by centrifugation at 1,000 x *g* for 5 min. The haemoglobin concentration in supernatant was measured using a microplate reader (FLUOROstar OPTIMA, BMG, Labtech) at an absorbance of 540 nm. Data were normalized to percentage of water lysis, and osmotic fragility curves were plotted using GraphPad Prism 5.0.

2.6 Parasite growth competition via co-culture

Wild-type and PFD knockout parasites in 10 mL culture were synchronized twice 4 hours apart with 5% sorbitol as described previously (see section 2.1.5). Twenty four

hours after the second synchronisation, the synchronous trophozoites were expanded into 30 mL culture. Another 24 hours later, parasitemias were determined by counting a total number of 1,000 erythrocytes on a Giemsa-stained thin smear. The co-culture assay was established in biological triplicate in 10-mL petri dishes containing both 0.1% of both CS2 wild-type parasites and CS2-ΔPFD parasites in 4% haematocrit incubated at 37°C and 41°C. The cultures were maintained below 2% parasitemia over a period of 3 weeks. Parasites from each culture were collected every 7 days and the parasite gDNA was extracted using the DNeasy blood & tissue kit (Qiagen) (see 2.1.13).

For the hydrolysis probe based real-time PCR, primer and probe sets (Appendix 2, supplementary table S2) were custom synthesised by Integrated DNA Technologies for *PFD1170c* gene (PFD) (to quantitate wild-type gDNA) and *hDHFR* gene (to quantitate PFD knock-out gDNA). The PCR conditions consisted of an initial incubation at 95°C for 3 min and then 45 cycles at 95°C for 15 s, 60°C for 60 s, and 72°C for 1 s. An approximate 40ng DNA was used per reaction, and all samples were tested in triplicate. The reaction was performed with a Light Cycler 480 (Roche) to detect *PFD1170c* gene amplification in the FAM channel and *hDHFR* gene in the HEX channel concurrently in the same reaction. The relative numbers of wild-type and knock-out parasites were then calculated based on a standard curve established with 10-fold serial dilutions of parasites (Lopaticki et al, 2011). The ratio of wild-type to knock-out parasite numbers were plot using GraphPad Prism 5.0. All experiments were performed in biological triplicates.

2.7 Cellular retention determination via microsphiltration system

The retention of iRBC was quantitated via a microsphiltration system in Dr. Pierre A Buffet's lab at the Pitié-Salpêtrière Hospital, Paris according to a previously described protocol (Deplaine et al, 2011). The microsphiltration device included metal micro-beads, a 1,000 μL anti-aerosol pipette tip (Neptune, BarrierTips), and an electric pump (Syramed μsp6000, Arcomed'Ag). The metal micro-beads (containing 96.50% tin, 3.00% silver and 0.50% copper) in 5-25 μm diameters mimicking the geometry of inter-endothelial splenic slits were manufactured by Industrie des poudres Sphériques, Annemasse, France. Two g of beads of each size was mixed and then suspended in 5 mL RPMI medium supplemented with 10% (v/v) human serum. Eight hundreds μL of the bead suspension was poured into an inverted 1,000 μL anti-aerosol pipette tip and allowed to settle, leading to the formation of a 5 mm-thick bead layer above the anti-aerosol filter.

CS2 wildtype and CS2-ΔPFD parasites were tightly synchronised by 5% sorbitol (see section 2.1.5). Mature parasites were collected through the magnetic cell sorting columns (CS columns; MACS Cell Separation, MiltenyiBiotec) the following day. The parasites were then resuspended in 10 mL warm complete media supplemented with fresh blood. 24 hours later, ~ 3 – 5% rings in 2% haematocrit were observed. The parasitemias were counted on a Giemsa stained thin smear and also by flow cytometry. SYBR® Green I (Invitrogen) was used to stain the parasite's nucleic acids for 15 min which were then counted on a BD Accuri™ C6 Flow Cytometer. The cultures (1 mL / tube) were incubated at 37°C and 41°C for 2 hours before loaded on the micro-bead layer. A flow of 1mL/min was controlled by an electric pump. The bead layer was then washed with 5 mL of 10% human serum in RPMI medium. The

downstream parasites were retrieved and counted by FACS. Parasite retention rate was calculated as a percentage of parasites retained in the micro-beads (retention rate = [input – output] / input * 100, in which input and output were the numbers of parasites loaded and flown through the micro-beads, respectively). Each culture was measured in technical triplicates. A total of 3 biological replicates were performed.

2.8 *Ex-vivo* human spleen perfusion

Isolated-perfused spleen experiments were performed as previously described (Buffet, 2006; Safeukui et al, 2008), in a Plexiglas chamber maintained at 37°C with a regulated warmed airflow. Briefly, a human spleen was connected to a perfusion device, and a progressive warming from 6°C to 10°C to 37°C was performed by increasing the Krebs-albumin medium flow from 1 mL/min to 50 to 150 mL/min over 40 to 60 min. Pressure, haematocrit, K^+, Na^+, glycemia and glucose concentrations were artificially controlled mimicking the conditions in human body. During this adaptation period, the remained RBCs in the spleen were flushed out in order to bring the haematocrit to less than 0.1% at the end of the warming period. Once the spleen temperature reached 35°C, uninfected O^+ RBCs were added (5% final haematocrit) and allowed to circulate for 30 to 60 min. Glucose, Na^+, K^+ concentrations, O_2, CO_2 partial pressures, and pH in the vein, artery, and reservoir were monitored every 10 min using an iStat device (Abbott Laboratories, Abbott Park, IL). At steady state, key physiologic markers were maintained in the following ranges: perfusate flow (0.8 to 1.2 mL/g of perfused spleen parenchyma per min), temperature of the spleen capsule (36.7°C to 37.2°C), Na^+ (135 to 148 mEq/L), K^+ (4 to 5 mEq/L), glucose (4 to 12 mM), pH 7.2 to 7.35, haematocrit (4% to 10%), and arterial-venous oxygen partial pressure decay (60 to 120 mmHg). Finally, the RBCs were rinsed out for 5 to 10 min

by using the Krebs-albumin medium before a mixture of 10-hour ring-iRBCs and 22-hour young troph-iRBCs at 0.2% to 6% parasitemia was introduced into the circulating system for 2 hours. Samples were collected from the reservoir every 20 min. Parasitemias were quantitated on Giemsa-stained thin smears and also by flow cytometry after staining CS2-wildtype parasites with red PKH26 and CS2-ΔPFD parasites with green PKH67 (fluorescent cell linker kit, Sigma). Data were analysed using the CELLQuest software (BD Biosciences).

2.9 Cytoadhesion assay

The adhesion assay was performed as previously described (Boeuf et al, 2011). CS2-ΔPFD and 3D7-ΔPFD and the parental CS2 and 3D7 cell lines were highly synchronised and magnet purified to enrich young trophozoite infected erythrocytes. The iRBCs were diluted to 500 cells / μL for each cell line in complete medium supplemented with 10% heat-inactivated pooled human serum. One hundred μL of the iRBCs were incubated with the stained PKH67 (Sigma) vesicles (prepared by Philippe Boeuf, the University of Melbourne) in a final volume of 150 μL in 96-well U-bottom newborn calf serum-coated culture plates. The plate was gently agitated at RT for 1 hour. Ethidium bromide (100 mg/mL final concentration) was added to stain the parasite's nucleic acids for 15 min before parasites were centrifuged at 500 x *g* for 3 min and washed 3 times with PBS. After being fixed with 0.5% formaldehyde, parasites were counted using a FACSCalibur cytometer. A minimum of 20,000 events was acquired. Percentage of parasite adhesion was calculated as follow:

% adhesion = iRBCs bound vesicles / ΣiRBCs * 100,

in which iRBCs bound vesicles were the number of PKH67 (green) positive / EtBr (red) positive events; and ΣiRBCs were the number of all EtBr (red) positive events.

2.10 Statistical analysis

Data were analysed and graphed using GraphPad Prism 5.0. In microsphiltration and adhesion assays, statistical significance was assessed using two-tailed unpaired Student *t*-test.

Chapter 3

Molecular interactions of a *P. falciparum* exported protein (PFD) in the RBC membrane

Abstract

Hundreds of *Plasmodium falciparum* parasite proteins are exported to the erythrocyte membrane after the invasion of host cells. Virulence proteins are accumulated in the erythrocyte membrane or associated with the erythrocyte cytoskeleton. Consequently, physiology of the host cell membrane is altered, which facilitates the adhesion of the infected cells to the host endothelial cells and thus, their survival in the human body. We found that a novel exported protein - named as PFD - is also localised to the host cell membrane and interacts with one of the known RBC cytoskeletal-binding protein – ring erythrocyte surface antigen (RESA). In order to characterize the molecular interactions of PFD, we investigate the expression, localisation, solubility and interacting partners of the protein. We show that PFD protein is expressed in all asexual parasite stages with a slight increase in ring stage. In microscopy studies, we observed that the protein displays in the iRBC membrane and not in the knob regions. PFD is a peripheral membrane protein and forms a ~ 400 kDa complex with RESA. RESA plays an important role in protecting the ring-iRBC membrane from heat-induced damage. We propose a role for PFD in remodelling the iRBC membrane via interactions with RESA. The findings open new avenues for investigation of the host cell membrane modifications by the malaria parasites.

3.1 Introduction

After invading the RBCs, the parasites establish their own machinery and export hundreds of proteins to the host cytoplasm. The infection thus leads to the dramatically changed structural and functional properties of the RBCs that include decreased deformability and the formation of knobs at the host cell surface. Consequently, the RBCs become rigid and cytoadhesive to the vascular endothelium (see (Cooke et al, 2001; Cooke et al, 2004) for review), which facilitates the parasite sequestration in many organs and causes the most severe complications (Miller et al, 2002).

The exported proteins implicated in the cytoadherence mechanism are mainly associated with the erythrocyte membrane and cytoskeleton (Cooke et al, 2001; Cooke et al, 2004). Identified cytoskeleton binding proteins include the knob-associated histidine-rich protein (KAHRP) (Biggs et al, 1989; Crabb et al, 1997), *P. falciparum* erythrocyte membrane protein 1 (PfEMP1) (Scherf et al, 2008), the ring-parasite-infected erythrocyte surface antigen (RESA) (Mills et al, 2007), the mature-parasite-infected erythrocyte surface antigen (MESA) (Black et al, 2008) and *P. falciparum* erythrocyte membrane protein 3 (PfEMP3) (Glenister et al, 2002). As mentioned in the chapter 1, all these proteins are exported and transported to the erythrocyte membrane via the signal sequence and PEXEL or in the case of PfEMP1 with a PEXEL-like motif. While PfEMP1 contains a C-terminal transmembrane domain (TMD), the others do not possess any TMD sequences and are identified as proteins associated with the RBC cytoskeleton (Favaloro et al, 1986; Lustigman et al, 1990; Pasloske et al, 1993; Pologe et al, 1987). Any disruptions in the interactions between these parasite proteins and the erythrocyte membrane cytoskeleton lead to a

reduced cytoadherence of the iRBCs to the host cell (Cooke et al, 2002), reduced rigidity of the iRBCs membrane (Glenister et al, 2002), lack of knobs in the iRBCs surface (Crabb et al, 1997), blocking the transportation of PfEMP1 (Waterkeyn et al, 2000) and inhibition of parasite growth at heat-shock condition (Silva et al, 2005). Thus, there is no doubt that the cytoskeletal parasite proteins play various important roles in supporting the parasite survival, parasite cytoadherence and sequestration in human organs.

Despite the fact that several recent studies are focusing on these cytoskeleton parasite proteins, most of their functional mechanisms are still unknown since only a few of them have been characterizing. In order to contribute to our understanding of the important aspect, we are interested in characterizing the molecular interactions of an exported protein called PFD - encoded by *PFD1170c* gene. Similar to PfEMP1, the protein sequence is found only in *P. falciparum*, suggesting that its function might also be *P. falciparum* specific. In addition, this molecule shows a high sequence homology with RESA and hence it is called RESA-like protein (Lanzer et al, 2005; Vincensini et al, 2005; Wu & Craig, 2006). Interestingly, both molecules belong to the *Plasmodium* helical interspersed subtelomeric (PHISTb) family protein (Sargeant et al, 2006). As shown in chapter 1, the PFD protein contains a signal sequence, a PEXEL motif in the N-terminus and a PHISTb domain in the C-terminus which may play an important role in protein-protein interactions and host erythrocyte remodelling (Marti et al, 2005). Furthermore, in a large scale functional screen of knock-out parasites, the deletion of PFD resulted in a reduction of ~ 50% adherence of the iRBCs to CSA under a physiological flow condition, although transportation of PfEMP1 and expression of KAHRP were normal (Maier et al, 2008). The authors also showed the molecule may be involved in knob formation since the PFD disrupted

cells lacked knobs on the surface via scanning electron microscopy (SEM) and exhibited no rim fluorescence of KAHRP on the iRBCs via immunofluorescence assay (IFA) (Maier et al, 2008). It is thought that PFD might support the KAHRP transportation to the erythrocyte membrane and hence the knob formation is altered in its absence (Maier et al, 2008). However, in order to clarify the functions of the protein and to gain a deeper understanding of the molecular mechanisms in which it is involved, more experimental evidences are required. We propose that the PFD protein may play a role in remodelling the iRBCs membrane via interactions with other parasite proteins. To test this hypothesis we generated antibodies recognizing PFD, *P. falciparum* transfectants lacking the expression of the protein and transfectants expressing GFP tagged version of the PFD molecule. Fractionation, immune-precipitation (IP) and blue native – polyacrylamide gel electrophoresis (BN-PAGE) experiments were performed to investigate the protein expression level, localisation, solubility and its interacting partners.

3.2 Results

3.2.1 Expression of PFD protein and generation of antibodies against PFD

PFD1170c (or *PFD*) is a single-copy 1.1 kb gene, comprising of 2 exons located on chromosome 4 of the *P. falciparum* genome. We generated glutathione S-transferase (GST) tagged PFD fusion proteins in *E. coli* and purified them for antibody production. Two fragment proteins were designed: one represents the N-terminal of PFD starting after PEXEL (aa 91 - 190, fragment A); the other is the C-terminal (aa 191 - 309). The sequences were amplified and cloned into the pGEX-4T-1 expression vector (Appendix 3, supplementary Figure S1, S2, S3, S4). Upon IPTG induction, only fragment A (~ 37 kDa) could be expressed in *E. coli* BL21 bacteria and

subsequently purified with more than 80% purity (Figure 3.1). The lower band of ~ 27 kDa was the GFP itself.

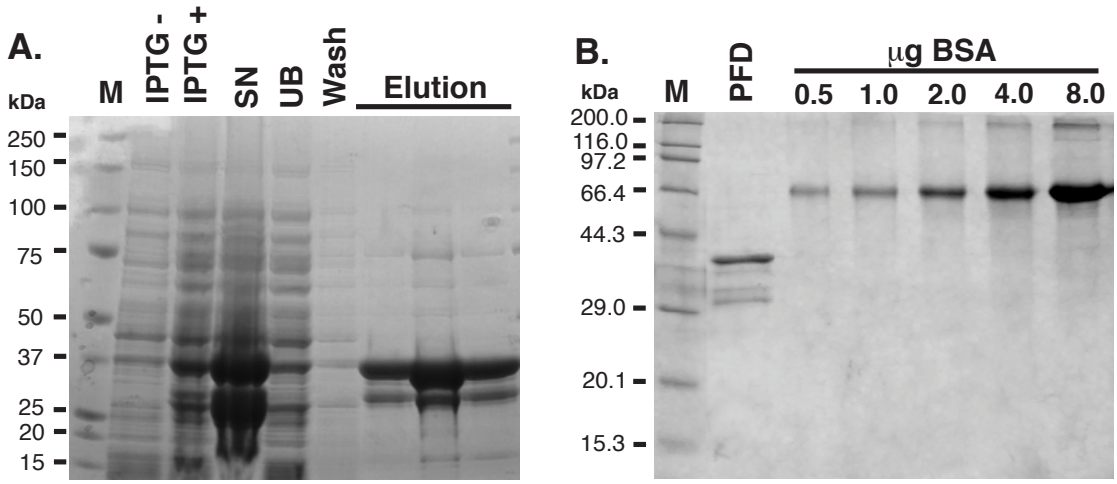

Figure 3.1. Generation of anti-PFD antibodies. (A) Expression of GST tagged PFD-A in *E. coli* BL21. PFD-A-GST protein was expressed in *E. coli* BL21 with 0.1 M IPTG induction. The fusion protein was purified by Glutathione Sepharose 4B resin (1 mL resin/1 L bacteria culture) and eluted in 3 fractions (10 mL/each). M, molecular weight marker (Bio-Rad). UB, unbound. SN, supernatant. **(B)** The protein concentration was estimated by comparing to the quantity of BSA loaded (0.5 μg to 8.0 μg). One μL of the purified PFD protein was loaded. The protein purity was higher than 80% and the protein concentration was approximately 1 mg/ml, respectively. M, molecular weight marker (Invitrogen).

The purified fusion protein was then injected to rabbits for anti-PFD antibody production. The rabbit anti-PFD antibodies were evaluated by Western blot analysis on the uninfected RBCs, CS2 wild-type, GFP tagged PFD and PFD knock-out parasites materials (Figure 3.2). The results indicated that the antisera could be used to specifically detect PFD at ~ 28.5 kDa in CS2 wild-type and PFD-GFP at ~ 52 kDa band in CS2-PFD-GFP parasite samples (also detected with anti-GFP antibodies). The specific bands were absent when prebleed antisera, the uninfected RBCs or PFD knock-out extracts were used. Having loaded excess material for the CS2-WT cells could have increased the number of non-specific bands that were detected in the blot by probing the membrane with the PFD antibodies. The optimal signal to noise ratio

was achieved by diluting the antibodies 1: 3000, as determined in serial dilutions. Hence, from here onwards this antibody concentration was applied for further Western analysis.

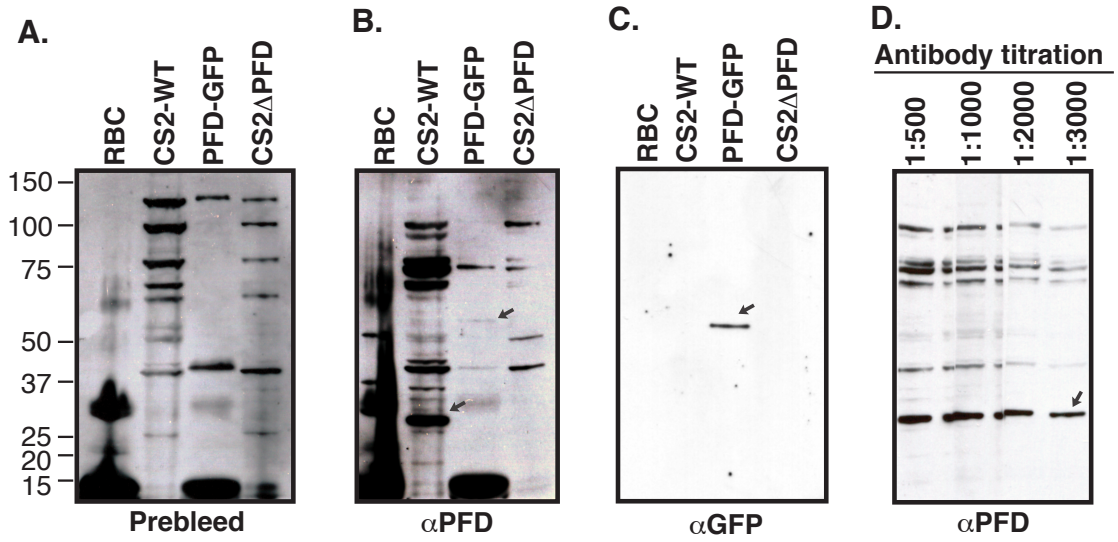

Figure 3.2. Quality control of anti-PFD antibodies. RBCs, CS2-wildtype, CS2-PFD-GFP and CS2-ΔPFD extracts were used to distinguish the specific band of PFD protein from other non-specific bands. Five µL of these samples were loaded. **(A)** Prebleed sera (dilution 1:500) were used as a negative control. **(B)** Antibodies against PFD (region A) (dilution 1:500) were used to detect expression of PFD in CS2-wildtype. **(C)** Antibodies against GFP (dilution 1:1000) were used to detect expression of PFD in CS2-PFD-GFP parasites (arrows show the specific bands) but not in the uninfected RBCs and CS2-ΔPFD extracts. **(D)** Antibodies against PFD worked well at up to the dilution of 1: 3000.

To determine whether the anti-PFD antibodies are suitable for immunofluorescence assay (IFA), we performed an IFA on the PFD-GFP parasites (the PFD-GFP cell line will be mentioned in section 3.2.2) by labelling the cells (RBCs and iRBCs) with anti-GFP (represented in green fluorescence) and anti-PFD antibodies (represented in red fluorescence). It is clearly seen that although the red pattern of PFD was also shown in rim fluorescence similar to the green pattern of PFD-GFP, there were also non-specific fluorescence on the uninfected RBCs membrane when using the anti-PFD antibodies from dilution of 1:20 up to 1:3000 (Figure 3.3). Therefore, the anti-GFP

antibodies were used to detect PFD-GFP fluorescence in IFA instead of the PFD antibodies.

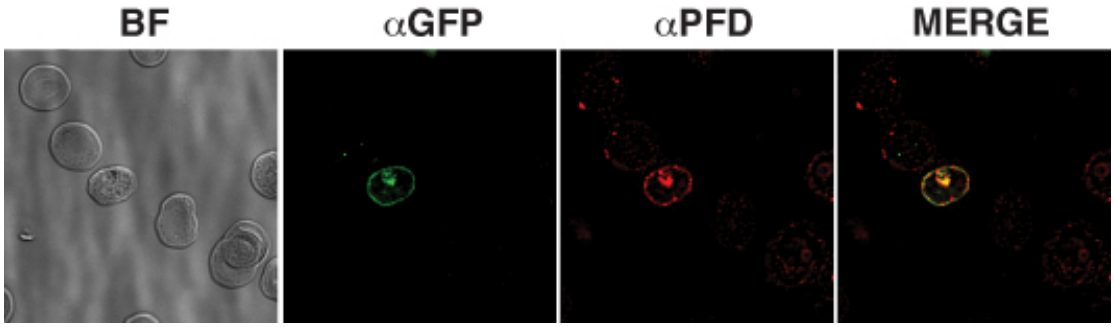

Figure 3.3. Anti-PFD antibodies cross-react with uninfected RBC proteins. A transgenic PFD-GFP line was used to examine the specificity of the PFD antibodies compared to the anti-GFP antibodies in immunofluorescence assay. The PFD antibodies were titrated from 1:20 to 1:3000 to optimize the antibodies titration for IFA. The image was observed with the 1:3000 dilution of the antibodies. BF, bright field. αGFP, rabbit anti-GFP antibodies. αPFD, rabbit anti-PFD antibodies.

3.2.2 PFD is expressed in all asexual blood stages

In order to monitor expression of the PFD protein we used a 3' replacement strategy to generate CS2 parasites expressing PFD protein fused to a green fluorescent protein (GFP). This resulted in the expression of this chimeric protein under the control of the endogenous PFD promoter.

Asexual parasite infected cells were collected 6 hours apart over 42 hours after double sorbitol synchronization (see section 2.1.5) and treatment with tetanolysin to lyse the uninfected RBCs (see section 2.1.6). Protein extracts derived from 10^6 iRBCs were loaded onto SDS-PAGE. Western blot analysis using anti-GFP antibodies reveals that the chimeric protein of approximately 52 kDa could be detected in all asexual parasite stages with a slight increase in expression in ring stages (Figure 3.4A).

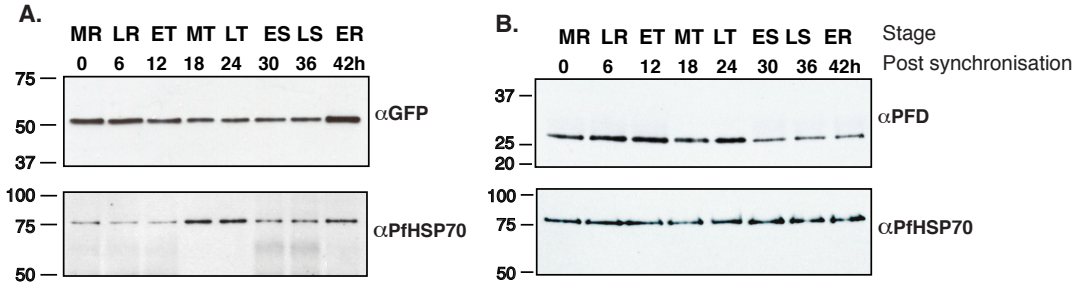

Figure 3.4. PFD is expressed in all asexual blood stages with a slight increase in rings. Time-course of the PFD expression over a 42 h period. PFD-GFP (A) and wild-type (B) parasites were synchronized by two consecutive sorbitol treatments 4 h apart (time zero corresponds to the second sorbitol lysis), collected 6-hour apart and tetanolysin lysed. Tetanolysin lyses the non-infected erythrocyte membrane, hence the treated samples contained the iRBCs only. The membrane was probed with anti-GFP antibodies to detect a chimera PFD-GFP (~ 52 kDa) in PFD-GFP cells (A, top panel) or anti-PFD antibodies to detect PFD (~ 26 kDa) in wild-type cells (B, top panel). Anti-PfHSP70 antibodies (bottom panel) served a control for differences in loading. Stages were determined optically by Giemsa stained smears. MR, mid ring. LR, late ring. ET, early trophozoite. MT, mid trophzoite. LT, late trophozoite. ES, early schizont. LS, late schizont. ER, early ring.

The membrane was stripped and re-probed with antibodies against PfHSP70 (PlasmoDB accession number PF08_0054) to control for the loading. Expression of the house-keeping gene PfHSP70 gradually increased during the development of the asexual parasites (Le Roch et al, 2004). The loadings in this experiment are quite equal among the stages with the increased expression of PfHSP70. In order to confirm the expression of PFD, a similar experiment was performed on the parental CS2 wild-type parasite extracts using anti-PFD antibodies and a similar pattern of expression was observed (Figure 3.4B).

3.2.3 PFD localises to the membrane of the iRBCs

To determine the localization of PFD, live cell fluorescence microscopy was performed on the CS2-PFD-GFP cells. GFP fluorescence accumulated in the host cell membrane (Figure 3.5). A fluorescence signal was also found in the parasite cytoplasm at early ring stage. The result indicates that the PFD protein might be synthesized at the early stages in order to be exported in the later stages of the parasite asexual life-cycle.

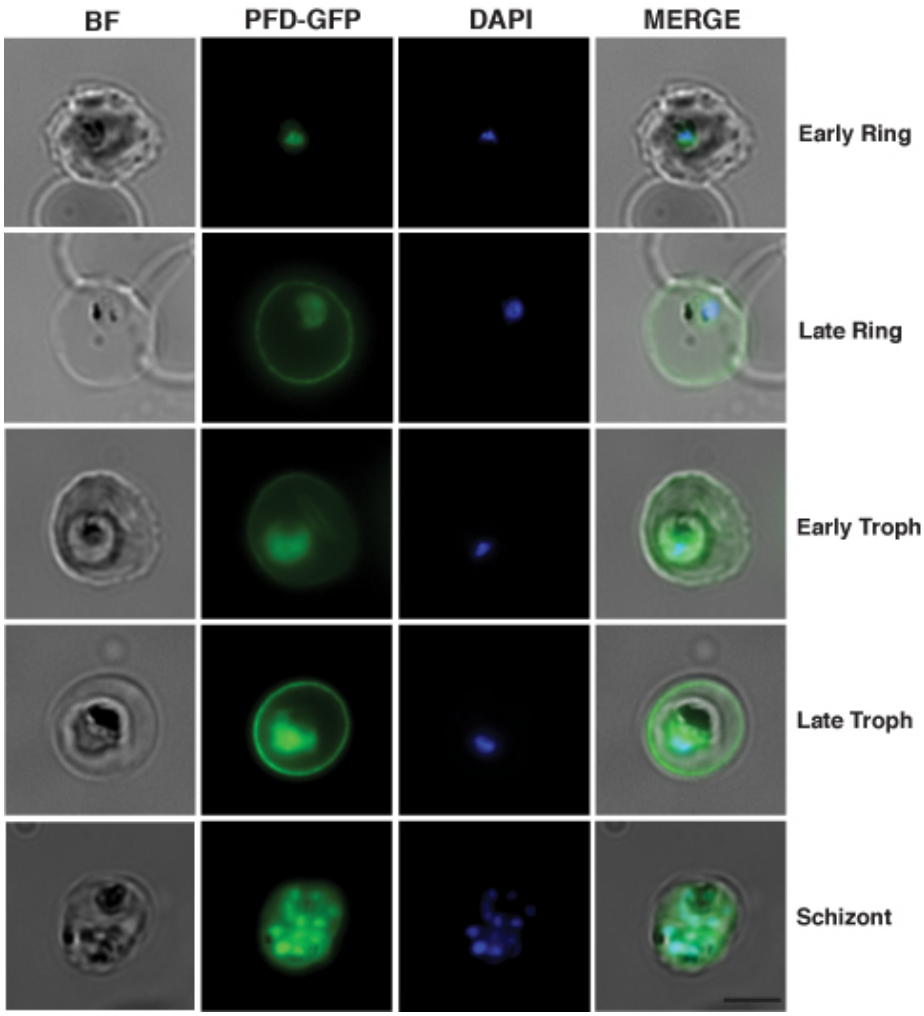

Figure 3.5. PFD localises to the host cell membrane and parasite cytoplasm. Live cell fluorescence microscopy of cells expressing GFP tagged PFD was performed at different stages of asexual cycle. Pictures were taken at the same setting of light intensity and exposure time. The parasite DNA was labelled by DAPI. BF, bright field. Scale bar: 5 μm.

To localize the GFP signal in relation to other exported proteins that are involved in RBC remodelling, the PFD-GFP expressing parasites were used in the IFA (Figure 3.6). Immunofluorescence assays were performed using anti-GFP (green) antibodies for PFD, anti-PfEMP1, anti-KAHRP, anti-PfEMP3, anti-MESA and anti-RESA (red) antibodies. PfEMP1 and KAHRP accumulated in several punctae on the infected erythrocyte membrane, which is consistent with their localisation in knob protrusions. In contrast, PFD showed rim fluorescence but the signal was more proximal to the cell in comparison to the KAHRP signal. This suggests a location of PFD could be in or underneath the RBC membrane. PfEMP3 and MESA showed a partial overlay (yellow) with PFD (Figure 3.6, row 3 and 4). Only RESA completely overlaid with PFD suggesting that PFD might locate to the erythrocyte cytoskeleton, which was observed for RESA (Da Silva et al, 1994; Foley et al, 1991; Silva et al, 2005).

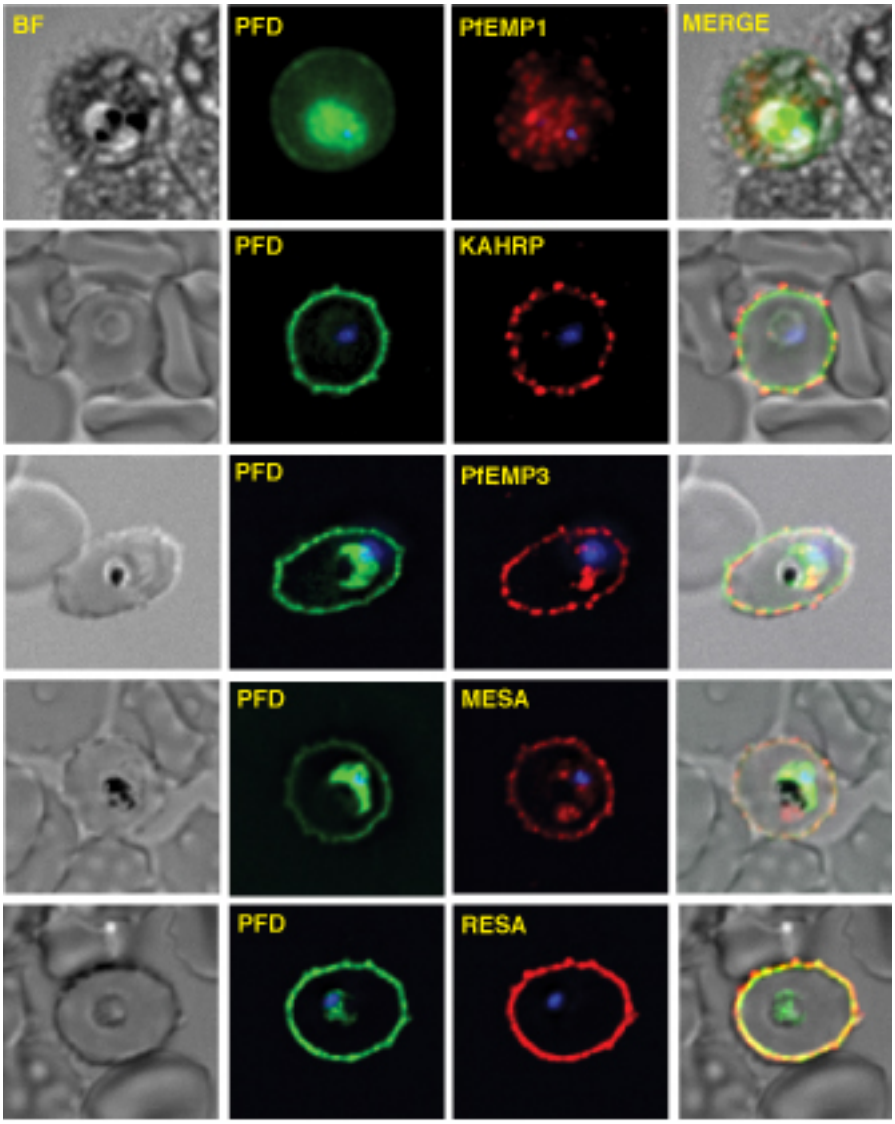

Figure 3.6. Localisation of PFD in relation to other known exported proteins associated with the erythrocyte cytoskeleton and membrane. PFD signal is overlaid with RESA. Immunofluorescence microscopy of paraformaldehyde/glutaraldehyde fixed CS2-PFD-GFP parasites was performed using anti-GFP (green), anti-PfEMP1, anti-KAHRP, anti-PfEMP3, anti-MESA and anti-RESA (red) antibodies at the same setting of light intensity and exposure time. The parasite DNA was labelled by DAPI (blue). BF, bright field. Scale bar: 5 µm.

In an effort to further elucidate the location of PFD in the iRBC membrane, an immune electron microscopic (EM) analysis of CS2-PFD-GFP cells was performed using anti-GFP antibodies. The cells were pre-embedded and treated with Equinatoxin to remove haemoglobin in order to get a clear background in the erythrocyte cytosol for later labelling with gold-conjugated anti-rabbit IgG (Hanssen et al, 2008). The EM

image shows that gold particles labelled PFD located to the erythrocyte membrane but not to the knob regions (Figure 3.7).

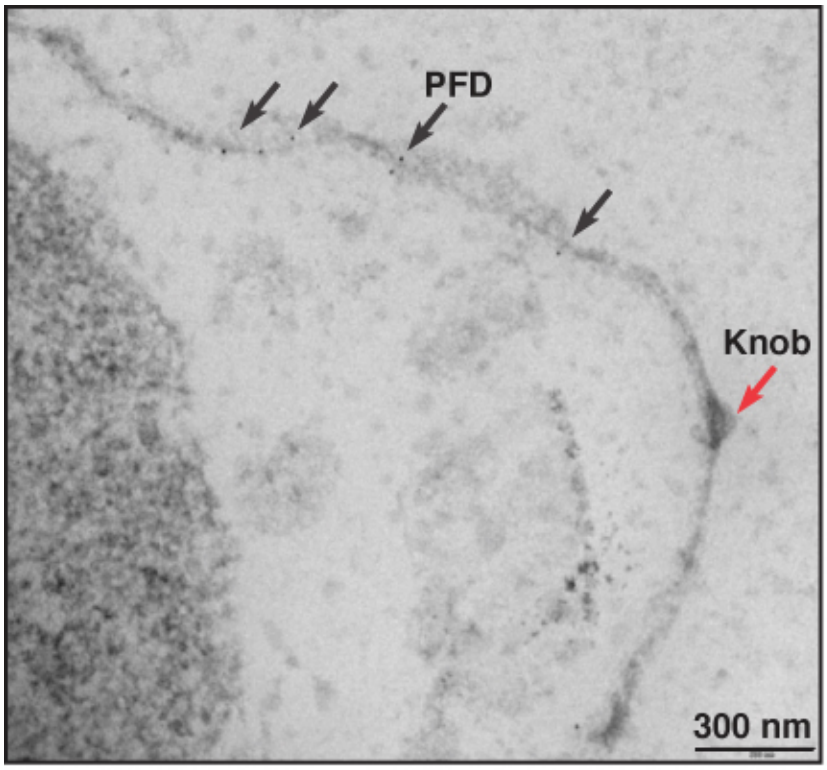

Figure 3.7. PFD-GFP located to the erythrocyte membrane and not in knob protrusions. Immuno electron microscopy of CS2-PFD-GFP parasites was performed using anti-GFP by Eric Hanssen, Bio21 Institute. The cells were permeabilized by Equinatoxin and incubated with primary rabbit anti-GFP antibodies and fixed with gold-conjugated anti-rabbit IgG. Black arrow indicates the gold particles labelled PFD and red arrow indicates knob. Scale bar: 300 nm.

3.2.4 PFD is not transported via Maurer's clefts (MC).

PFD had been predicted to be a novel protein in MC via a global proteomic analysis of ghost fraction from *P. falciparum*-infected erythrocytes (Vincensini et al, 2005). The ghost fraction included the RBC membrane, the RBC cytoskeleton and the MC. Of 78 candidates identified, 7 are MC proteins. The others including PFD are still unknown. In order to clarify the question whether PFD has any transient association with the MC, immunofluorescence assays had been performed on the CS2-PFD-GFP

cells to localize PFD with a known MC protein, ring exported protein 1 (REX1) (Dixon et al, 2008a). The result showed that PFD signal is not overlaid with REX1 signal (Figure 3.8), suggesting that PFD could diffuse across the erythrocyte cytosol and then bind to the erythrocyte membrane directly.

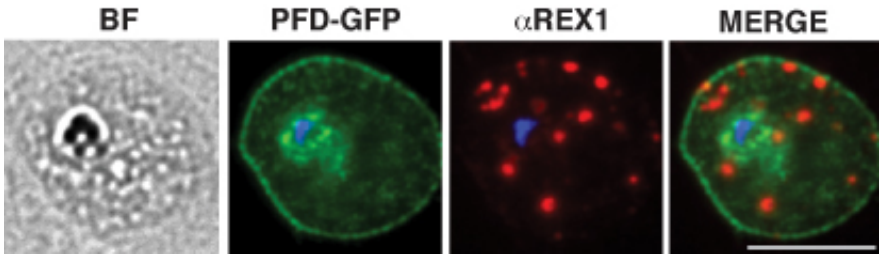

Figure 3.8. PFD does not co-localise with REX1 (ring exported protein 1). Immunofluorescence microscopy of aceton/methanol fixed cells was performed using anti-REX1 antibodies. REX1 resides in MC's cleft membrane. Mouse antibodies anti-REX1 (1:2000) (a gift from Matthew Dixon, University of Melbourne) was used to label the transgenic CS2-PFD-GFP cell line.

3.2.5 PFD is a peripheral membrane protein

In order to further study the localisation of PFD, parasitized RBCs were fractionated by saponin, Triton X-100, Triton X-114 and sodium carbonate. Erythrocyte membrane and parasitophorous plasma membrane (PVM) of CS2-PFD-GFP cells were lysed with saponin to allow a separation of the RBCs cytosol and the soluble content of the parasitophorous vacuole (PV) (called supernatant fraction – S) from intact parasites, PVM and erythrocyte membranes (called pellet fraction – P) (Ansorge et al, 1996; Siddiqui et al, 1979). Western blot analysis was performed on these two fractions using anti-GFP (to detect PFD), anti-PfHSP70 (a soluble marker for parasite cytosol (Joshi et al, 1992; Kappes et al, 1993)) and anti-EXP1 (insoluble transmembrane protein in the PVM (Günther et al, 1991)) antibodies (Figure 3.9). PFD-GFP protein was mainly present in the pellet fraction, indicating that PFD location is restricted to intact parasites, PVM and/or the erythrocyte membranes. This

result is consistent with the localisation of PFD seen under the microscope. A far less abundant 52 kDa band representing PFD-GFP protein detected in the supernatant fraction indicates that a small amount of PFD might also be present in PV or erythrocyte cytoplasm during trafficking process.

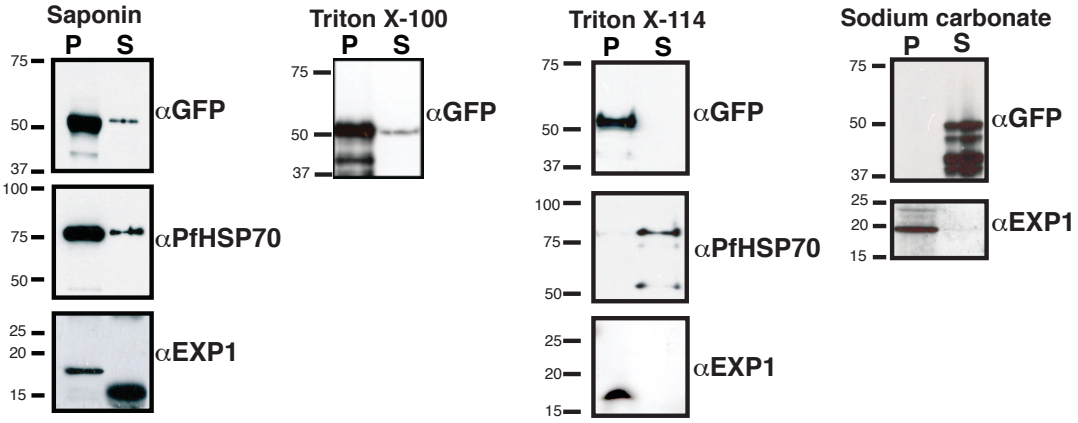

Figure 3.9. Fractionation of PFD-GFP cells by different detergents to examine the characteristics of PFD protein. PFD-GFP parasites were magnet purified and lysed by saponin, Triton X-100, Triton X-114 or carbonate extraction. Supernatant and pellet fractions were separated by centrifugation and resolved in 4 -12 % SDS-PAGE. The gels were transferred onto nitrocellulose membrane and probed with antibodies against GFP, PfHSP70 or EXP1. PFD is an insoluble protein in saponin, Triton X-100 and Triton X-114 but soluble in sodium carbonate, suggesting that PFD is a peripheral membrane protein. The lower band of ~15 kDa (bottom panel of saponin lysis) could be the N-terminal protected peptide of EXP1 that is exposed to the lumen of PV (Günther et al, 1991). It is possible that the intact EXP1 protein was digested by the parasite endogenous proteases (Günther et al, 1991) and the N-terminal fragment faced to the PV therefore it was detected in the supernatant sample when probing with anti-EXP1.

In order to examine whether PFD is membrane-associated protein, the CS2-PFD-GFP pellet fraction from saponin lysis was subjected to extraction with equilibrated Triton X-114 (TX-114) to separate detergent phase (P fraction) and aqueous phase (S fraction) (Figure 3.9). The P fraction contained membrane proteins including membrane-associated, hydrophobic and amphipathic proteins whereas the S fraction contained hydrophilic proteins (Bordier, 1981; Mattow et al, 2007; Punjabi & Traktman, 2005). EXP1, a *P. falciparum* integral membrane protein served as a

control for the pellet fraction (Günther et al, 1991) while PfHSP70, a soluble parasite protein, served as a control for the supernatant fraction (Joshi et al, 1992; Kappes et al, 1993). The result showed that PFD-GFP was only present in pellet fraction, suggesting that PFD is membrane-associated. The data is consistent with the insoluble profile of PFD in Triton X-100 (TX-100) (Figure 3.9).

In order to clarify whether PFD is a peripheral or an integral membrane protein, the saponin lysed CS2-PFD-GFP cells were incubated with a high ionic strength buffer (Na_2CO_3, pH 11.5) (Fujiki et al, 1982) followed by high-speed sedimentation centrifugation. The transmembrane proteins were spun down in the insoluble fraction (P) whereas peripheral membrane proteins and soluble proteins were in the supernatant fraction (S). The result (Figure 3.9) showed that PFD-GFP protein was present in the supernatant, while EXP1 remained in the pellet, suggesting that PFD is a peripheral membrane protein. This is consistent with the fact that PFD does not contain a transmembrane domain while EXP1 contains the domain (Appendix 3, supplementary Figure S8).

3.2.6 PFD interacts with RESA to form a ~ 400 kDa complex

The identification of interacting partners could give clues on the function and molecular mechanism of PFD that might be similar to those of its partners. In order to precipitate complexes containing PFD and its possible partners without interfering its nature, we simultaneously screened the solubility of PFD-GFP in detergents belonging to 3 different groups including non-ionic (OGP, OTGP, NP-40, Digitonin and Triton X-100), ionic (DOC) and Zwitterionic detergents (CHAPS, Zwittergent 3-14). Non-ionic detergents break up lipid-lipid and lipid-protein interactions and hence solubilize membrane proteins in a gentler manner. Ionic detergents possess the net charge in the head groups. On the other hand, Zwitterionic group combines the properties of ionic and non-ionic detergents (Jones et al, 1987). Non-ionic detergents are less effective in solubilizing hydrophobic proteins while Zwitterionic detergents such as CHAPS and Zwittergent 3-14 provide higher solubilisation efficiency (Luche et al, 2003) with the later being more stringent than the former. In the first screen, we used a mild detergent concentration of 1% for all detergents in order to maintain the specific protein-protein interactions. The abundance of PFD-GFP band in the supernatant (S) fraction increased from ~10% in non-ionic detergents to 50% in ionic detergents whereas the solubility of PFD protein increased to 70%-90% in CHAPS and Zwitterent 3-14 detergents (Figure 3.10). The combination of non-ionic and ionic properties in Zwitterent 3-14 detergent gave the best efficiency to solubilize PFD-GFP protein. The Zwittergent 3-14 was used in the immunoprecipitation (IP), pull-down and BN-PAGE experiments for further investigations of PFD's partners.

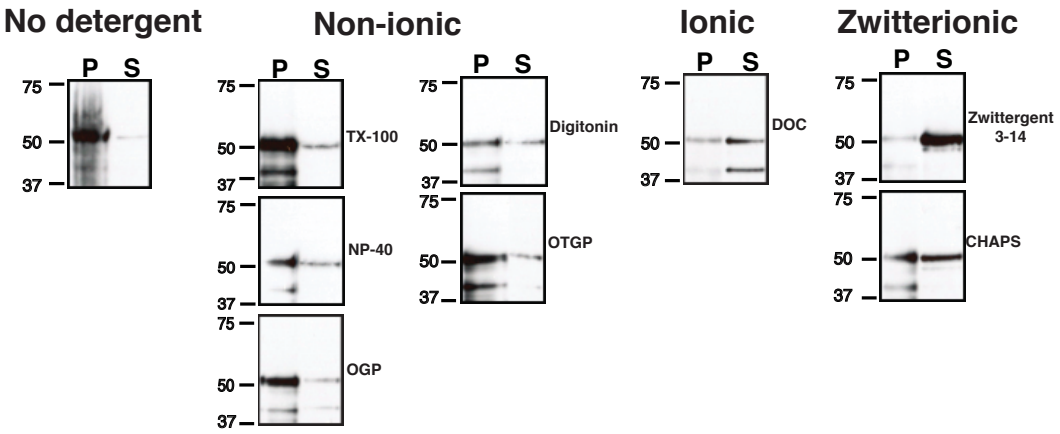

Figure 3.10. Solubility of GFP tagged PFD protein was examined by a range of detergents. The saponin-lysed CS2-PFD-GFP samples were incubated with solubilisation buffer without detergent as a control and with 1% of the following detergents: TX-100, Triton X-100; NP-40, nonyl pheroxy-polyethoxylethanol NP-40; OGP, n-Octyl-β-D-glucopyranoside; Digitonin; OTGP, n-Octyl-β-D-thioglucopyranoside; DOC, Deoxycholic acid, Zwittergent 3-14, n-Tetradecyl-NN-dimethyl-3-ammonio-1-propanesulfonate; CHAPS, 3-[(3-cholamidopropyl) dimethylammonio]-1-propanesulfonate. PFD-GFP protein in the soluble (S) and insoluble (P) fractions was detected by immunoblotting using antibodies against GFP.

In order to identify the interacting partners of PFD, we performed co-immunoprecipitation (co-IP) analysis on the CS2-wildtype cells. The iRBCs were collected by magnet purification at early/mid trophozoite and mid/late trophozoite stages. Co-IP allows us to co-precipitate proteins interacting with the protein that the antibody recognizes. The first immunoprecipitation (IP) was established by using anti-PFD antibodies to precipitate PFD's complexes. The pre-clear and pre-bleed antisera were loaded to evaluate non-specific bindings of other proteins in lysate (input) and non-specific antibodies to resin. The precipitated protein complexes were denatured and subjected to immunoblottings using anti-RESA, MESA, KAHRP, PfEMP1 and PfEMP3 antibodies to identify possible interactions of PFD with these known exported proteins. Only RESA (155 kDa) was clearly found in a complex precipitated with anti-PFD antibodies (Figure 3.11A and Appendix 3, supplementary Figure S9), indicating that RESA could bind to PFD. The interaction was confirmed

by the reciprocal co-IP in which anti-RESA antibodies were used to precipitate RESA containing complex followed by immunoblotting using anti-PFD antibodies. The result showed that PFD (~ 30 kDa) was detected in fraction precipitated by anti-RESA antibodies (Figure 3.11B). The abundance of both RESA and PFD detected in these co-IP experiments was higher in young-trophozoite extract than in late-trophozoite, suggesting that the interactions between PFD and RESA might happen more abundantly in earlier stages; and reduce in the later stages of the parasite erythrocytic life-cycle.

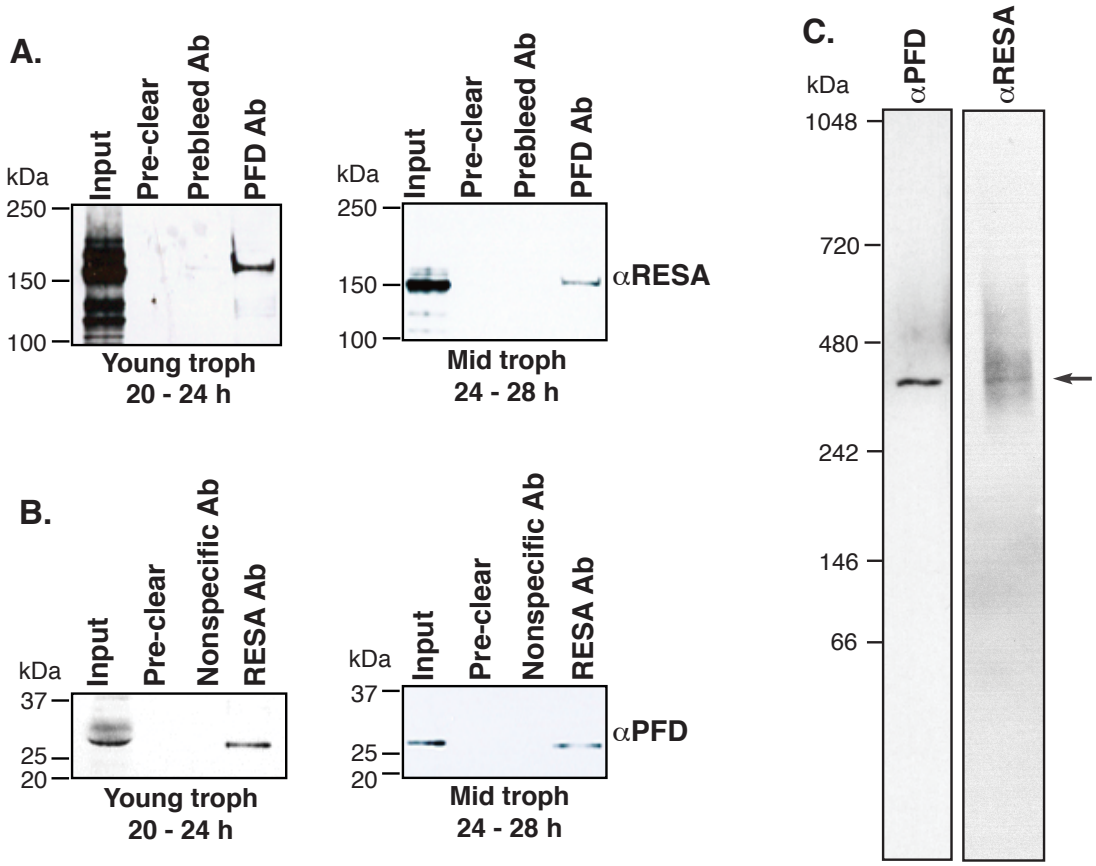

Figure 3.11. PFD interacts with RESA to form a complex of approximately 400 kDa. Co-Immunoprecipitation assay was performed on 1% Zwittergent 3-14 lysed CS2-wildtype cells at young troph (20 – 24 h) and mid troph (24 – 28 h) stages. Anti-PFD antibodies were used to precipitate PFD complexes **(A)** and anti-RESA antibodies were used to precipitate RESA complexes **(B)**. The immunoblottings of precipitated complex were performed using anti-RESA and anti-PFD antibodies. Input, parasite lysate before IP; Pre-clear, precipitation without using antibodies; Pre-bleed Ab, precipitation with pre-bleed antisera (before immunisation); Non-specific Ab, precipitation with non-

specific antibodies. **(C)** BN-PAGE analysis was performed on young trophozoite parasites lysed with 1% Zwittergent 3-14 and the immunoblottings were performed using anti-RESA and anti-PFD antibodies. PFD and RESA are both present in a complex of ~ 400 kDa.

To investigate the native complex of PFD and RESA, we performed BN-PAGE on the young trophozoite cells. Three hundred μg of 1% Zwittergent 3-14 solubilized proteins were loaded onto a 4% - 16% BN-PAGE gel and subjected to immunoblotting using anti-PFD and anti-RESA antibodies. The result showed that both PFD and RESA were present in complexes of 400 kDa (Figure 3.11 C).

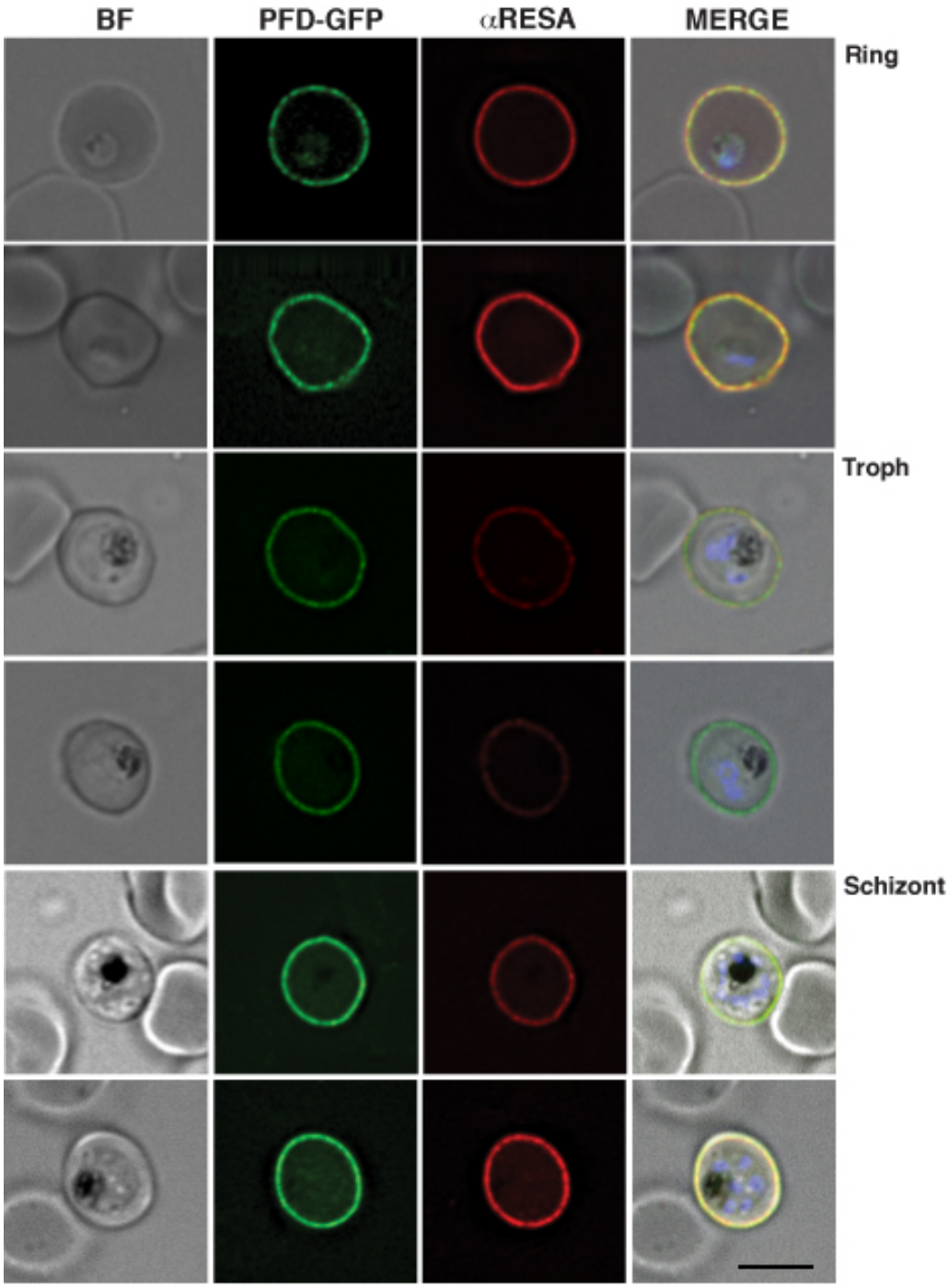

Figure 3.12. RESA is highly expressed and co-localized with PFD at ring and late schizont stages. Immunofluorescence microscopy was performed on paraformaldehyde/glutaraldehyde fixed GFP tagged PFD parasites in different asexual blood stages using anti-GFP (Green) and anti-RESA (Red) antisera at the same setting of light intensity and exposure time. The nuclei were visualised with DAPI (Violet). BF, bright field. Scale bar: 5 μm.

To compare the localization of PFD and RESA from ring to schizont stages, we performed the immunofluorescence assay on the PFD-GFP cells (Figure 3.12). Labelling of the cells with anti-GFP antibodies showed the constant expression of PFD protein (green) throughout the asexual stages, while a faint signal of RESA protein (red), when anti-RESA antibodies were used to label the cells, was seen in the trophozoite infected RBCs. Both signals were rim fluorescence and almost overlayed in ring and late schizont stages (yellow patterns). The data is consistent with the RESA expression profile in previous studies (Foley et al, 1991; Le Roch et al, 2004; Rug et al, 2004) and the higher amount of PFD and RESA proteins detected in younger trophozoite stage in the co-immunoprecipitation assays (Figure 3.11 A and B).

In order to identify additional components of the PFD complex, we generated parasites in which the endogenous *PFD1170c* was tagged at the 3' terminus with 3 x hemagglutinin epitope tags (HA) and streptavidin (STREP) (Figure 3.13A). The integration event of the 3 x HA / STREP tag to the PFD gene locus and the chimeric expression proteins were confirmed by Southern blot analysis (Figure 3.13B) and Western blot analysis (Figure 3.13C). The PFD-HA/STREP protein of ~ 37 kDa was detected using anti-HA and anti-STREP antibodies (Figure 3.13C).

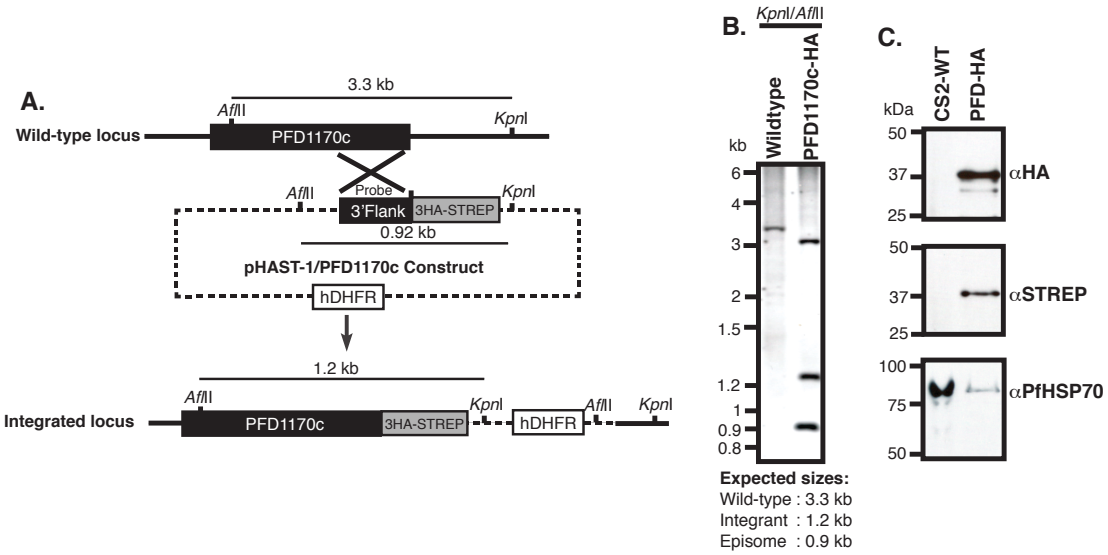

Figure 3.13. Generation and analysis of transgenic *P. falciparum* CS2 expressing a HA-STREP integrated PFD chimera. (A) Schematic representation of the integration plasmid used to generate the 3HA-STREP tagged *PFD1170c* parasites and the target locus for genomic integration by single crossover (not scaled). The plasmid used contained the *HA-STREP* sequence following the 3' coding region of *PFD1170c* gene and *hDHFR* selection cassette. Black box, *PFD1170c* coding region; open box, *hDHFR* selection cassette; grey box, 3HA-STREP. **(B)** Southern blot analysis of digested genomic DNA from wild-type and 3HA-STREP tagged *PFD1170c* parasites demonstrated the correct integration of 3HA-STREP into *PFD1170c* locus. **(C)** Western blot analysis of the expression of 3HA-STREP tagged PFD1170c in the transgenic parasites. The fusion protein in the transgenic cell line was detected using antibodies against HA and STREP. Antibodies against PfHSP70 were used as a control for the amount of protein loaded.

Large-scale pull-down on the CS2-PFD-HA cell line by using anti-HA affinity matrix (Roche) was performed. Three independent experiments were performed on the CS2-PFD-HA and CS2-wildtype cells. The representative result of the Western blot and silver gel analysis confirmed the target PFD-HA protein was efficiently precipitated (Figure 3.14). Using the monoclonal anti-HA antibody on the Western blot analysis, the PFD proteins were only detected in the input (before pull-down) and the eluted samples of the HA tagged PFD cell line, but not in the wild-type samples (Figure 3.14A). The eluted samples from the two cell lines were subjected to denatured SDS-PAGE followed by silver staining. As a result, a specific ~ 35 kDa band of PFD-HA protein (black arrow) was observed in the PFD-HA cells but not in the parental CS2

cells (Figure 3.14B). By comparing the silver-stained protein pattern of the PFD-HA cells with the nonspecific precipitated proteins derived from the wild-type extract, we found that other proteins of approximately 27 and 30 kDa (brown arrows) were also present in the elution of the CS2-PFD-HA cells, but not in the wild-type (Figure 3.14B).

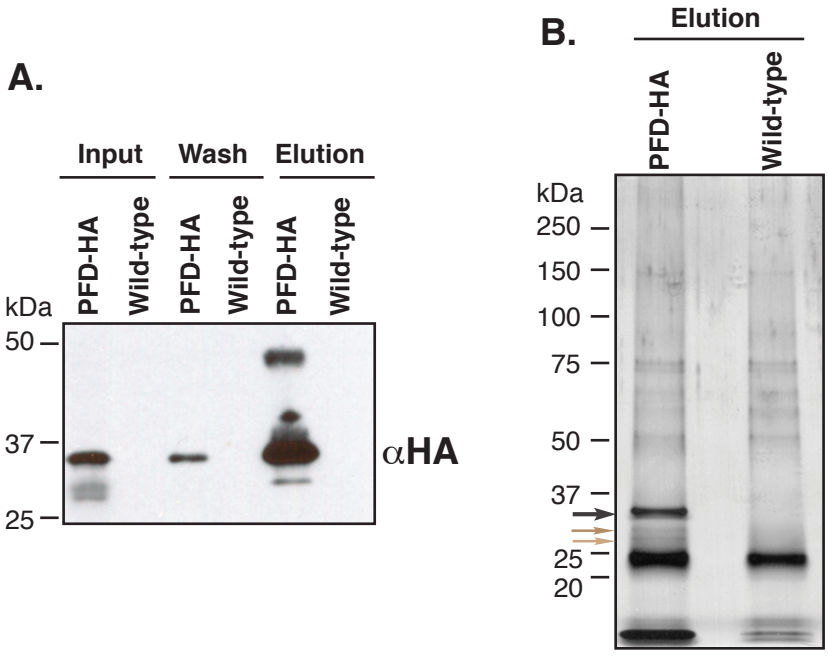

Figure 3.14. Pull-down of PFD-HA complex visualized by silver gel staining. (A) Pull-down assay was performed on the CS2-PFD-HA and CS2 wild-type cells at young trophozoite stage. Each sample was harvested from 6 x 30 mL *P. falciparum* culture with 4% haematocrit and ~ 5% parasitemia. The immunoblotting of denatured precipitated complex was performed using monoclonal anti-HA antibody. Input, parasite lysate before pull-down; Wash, the supernatant of unbound proteins; Elution, PFD-HA and its potential interacting proteins binding to resin. The target band of PFD-HA was observed at ~ 35 kDa in the lanes of HA-tagged samples. **(B)** The elution samples of HA tagged PFD and wild-type cell lines were analysed on a high sensitive silver gel staining. The specific band of PFD-HA (black arrow) was seen in the lane of HA-tagged elution. Brown arrows indicate unknown proteins, which are only detected in CS2-PFD-HA precipitation.

To identify any other potential interacting partners of PFD, the HA antibodies precipitated proteins from the CS2-PFD-HA cells were identified by mass spectrometry. The mass spectrometry was performed and the data were analysed by Pierre Faou and Ira Cooke (La Trobe University). To exclude any non-specific

bindings of other iRBCs proteins to the HA antibodies coated beads, the same experiments were performed on wild-type cells, serving as negative control. The potential interacting partners of PFD, which were identified in the PFD-HA cells but not in the wild-type cells, were shown in Table 3.1.

Protein Name	MW	Organism	Protein Identification Probability			
			PFD-HA	PFD-HA	PFD-HA	WT
PFD (*PFD1170c*)	36 kDa	*P. falciparum*	100%	100%	100%	0%
Keratin, type II cytoskeletal 6A	60 kDa	*H. sapiens*	100%	100%	100%	0%
Keratin, type II cytoskeletal 2	65 kDa	*H. sapiens*	45%	92%	100%	0%
Flotillin-2	47 kDa	*H. sapiens*	100%	100%	0%	0%
Flotillin-1	47 kDa	*H. sapiens*	100%	100%	0%	0%
Myosin light chain kinase 2, skeletal	65 kDa	*H. sapiens*	0%	100%	30%	0%

Table 3.1. Potential interacting partners of PFD were identified by mass spectrometry (MS) analysis in the samples of pull-down assays with anti-HA antibodies. The experiments were performed on the CS2-PFD-HA and the parental CS2 cells (to exclude any non-specific bindings of other iRBCs proteins to the HA antibodies coated beads, serving as negative control) in biological triplicate. The proteins with higher than 90% of protein identification probability were considered the reliable hits. PFD was the only *P. falciparum* protein found in the analysis whereas the others were human (*H. sapiens*) proteins. PFD-HA, HA tagged PFD cells; WT, wild-type cells; MW, molecular weight.

As expected, PFD was found in all the PFD-HA samples but not in the wild-type. The result was consistent with the observation on the Western blot analysis and the silver gel staining (Figure 3.14). However, PFD was the only *P. falciparum* protein found in the pull-down and MS experiments. The others were human proteins including keratin, flotilin and myosin, suggesting that they potentially interact with PFD.

3.2.7 Disruption of PFD does not influence the location of RESA and KAHRP and the formation of knobs

3.2.7.1 Disruption of PFD

To determine the influence of PFD function on RESA, KAHRP and knob formation, we generated parasites in which the corresponding gene locus (*PFD1170c*) was

disrupted by transfecting the *pHHT*-TKΔPFD1170c plasmid into *P. falciparum* CS2 (Maier et al, 2008) and 3D7-infected erythrocytes, leading to homologous double crossover recombination (Figure. 3.15A). Additional knock-out in 3D7 cell line was also generated to exclude any off-target mutations during transfection, culturing and to increase the confidence in the results (Goldberg et al, 2011). The Southern blot analysis revealed an absence of wild-type bands in the transfected, drug selected cell-lines, with new DNA fragment sizes at around 1.3 kb for the 5' flank and 3.5 kb for the 3' flank, indicating the correct integration of the resistance cassette and consequent disruption of the *PFD1170c* locus (Figure. 3.15B). Western blot analysis confirmed the complete disruption of PFD protein in the knock-out cell lines compared to the parental cells (Figure 3.15C).

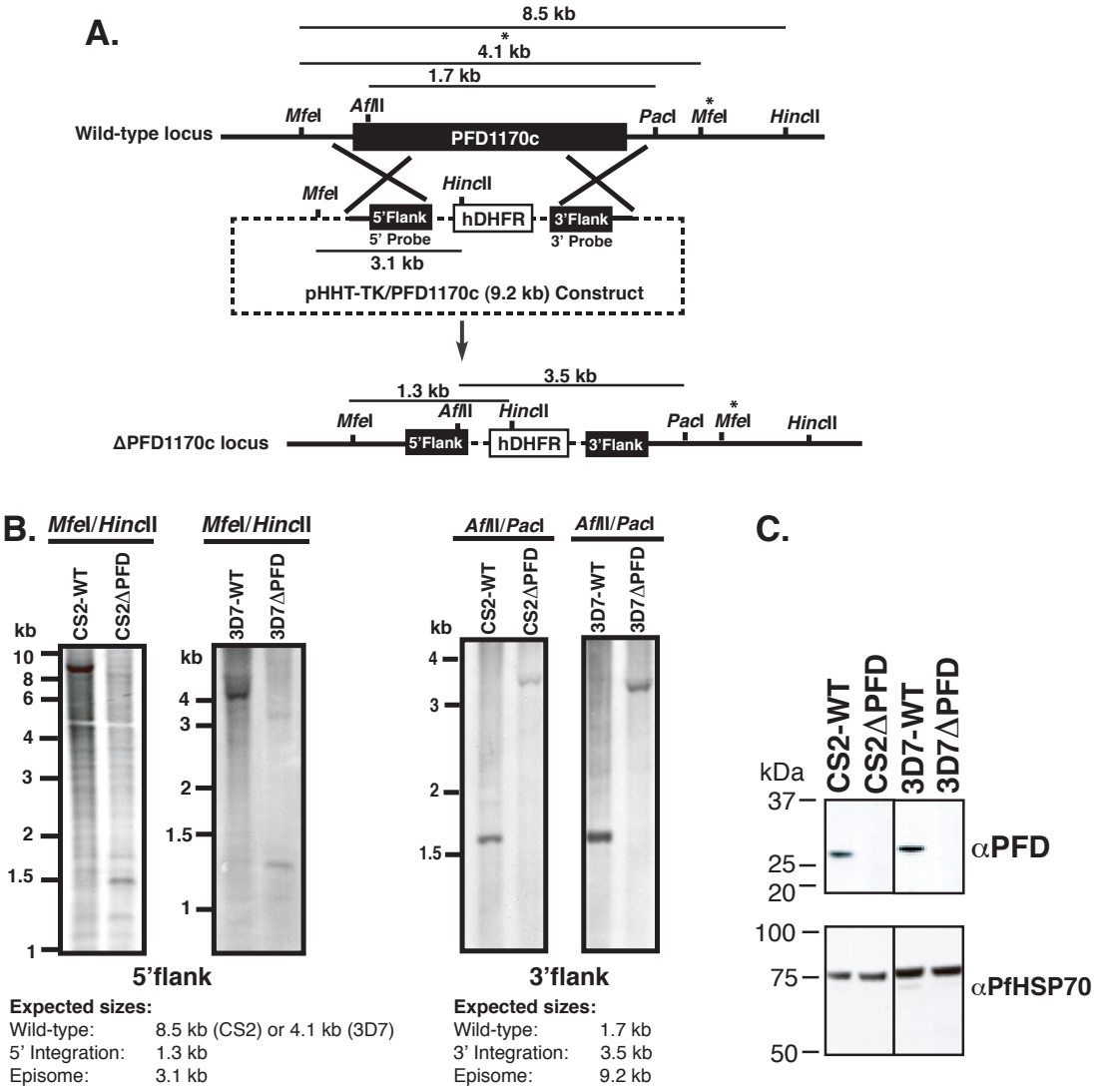

Figure 3.15. Disruption of *PFD1170c* in *P. falciparum* CS2 and 3D7 parasite lines. **(A)** The schematic representation of the vector (pHHT-TK) used to disrupt *PFD1170c* and the genomic loci before and after insertion of the vector (not scaled). The vector contained the *hDHFR* selection cassette flanked by two *PFD1170c* targeting sequences. Black box, *PFD1170c* coding region; open box, *hDHFR* selection cassette, *, restriction site present in the 3D7 genome, but not in the CS2 genome. **(B)** Southern blot analysis of digested genomic DNA from CS2 and 3D7 wild-type and knock-out parasites demonstrates the disruption of *PFD1170c*. **(C)** Western blot analysis shows the absence of PFD protein in knock-out parasites cell lines.

3.2.7.2 Localisation of RESA or KAHRP in the PFD deleted iRBCs

In order to examine whether the PFD influences the localisation of other exported proteins. We performed immunofluorescence microscopy on PFD knock-out and wild-type cell lines by labelling the iRBCs with anti-KAHRP and anti-RESA

antibodies. In the absence of PFD, KAHRP (Figure 3.16A) and RESA (Figure 3.16B) were still exported to the erythrocyte membrane as seen in the parental cells. The rim fluorescence patterns were similar to the patterns in the parental line, indicating a correct location of KAHRP and RESA in the PFD disrupted cells.

Anti-PFD antibodies cross-reacted with other proteins, and thus could not be used for IFA (Figure 3.3). In order to investigate whether disruption of RESA has an impact on PFD localization, we transfected episomal pGLUX-6/endo/PFD-GFP vector (Appendix3, supplementary Figure S6) into the CS2-ΔRESA cell line (Appendix 3, supplementary Figure S7) (the RESA knock-out cell line was created by Alex Maier). The resulting parasites were episomally expressing a chimeric PFD-GFP protein under the control of PFD endogenous promoter. Rim fluorescence of PFD-GFP in the RESA-knockout was still observed in wild-type cells (Figure 3.16C), suggesting that disruption of RESA does not influence the localisation of PFD.

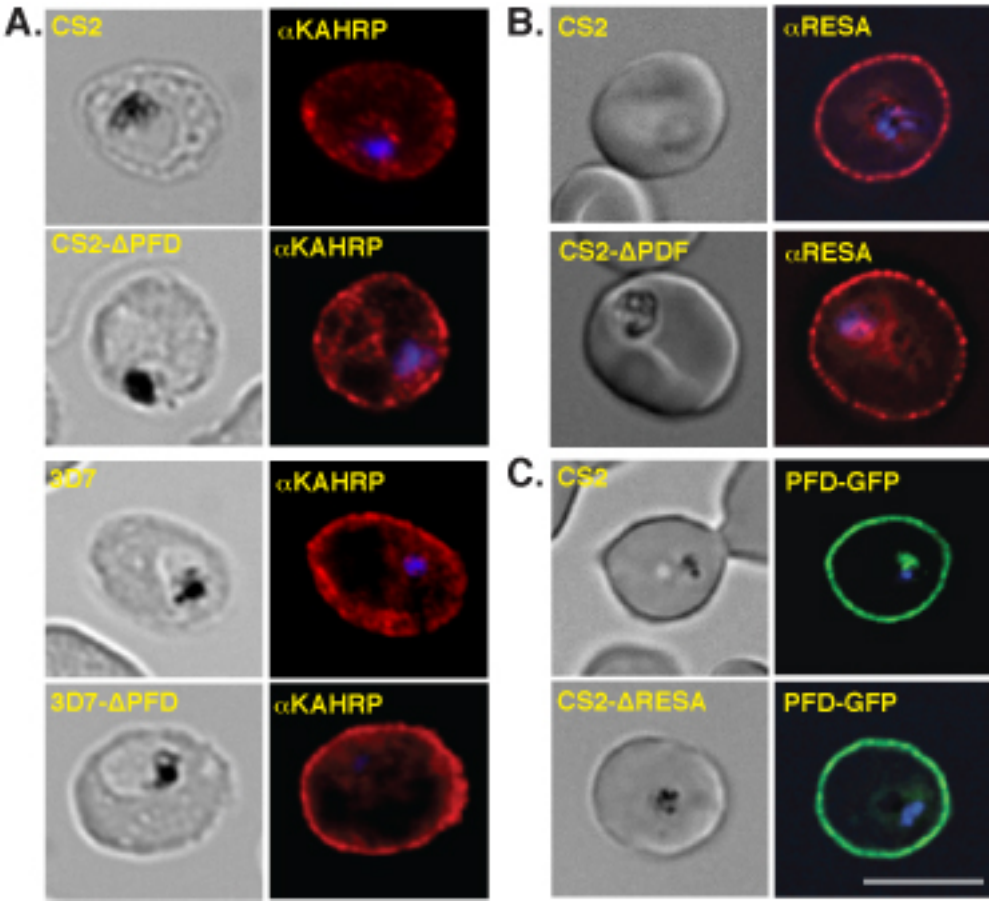

Figure 3.16. Disruption of PFD does not influence KAHRP and RESA localisation. Immunofluorescence microscopy of paraformaldehyde/glutaraldehyde fixed cells was performed using anti-KAHRP, anti-RESA and anti-GFP antibodies. The pattern of KAHRP **(A)** and RESA **(B)** was similar between the RBCs infected with wild-type and PFD disrupted parasites. **(C)** PFD-GFP was detected in CS2-ΔRESA cells as seen in parental CS2 wild-type cells. The first row is the fluorescence of PFD-GFP (episomal pGLUX-6/endo/PFD-GFP vector) complemented in CS2-wildtype. The second row is the fluorescence of PFD-GFP complemented in CS2-ΔRESA. The PFD-GFP expression was controlled by the PFD endogenous promoter. The DNA were visualised with DAPI (blue). BF, bright field. Scale bar: 5 μm.

Scanning electron microscopic (SEM) analysis on PFD disrupted parasites was also performed to assess the role of PFD in knob formation. The result showed that in the absence of PFD, knobs were still formed as seen in wild-type cells (Figure 3.17). The result is consistent with the fact that PFD did not co-localise with KAHRP (Figure 3.6) and was not found in knob protrusion (Figure 3.7). Together, the findings

indicate that the deletion of PFD does not influence RESA, KAHRP localisation and the formation of KARHP rich knobs.

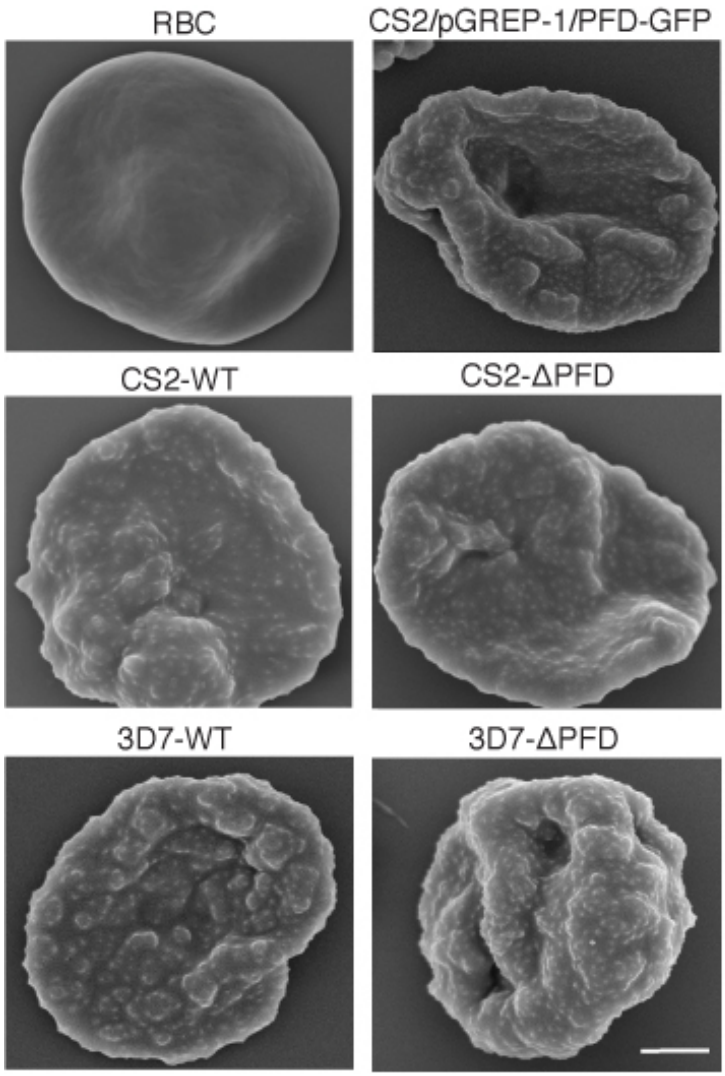

Figure 3.17. Knobs are still formed in the PFD disrupted and PFD-GFP iRBCs. Scanning electron microscopy (SEM) was performed on the parental CS2, 3D7 and the CS2-PFD-GFP and PFD disrupted cells. The presence of knob structures in the PFD disrupted iRBCs was similar to its parental iRBCs and distinguished to the smooth surface of the uninfected RBCs. The images show a representative trophozoite-infected erythrocyte for each cell line. RBC, uninfected red blood cell; WT, wild-type. Scale bar: 2 μm.

3.3 Discussion

In this study, we report that PFD is a peripheral membrane protein that co-localises and interacts with RESA to form a ~ 400 kDa complex in the RBC membrane, probably in the cytoskeleton. The protein is not located in knob protrusions and not overlaid with either knob proteins such as PfEMP1 and KAHRP. In addition, PFD deletion does not influence knob formation and does not affect KAHRP and RESA localisation. The protein is expressed in all asexual stages with a slight increase in ring stages.

PFD is the first *P. falciparum* parasite protein showing interactions with RESA, a protein involved in protecting ring cells against heat-shock temperature. The localisation study of PFD in relation to other exported proteins in the erythrocyte membrane showed that PFD is overlaid with RESA. The interactions between the two molecules are convincing since they were co-precipitated in IP assay. We also found that the detected protein level of the two molecules in the co-IP assay was different between young and mid trophozoite stages with higher grade for the former. This could be explained by the fact that RESA protein is gradually disappearing and disassociated with the erythrocyte cytoskeleton at later stages (after 24 hours in the asexual erythrocytic cycle) (Foley et al, 1990; Rug et al, 2004). Furthermore, these two proteins were also present in the complexes of a similar size at ~ 400 kDa in native condition. The complex could include PFD and RESA and/or also other unidentified proteins. The finding that PFD and RESA are co-expressed in field isolates in different transmission areas in Africa (personal communication with Margaret Mackinnon, unpublished data) implies that they potentially contribute to each other's functions. However, the disruption of PFD does not influence the

localisation of RESA and vice versa, suggesting that the trafficking of the molecules is not affected by each other. Overall, these data are consistent with PFD interacting with RESA.

Mass spectrometry analysis on pull-down elution samples has identified human proteins keratin, flotillin-1, flotillin-2 and myosin as other potential interacting partners of PFD whereas failed to detect any other *P. falciparum* proteins. Keratin, which is abundantly present in human skin, hair and laboratory dust, is a common contaminant in the MS analysis (Keller et al, 2008). Flotillin-1 and flotillin-2 are integral proteins located in the lipid rafts of the erythrocyte membrane and in the PVM in the *P. falciparum* infected RBCs (Murphy et al, 2006; Salzer & Prohaska, 2001). They are also partly associated with the erythrocyte cytoskeleton (Murphy et al, 2006; Salzer & Prohaska, 2001). Myosin is found in the erythrocyte cytosol and the erythrocyte membrane (Pasternack. & Racusen, 1989). The identification of flotillin and myosin as potential binding molecules of PFD partly supports our hypothesis that PFD locates to the host cell membrane and/or underneath the membrane. However, whether the human erythrocyte proteins specifically interact with PFD requires further investigations. That no *P. falciparum* protein was detected in the HA antibody-precipitated elutes might be due to HA tag interfering with the interactions of PFD with other parasite molecules. Therefore, it is necessary to repeat the experiments on the wild-type cells using anti-PFD antibodies. At this stage, it is difficult to draw definitive conclusions in this regard.

PFD is a peripheral membrane protein and likely associates with the cytoskeleton since its interacting partner – RESA is known to bind to the membrane at ring stage (Foley et al, 1991). Some *P. falciparum* exported proteins, which have been shown to

be soluble in sodium carbonate and insoluble in TX-100 detergent, are RBC-cytoskeleton binding proteins (Nilsson et al, 2012; Proellocks et al, 2014). In our study, PFD does show a similar solubility profile to these cytoskeleton proteins, suggesting that PFD could be associated directly with the cytoskeleton or via RESA interactions. PFD sequence contains a PHISTb domain that might play a role in interacting with RESA and/or the cytoskeleton.

The time course experiment analysed by Western blot and IFA showed that PFD is expressed in all asexual stages with a slight increase in ring stages. The data are coherent with mRNA expression of PFD peaking at merozoite stage (Le Roch et al, 2004), suggesting a high level translation of the protein in ring stage at which the host cell remodelling occurs (Marti et al, 2004). Interestingly, the expression profile of PFD was similar to that of RESA, which is additional evidence supporting that they might interact. The only difference is that PFD is still detectable at trophozoite stages whereas RESA is almost not detected (Figure 3.12). Based on these findings, it is conceivable that PFD could contribute to RESA function at ring stage in protecting the ring-iRBC membrane against the transient fever temperature for their survival in human. When RESA starts to be degraded at later parasite stages (Rug et al, 2004), PFD remains in/under the erythrocyte membrane, suggesting that the protein may play other roles or be involved in other molecular mechanism at these stages in facilitating other proteins transportation to the erythrocyte membrane and exposing their virulence. It is possible that PFD might interact shortly with other exported proteins in/under the erythrocyte membrane, and hence leading to the modifications of the iRBC membrane properties. This could be partly explained by the observation that the adhesion of CS2 cells to CSA in microslide flow chambers reduces by 50% in the absence of PFD (Maier et al, 2008). Therefore, PFD might play an important role

in the host cell remodelling at early stages of parasite development when RESA is expressed and also possibly support the presentation of other exported proteins to the membrane of mature parasite infected cells.

The observation that PFD-deleted parasites in either CS2 or 3D7 still produce knobs as normal as the parental lines via SEM suggests PFD is not crucial for knob formation on the iRBCs surface. The results are consistent with the localisation study showing PFD location is distinct from that of knob proteins such as PfEMP1 and KAHRP. Particularly, while KAHRP is distributed to several puntae in the erythrocyte membrane, PFD is likely accumulated underneath the host cell membrane. Moreover, the higher resolution EM image showed that PFD is not located in the electron-dense of knob protrusions but rather in the other locations of the host membrane. In addition, disruption of PFD does not influence KAHRP expression and PfEMP1 transportation to the iRBC membrane (Maier et al, 2008). We also failed to detect KAHRP, PfEMP1 and PfEMP3 as PFD interacting partners via co-IP assay and BN-PAGE. These findings imply that PFD hardly affects knob formation in the iRBCs, which contradicts the previous finding that disruption of PFD showed lack of knobs in the surface of the iRBCs (Maier et al, 2008). The disappeared rim fluorescence of KAHRP in the PFD disrupted cells had implied that the PFD is required for the correct assembly of KAHRP into knobs (Maier et al, 2008). However, as discussed above, we failed to provide any evidence that KAHRP and other known exported proteins were interacting with PFD, except for RESA. It is possible that the Maier et al. functional study screening on a large number of the knock-out parasites for the defect of knob formation potentially overlooked the tight synchronisation of the analysed wild-type and PFD disrupted parasites to the same developmental stage on which the knob formation is dependent. It is also plausible

that some unknown knob proteins might transiently interact with PFD, leading to some effects of PFD on the knob formation in the iRBCs. Whether the abnormal knobs or the un-stabilization of the iRBC membrane due to the disruption of PFD results in the reduced binding of the host cells to CSA (Maier et al, 2008) is unknown. At this stage, we do not have tool to further explore the issue.

We have provided experimental evidences that PFD interacts with RESA, an important molecule protecting parasites against the host febrile temperature at ring stage. The findings raise the possibility that PFD might support the function of RESA in regulating the host cell membrane stabilization at the heat-shocked temperature and/or involve in other unknown mechanisms that related to the febrile temperature, deformability and/or knob formation of the iRBCs. This study may open some new aspects for further functional studies of these two proteins, which may help to understand the RESA and PFD mechanism in detail. Gaining more insights into the molecular mechanisms of the *P. falciparum* exported proteins might promote novel therapies to reduce the serious modifications of RBC properties by the malaria parasite proteins.

Chapter 4

Physiological role of PFD *in vitro* and *in vivo*

Abstract

Mature *P. falciparum* infected erythrocytes can avoid clearance by the human spleen through sequestering themselves in other organs, whereas cells are infected by younger parasites found in the peripheral circulation. However, recent studies on human spleen showed that a proportion of ring-iRBCs could be retained and destroyed by the spleen due to their reduced deformability. In order to study the influence of PFD on the erythrocyte membrane modifications and on the parasite growth, we performed a range of *in vitro* and *ex vivo* experiments. We show that the presence of PFD leads to an increase in retention of the ring-iRBCs in both *in vitro* microsphiltration (mimicking the mechanical retention process in the spleen) and *ex-vivo* perfused human spleen at elevated temperature. Furthermore, the increased retention subsequently results in increased phagocytosis of the wild-type cells. We also demonstrate that PFD likely supports the iRBCs growth *in vitro* at body temperature in competitive co-culture assays. In order to access the influence of PFD on the modified-iRBCs membrane, we performed osmotic fragility and adhesion assays. PFD deleted parasites exhibit a slight difference in osmotic fragility at low tonicity and normal binding to placental vesicles compared to wild-type. Based on these findings we propose a crucial role for PFD in increasing the parasite growth at normal body temperature and increasing the splenic clearance of the parasites at febrile temperature.

4.1 Introduction

Parasitised-iRBCs can cytoadhere to vascular endothelial cells (Udeinya et al, 1981), which consequently leads to the sequestration of the iRBCs in major organs resulting in severe complications including cerebral malaria and death (Macpherson et al, 1985). It is clear that the sequestration is an important mechanism that needs to be explored in malaria research.

Plasmodium falciparum erythrocyte membrane protein 1 (PfEMP1) is the virulence factor that mediates the cytoadherence between the iRBCs and the host cells (see (Cooke et al, 2002; Maier et al, 2009) for review). A number of exported parasite proteins are probably required for virulence and rigidity of the iRBCs (Maier et al, 2008). Some of them are exported to the erythrocyte cytoplasm such as in knob protrusions and/or in association with iRBCs membrane and cytoskeleton. KAHRP is an essential protein for knob formation and plays a role in strengthening the cytoadhesion between PfEMP1 and endothelial cells (Crabb et al, 1997). Some exported proteins interacting with the RBC membrane were found to contribute to increased membrane rigidity (Cooke et al, 2002; Glenister et al, 2002). For example, PfEMP3 has an approximately 15% and 30% effect on the rigidity and the adhesion, while KAHRP shows at least 3 – fold increase in these properties (Cooke et al, 2002; Glenister et al, 2002). In contrast, another protein associated with RBC cytoskeleton - RESA protein expressed at ring stage did not show significant difference in membrane rigidity (Silva et al, 2005) and iRBC adhesion to CD36 under physiologically relevant flow conditions (Cooke et al, 2002; Silva et al, 2005). However, the protein had previously been shown to stabilize the iRBC membrane against febrile temperature (Da Silva et al, 1994) and to decrease deformability of

ring-iRBCs membrane at this temperature (Diez-Silva et al, 2012). In order to survive in the human host, the parasites have to export their own proteins and alter the host membrane properties to facilitate their binding and/or their survival. Understanding the molecules involved in the mechanisms will be helpful to interfering the binding and the sequestration of the parasites in human and diminishing the risk of severe complications.

Exploring the mechanisms in the human spleen that corresponds to the removal of the parasitised-RBCs is also a crucial aspect to control and regulate the *P. falciparum* infection. The spleen plays an important role in clearing the parasitised-RBCs, where interactions between immune system and malaria parasite antigens on the iRBCs surface and/or mechanical sensing of less deformable ring-iRBCs occur (Buffet, 2006; Buffet et al, 2011). The organ is also a place for generating pathogen-specific T and B cells to respond to the parasites (see (Engwerda et al, 2005) for review). However research on the aspect is challenged due to the limitation of the human tissue. Buffet et al. had established the *ex vivo* perfusion of human spleen collected from the patients with left pancreas tumours whose spleen has to be removed due to vascular-related constraints (Buffet, 2006). Furthermore, the authors also created a new system - called microsphiltration, which mimics the mechanical retention of the spleen sinus based on the reduced deformability of the iRBCs (Deplaine et al, 2011). Gaining more insight into the mechanism of parasite retention in the spleen and micro-beads models can help to control of the parasite density and diminish the severe disease. The knowledge therefore will deepen our understanding of the disease pathogenesis, which is important for discovery of interventions against malaria.

In chapter 3, we have shown that PFD interacts with RESA, speculating that PFD might complement the function of RESA. RESA disruption exhibited an increase in deformability of ring-iRBCs at febrile temperature (Mills et al, 2007), and a decrease in retention of the iRBCs in a microsphiltration system (Diez-Silva et al, 2012). The protein possibly contributes to splenic retention and accelerating parasite clearance (Diez-Silva et al, 2012).

We propose that by forming a complex with RESA, PFD would also play an important role in the ring-iRBCs deformability. In order to define the influence of PFD on the host cell membrane modifications and its effects on the human spleen clearance, we examine the osmotic fragility, adhesion and deformability of PFD disrupted cells via retention experiments compared to parental cells. Moreover, we investigate the retention rate of iRBCs through both *in vitro* microsphiltration system and *ex-vivo* human spleen at normal body and febrile temperatures. We also show the percentage of iRBCs undergoing phagocytosis in the spleen. Lastly, the parasite growth in the absence of PFD is assessed via growth competition assay and quantitative PCR.

4.2 Results

4.2.1 Disruption of PFD shows a slight effect on osmotic fragility of the infected erythrocytes at low tonicity.

After invasion, the malaria parasite extensively modifies the host cell membrane. In order to investigate the influence of PFD on the host membrane's osmotic property, we performed an osmotic fragility assay on the CS2-wildtype and CS2-ΔPFD cells of young trophozoite stage (22 – 28 hours after invasion). At this time point the initial host cell modifications are manifested and the infected cells can be purified. The cells

were enriched to > 98% purity by magnet. A number of 10^8 cells from each parasite line were subjected to different concentrations of NaCl-PO_4 salt (see section 2.5). Haemoglobin released from lysed cells at various salt concentrations was measured at OD_{540} and normalised to that of water lysed cells. The result (Figure 4.1) showed that at low tonicity (< 0.2% NaCl-PO_4), the percentage of haemolysis of knock-out cells was marginally higher than that of wild-type cells and similar to the uninfected cells, although a similar osmotic resistance was observed for wild-type and knock-out cells at high tonicity (> 0.4%).

The finding indicates a small change in osmotic fragility of host cell membrane in the absence of PFD in the low tonicity environment, which was shifted to that of uninfected RBCs.

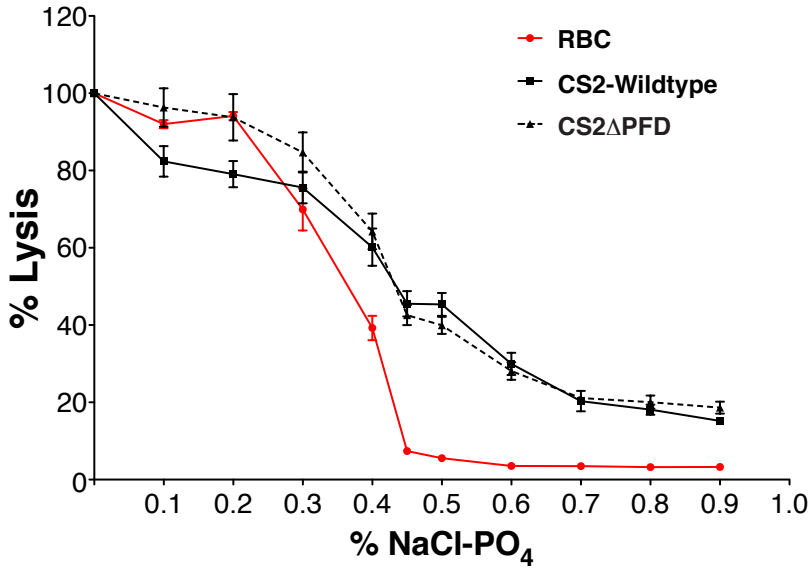

Figure 4.1. Osmotic fragility curves of CS2-wildtype, CS2-ΔPFD and uninfected RBCs. PFD knock-out and parental CS2 cells were enriched to > 98% purity by magnet purification at young trophozoite stage (22 – 28 hours). A number of 10^8 cells were subjected to different concentrations of NaCl-PO_4. Water was used for the point of 0% NaCl-PO_4, which corresponds to 100% haemolysis of RBCs and iRBCs. Concentration of haemoglobin released from lysed cells at various salt concentrations was measured at OD_{540} and normalised to that of water lysed cells. Error bars represent the standard deviation of three independent experiments in technical triplicate each.

4.2.2 Disruption of PFD does not influence the adhesion of infected RBCs to the CSA receptor on placental cells

One of the reasons *P. falciparum* causes threat to maternal and foetal health is the adhesive ability of the iRBCs to the placental epithelium. Chondroitin sulphate A (CSA) is abundantly expressed on the apical membrane of the placental syncytiotrophoblast epithelium and serves as a receptor for PfEMP1 variant var2csa (encoded by *PFL0030c*) (Duffy et al, 2006). The var2csa protein has a high affinity to CSA (Salanti et al, 2004) and is specific to placenta (Yosaatmadja et al, 2008). The CS2 parasite line steadily expresses the var2csa protein (Duffy et al, 2006) after being selected for adhesion to CSA (Duffy et al, 2005). On the other hand, the 3D7 parasite line shows a decreased affinity to CSA (Duffy et al, 2005), which was used as a negative control in our adhesion assay.

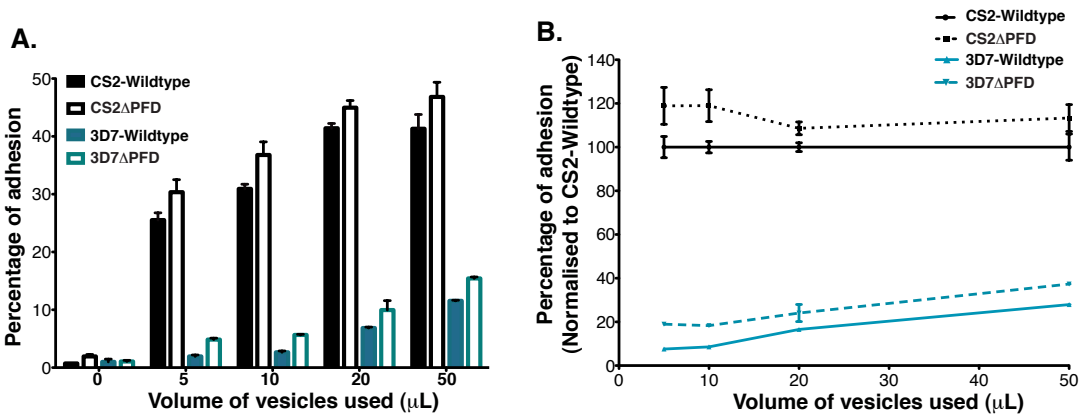

Figure 4.2. Disruption of PFD does not influence the adhesion of iRBCs to CSA receptor on placental cells. Apical epithelial vesicles were prepared from three different human placentas by Dr. Phillippe Boeuf, University of Melbourne. Increasing volumes of these vesicles (5 to 50 μL) were each incubated with 5 x 10^4 wild-type or PFD knockout cells in CS2 (CSA binding) and 3D7 (CSA non-binding). The apical epithelial vesicles were stained with green PKH67 and the infected cells were stained with red ethidium bromide and counted on a flow cytometer. Percentage of vesicles bound to the infected erythrocytes **(A)** and its normalisation to CS2-wildtype (CS2WT) cells **(B)** were plotted.

The difference in the adhesion between CS2-ΔPFD and CS2-WT was not statistically significant (*P* values (unpaired Student *t* test) > 0.1 for all volumes of vesicles used).

In order to investigate the role of PFD in the adhesion of infected RBCs to CSA on placental cells, CS2-ΔPFD and 3D7-ΔPFD cells were synchronized to trophozoite stage, magnet purified and a number of 5 x 10^4 cells from each cell line were then subjected to the placental adhesion assay with different amount of apical epithelial vesicles. Adhesion of parental cells served as a comparison. The vesicles were purified from the apical plasma membrane of several epithelia using Mg^{2+} precipitation and differential centrifugation (Glazier & Sibley, 2006). The plasma membrane fragments were forced to vesiculate by shear force, orientate right-side-out (Glazier & Sibley, 2006). The vesicles used in the placental assay were prepared by Dr. Phillippe Boeuf (University of Melbourne) (Boeuf et al, 2011). The green PKH67 stained apical epithelial vesicles and the red ethidium bromide stained infected cells were counted on a flow cytometer to assess ability of the iRBCs to adhere to the placental vesicle. The results (Figure 4.2) showed no significant difference (*P* value > 0.1) in adhesion of PFD disrupted cells to vesicles carrying CSA receptors compared to CS2 wild-type line. The negative control 3D7 cells showed a much lower adhesion to the vesicles compared to the CS2 lines. The data suggested that PFD is not required for the promotion of infected cells adhesion to CSA expressing placental epithelia.

4.2.3 Disruption of PFD leads to a reduced retention rate of ring stage parasites in human spleen

In order to examine the role of PFD in the retention rate of infected RBCs in human spleens, highly synchronous CS2-ΔPFD cells of different stages (14 - 22, 22 – 30 and 30 – 38 hours after invasion) were subjected to a retention assay in a microsphiltration device. The microsphiltration device contains micro-beads mimicking the geometry

of inter-endothelial slits of the human spleen and hence imitating the stringent challenge in the red pulp of the human spleen (Deplaine et al, 2011; Diez-Silva et al, 2012). In order to cross the narrow inter-endothelial slits of the sinuses the RBCs must undergo extensive deformation (Safeukui et al, 2008). The microsphiltration retains ring-stage iRBCs at a similar rate as isolated-perfused (IP) human spleen (Deplaine et al, 2011). This system allows us to monitor the filterability of iRBCs and hence the impact of the presence of PFD on the traversal of the microsphere layer.

The cells (~ 4% parasitemia in 2% haematocrit) were incubated at either 37°C or 41°C for 2 hours before loaded onto microspheres columns. Nucleic acids of the infected cells were stained with SYBR® green I (Invitrogen) before counted on a flow cytometer. Retention rates were calculated as percentage of the infected cells retained in the microspheres column. The data were obtained from three independent experiments in technical triplicate.

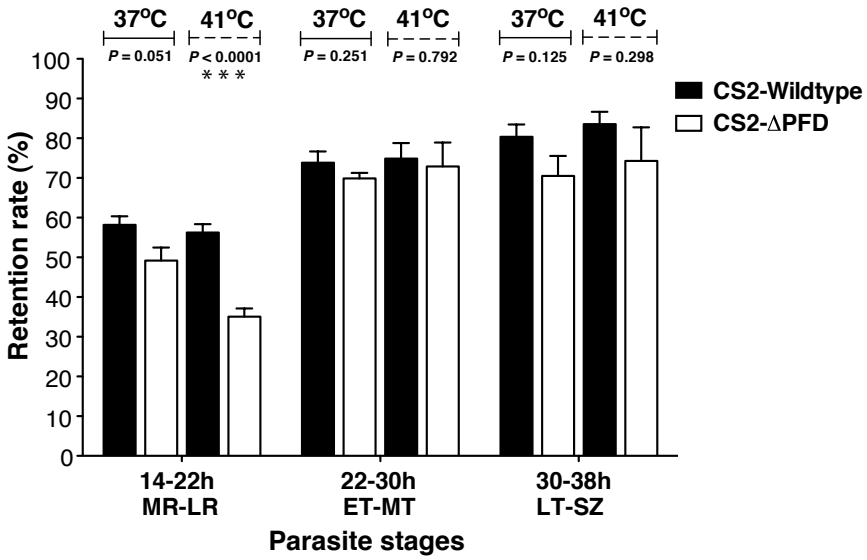

Figure 4.3. Ring stages PFD knock-out cells are retained less in a microsphiltration system mimicking human spleens compared to parental cells. Highly synchronous parasites at 14 – 22, 22 – 30 and 30 – 38 hours after invasion were incubated at either at 37°C or 41°C for 2 hours before loaded onto microspheres columns (these columns were incubated at 37°C or 41°C). Nucleic acids of the wild-type and knock-out cells were stained with SYBR® green I and counted on a flow cytometer. Retention

rate was calculated as percentage of total infected cells retained in the microspheres column. Error bars represent the standard deviation of three independent experiments in technical triplicate each. The *P* values shown represent a difference in retention rate between parental and knock-out cell lines and were calculated using unpaired Student *t* test. ***, statistically significant difference ($P < 0.001$). MR, mid ring. LR, late ring. ET, early troph. MT, mid troph. LT, late troph. SZ, schizont.

Overall, the ring-iRBCs showed less retention in the micro-beads compared to the mature trophozoite stages at both temperatures (Figure 4.3). At 37°C, the mid/late ring stage (14 – 22 hours) CS2-ΔPFD cells showed 15 % reduction in the retention ability compared to the parental cells ($P = 0.051$) and the difference is not considered significantly. Similarly, there were no differences in retention of the two cell lines in later stages (*P* value > 0.1). In contrast, at 41°C, a statistically significant reduction of 37 % was observed for the transiently heat-stressed ring-infected cells ($P < 0.0001$) despite no difference seen for the later stages.

This data suggests the disruption of PFD increased the deformability of ring-infected cells, particularly at transient febrile temperature, therefore leading to the decreased retention rate in the spleen-substituted device.

To validate the impact of PFD in the retention of the ring infected cells in human context at febrile temperature, we performed a similar procedure to microsphiltration (that I designed during the stay of 3 months in Pierre Buffet's lab) on the *ex vivo* isolated perfused human spleens (Buffet, 2006) using heat-shocked ring infected cells. In order to distinguish wild-type and PFD-knockout cell populations, these cells were independently stained with red PKH26 and green PKH67 stains (Sigma) before perfusion. Fifteen mL of packed labelled iRBCs at ~ 3.5% parasitemia of each CS2-ΔPFD and CS2-wildtype lines were mixed and subjected to the spleen perfusion system for 1 hour (see section 2.8). The cells before and after travelling through the spleen were counted on a flow cytometer and retention rate of each cell line was

calculated as percentage of total iRBCs retained in the spleen. Since the availability of the spleen is unpredictable and limited, I had observed the spleen experiment only one time during my research exchange in Pierre Buffet's lab. In order to maintain my workflow in the aspect, I had frozen down a number of tubes containing the iRBCs for the wild-type and the PFD disrupted cells for the first spleen experiment and also wrote the protocol for the microsphiltration that could be applied for the spleen experiments. Three independent spleen experiments were performed by Pierre Buffet's group. The quality of the spleens was dependent on the patient physiology and the surgical conditions in removing the spleen, leading to variations of the general retention ability of the iRBCs to the spleens. Due to this reason, we presented the data of the spleen experiments for each spleen experiment individually (Figure 4.4A). Overall, the result reveals that disruption of PFD reduced retention of ring-iRBCs in the spleen by ~ 41% at mid-ring and ~ 42% at late ring stages.

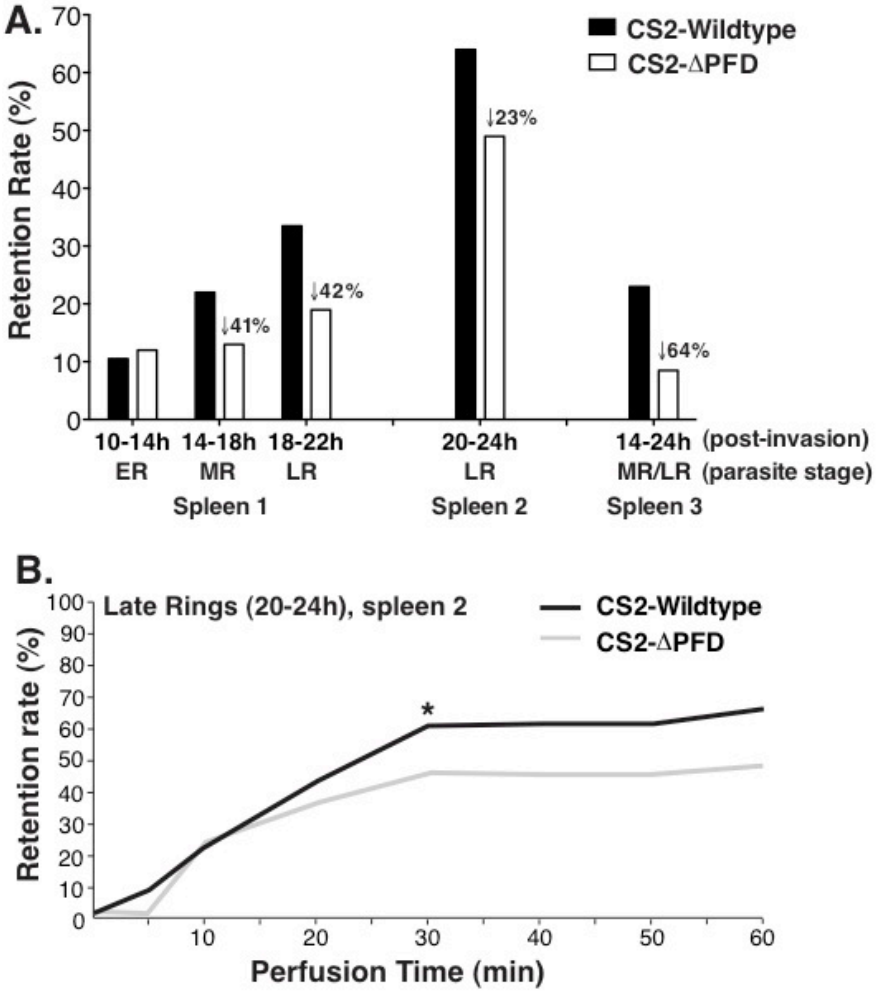

Figure 4.4. Reduction in retention rates of mid/late ring stage PFD disrupted cells compared to parental cells in isolated perfused human spleen system at febrile temperature. (A) Synchronous CS2-wildtype and CS2-ΔPFD parasites at ring stages were incubated at 41^{o}C for 2 hours before subjected to spleen perfusion at the elevated temperature. The iRBCs were stained with red PKH26 (for CS2-wildtype) and green PKH67 (for CS2-ΔPFD). The stained iRBCs from each CS2-ΔPFD and CS2-wildtype lines were mixed and perfused through the spleen system for 1 hour. The cells before and after travelling through the spleen were counted on a flow cytometer and retention rate of each cell line was calculated as percentage of total infected cells retained in the spleen. The data were collected from 3 independent spleen experiments (performed by Pierre Buffet and Papa Alioune Ndour). The reduction in retention rate of knock-out cells was shown on top of knock-out columns. ER, Early ring, MR, mid ring, LR, late ring. **(B) Kinetic of CS2WT and CS2-ΔPFD in the second spleen perfusate.** The retention of heat-shocked late-ring (20-24 hours after invasion) parasites was examined. Percentage of retained iRBCs was measured over 60 min perfusion. *, a reduction of 23% in retention rate of knock-out cells was observed at late ring stage.

Figure 4.4B showed a representative kinetic of CS2 wild-type and PFD knock-out parasites (the second spleen experiment) on the late-ring stage parasites (20-24 hours

after invasion). The difference in retention rate was observed by the reduced retention of 23% in the PFD disrupted cells compared to the wild-type cells after 30 min of the spleen perfusion (star, Figure 4.4B). In addition, the general retention rate of the late ring cells in the second spleen was higher than that observed in the other spleens: 50% - 65% in the second spleen compared to 20% - 35% in the first spleen and 8% - 23% in the third spleen. It could be due to the difference in the spleen quality.

The average reduced retention of the PFD deleted late-ring cells in the spleen experiments was approximately 42.5%, which is close to that seen in the microsphiltration (37%) (Figure 4.3). The results are consistent with the previous findings that the microsphiltration can mimic the mechanical retention in the spleen at a similar rate to some extent (Deplaine et al, 2011).

4.2.4 CS2-ΔPFD cells escape from phagocytosis human spleen

In order to answer the question whether the reduced retention of PFD-deleted cells will lead to a reduction in phagocytosis by white cells in the spleen, the perfusion output were labelled with a blue Hoechst 33342 dye (Molecular Probes). The DNA of white cells was stained by the dye that was counted by flow cytometry (Figure 4.5). The free immune cells labelled with Hoechst 33342 only (in blue) showed no phagocytosis. By contrast, in phagocytosis events, the white cells containing the dead parasite remnants exhibited the blue labelling by Hoechst 33342 on top of PKHs labelling of the parasites (red PKH26 for wild-type or green PKH67 for knock-out). The result showed that only the phagocytosis of the wild-type iRBCs was observed (Figure 4.5A).

In order to examine the percentage of iRBCs undergoing phagocytosis, the iRBCs in association with and without white cells were quantitated by flow cytometry. The

phagocytosed iRBCs showed a higher intensity of blue fluorescence compared to normal iRBCs due to the co-labelling of the iRBC DNA and white cell DNA. As shown in a representative experiment, a subpopulation (0.6% parasitemia) of phagocytosed wild-type iRBCs was detected at the end of perfusion, whereas no phagocytosis was found for the knock-out iRBCs (Figure 4.5B). The parasite mixture before perfusion did not contain any phagocytosed cells. Percentages of phagocytosis of the wild-type iRBC cells, which were calculated by dividing the number of phagocytosed cells by the total number of iRBCs, were 35.3% and 78.4% in two independent spleen experiments (Figure 4.5C). Phagocytosis of the knock-out iRBC cells was 0%.

The results suggest that disruption of PFD leads to the parasite escape from being phagocytosed by the white cells in the human spleen.

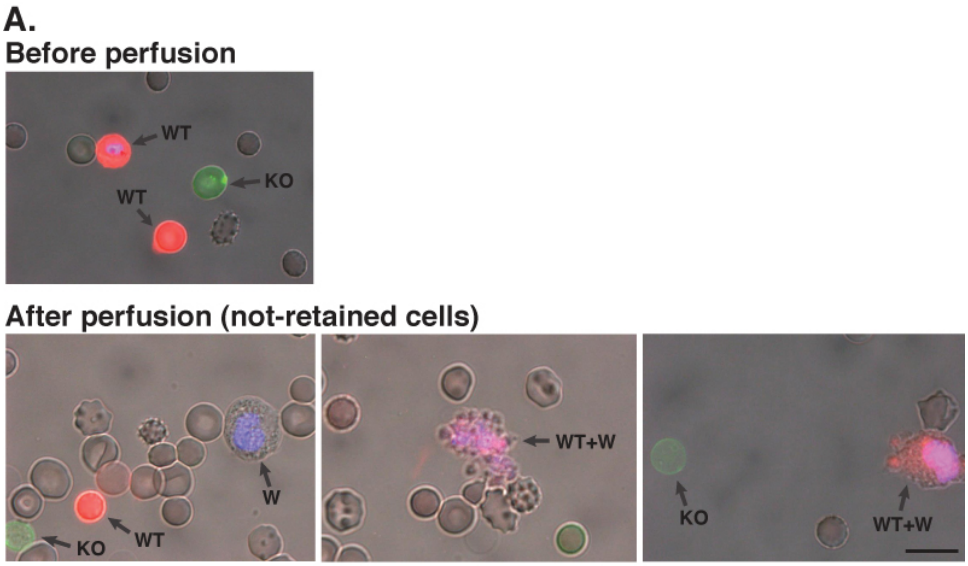

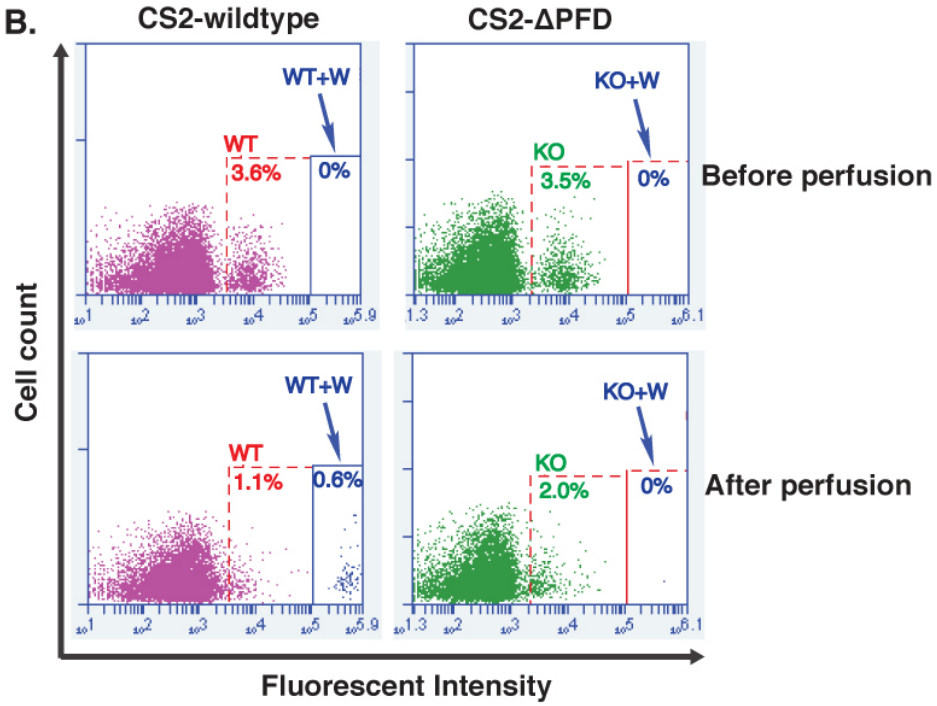

C.

	Percentage of iRBCs Phagocytosis	
	CS2-wildtype	CS2-ΔPFD
Spleen 1	35.3%	0.0%
Spleen 2	78.4%	0.0%

Figure 4.5. CS2-ΔPFD cells escape the phagocytosis from the white cells in human spleen at febrile temperature. (A) Synchronous parasites at ring stage of CS2-wildtype and CS2-ΔPFD were incubated at 41^{o}C for 2 hours before subjected to spleen perfusion at the same temperature. The iRBCs were stained with red PKH26 (for CS2-wildtype) and green PKH67 (for CS2-ΔPFD) dyes. An equal number of the stained iRBCs from each cell line were mixed with fresh blood (3.5% each cell line). The parasite mixture was perfused through the isolated human spleen for 1 hour before the cells, which

were not retained in the spleen, were collected. Nucleic acids of white cells were labelled with 1 μM Hoechst 33342 (blue) for 10 min. The cells before and after perfusion were imaged on a Zeiss Axiovision 200 M fluorescent microscopy in order to examine the phagosytosis of the infected RBCs. WT, wild-type (red); KO, knock-out (green); W, white cells (blue); WT+W, wild-type positive white cells (blue and red). Scale bar, 10 μM. **(B)** The number of iRBCs and white cells before and after perfusion was quantitated by flow cytometry. The population of labelled iRBCs, which was distinctive from the uninfected RBCs population, were gated and counted. The populations of red PKH26 labelled wild-type and green PKH67 labelled knock-out iRBCs were gated. Then, the population of the parasitized white cells, which contained both the iRBC DNA and white cell DNA, was gated with a stronger intensity of blue (Hoechst33342) fluorescence. WT, wild-type; KO, knock-out; WT+W, wild-type positive white cells; KO+W, knock-out positive white cells. **(C)** The phagocytosis of the iRBCs was estimated based on the proportion of the phagocytosed iRBCs in total iRBCs flowing through the human spleen. The data were obtained from two independent spleen experiments.

4.2.5 Deletion of PFD affects parasite growth

We performed growth competition assays in order to examine growth rate of PFD disrupted cells in comparison to wild-type under the same culture condition. An equal number of highly synchronous RBCs infected with ring-stage wild-type and knock-out cells were added into the same culture dish and maintained for 21 days either at constant 37°C or at transient febrile condition. Here the culture temperature was raised to 41^{o}C for 2 hours at ring stage of the parasite development every 48 hours (once every parasite lifecycle). The cultures were maintained by reducing the parasitemia to 0.2% with fresh blood and media addition every second day. The parasitemia was monitored by Giemsa-stained blood thin smears. We observed that the parasitemia of the heat-shocked cultures were always lower (0.5 – 1.5% after each cycle) than the normal cultures (3 - 4% after each cycle). The parasites were collected weekly and the genomic DNA from each cell line was quantitated by quantitative PCR with specific probes distinguishing between wild-type and knock-out parasites. The parasite numbers were calculated based on a standard curve obtained from a serial dilution of the parasites. The data were obtained from 3 independent

experiments and qPCR was performed in technical triplicate. After 21 days of co-culture (10 life-cycles of the parasite), the growth of CS2-ΔPFD cells was approximately 5-times less than that of wild-type at 37°C. No difference of the parasite growth was observed under the febrile condition (Figure 4.5). The data suggests an important role for PFD in the parasite growth *in vitro*.

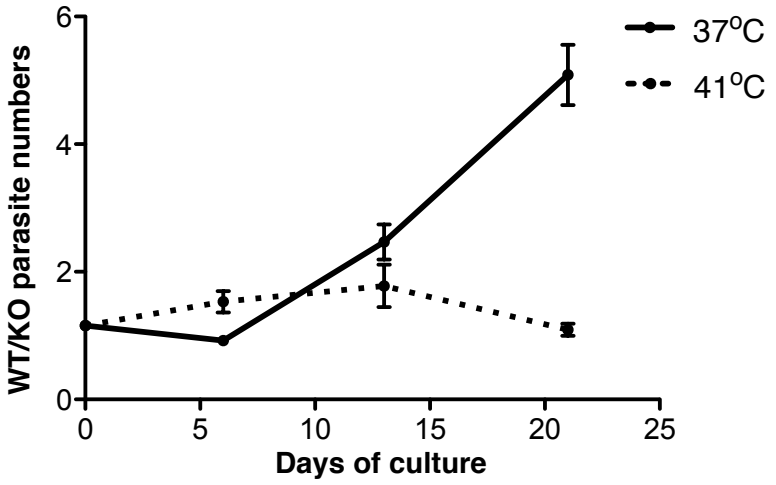

Figure 4.6. PFD disrupted parasites grow slower than parental cells in growth competition culture at constant 37°C. An equal number of highly synchronous knock-out and wild-type cells in ring stage were added into the same culture dish and maintained for 21 days either at normal culture condition or at febrile condition in which the culture temperature were raised to 41°C for 2 hours every 48 hours (once every parasite life-cycle). The genomic DNA from each cell line was quantitated by quantitative PCR weekly. The ratio of wild-type to knock-out parasite number was calculated based on the standard curve and plotted. Error bars represent the standard deviation of three independent experiments with technical triplicate. WT, wild-type; KO, knock-out.

4.3 Discussion

The results presented here demonstrate that the presence of PFD protein has a significant effect on retention rate of the ring-iRBCs and consequently increases the splenic clearance in the human spleen at febrile temperature. The reduced retention of the PFD disrupted ring-iRBCs also indicates that their deformability at the ring stage is higher than that of the wild-type cells. We also showed that PFD is important for parasite growth *in vitro* at human body temperature. In addition, we observed a slight impact of PFD on the osmotic fragility of the infected RBCs at low tonicity and no difference in the adhesion of the infected cells to CSA-containing vesicles of the placenta. Overall, the findings suggest that PFD has influence on the infected erythrocyte membrane deformability and is also involved in the mechanism of parasite retention in the human spleen at febrile temperature.

The expression of PFD protein reduces the deformability of the ring-iRBCs, which is even more obvious at elevated temperature. We examined the deformability of the ring-iRBCs via physiological retention mechanism in the *in vitro* microsphiltration system at both normal and elevated temperature. The device serves as a substitute method for spleen mechanic challenge of red cell deformability (Deplaine et al, 2011). Therefore, ring cells that are less deformable are retained in the micro-bead layers. Using the model, disruption of PFD leads to a significant decrease in retention of ring infected RBCs (14 hours – 22 hours after invasion) for heat-shocked cells. Filterability of PFD disrupted cells in the microsphiltration device was 15% lower than that of wild-type at 37ºC, and a more significant reduction of 37% was observed in the heat-shock condition. However, no difference in retention was observed for mature parasites (> 22 hours) due to their highly poor deformability. The result is

consistent with the previous finding that disruption of PFD does not result in any significant differences in the trophozoite-iRBCs deformability using a laser-assisted optical rotational cell analyzer (LORCA) (Maier et al, 2008). The contribution of PFD to the retention of ring infected cells in the micro-beads under the heat-shock stress is similar to that observed for RESA (Diez-Silva et al, 2012). Despite the fact that we showed interactions of both molecules and they are present in the same protein complex, disruption of either PFD or RESA did not influence the localisation of the counterpart (chapter 3). It is plausible that when any of the complex's components is deleted, the complex might function improperly in the cells, implying that the absence of both PFD and RESA might possibly lead to even greater defect to the increased deformability of host cells at the febrile temperature and consequently might decrease the parasites clearance from the spleen. The finding indicates that PFD has a similar function to that of RESA in reducing deformability of ring-iRBCs at febrile temperature and in increasing the mechanical retention.

The impact of PFD protein was also explored far further than its molecular aspect since the phenotype on the parasite retention was also investigated in *ex-vivo* perfused human spleens at the elevated condition. In addition to the mechanical filtering in the microsphiltration device, the iRBCs also cytoadhere to the sinus lumen of the spleen (Prommano et al, 2005). To minimize the possibility of the mature asexual parasites adhesion in the spleen, we performed the spleen experiment on the ring-infected parasites of CS2 cell line. However, the knob protrusions may be already present on the surface of the infected cells from about 16 hours after invasion (see (Maier et al, 2009) for review). Therefore, the cells that did not pass through the spleen probably include both retained and cytoadhered parasitised-RBCs. The retention phenotype seen for the knock-out parasites at mid/late ring (14 – 24 hours) at 41ºC was slightly

higher in the spleen experiments (42.5%) than in microsphiltration (37%). The more decreased retention of the knock-out cells in the spleen might indicate the presence of cytoadhrence phenomenon with the more cytoadherence of wild-type and less cytoadherence of the knock-out to the spleen. The argument is likely consistent with the previous finding showing that PFD disruption decreased the adhesion of the infected cells to CSA under physical flow condition (Maier et al, 2008). At this stage, we do not know which receptors on the CS2-iRBCs could bind to the spleen and how many receptor types could be present in the splenic lumen. There were no differences in the splenic retention observed for very early ring stage parasites (< 14 hours after invasion). This could be explained by the fact that at this early stage, the parasite just begins to export proteins and does not significantly modify the host cell membrane. In addition, PFD is located in the parasite cytoplasm at the early ring stage and not exported to the erythrocyte membrane until the mid-ring stage (Chapter 3, Figure 3.5), suggesting that PFD affects the host cell membrane only from the mid to late ring stages onwards.

PFD is important for parasite growth during its asexual cycle. A 5-time reduction in growth of PFD deleted parasites was observed after 10 parasite life cycles of growth competition culture at 37ºC. This is a slow delay in development of the knock-out parasites since one parasite can produce up to 32 progenies after completing its 48-hour asexual cycle. The slow growth defect was not observed at the transient 41ºC incubation condition. This could be explained by the fact that the 2-hour elevated temperature had a deleterious effect on parasite survival at least by 25% (Oakley. et al, 2007). It is conceivable that the transient heat-shock negatively affects the well-being parasites of both cell lines, therefore, the difference in parasite numbers, if any,

were hard to be seen in 21 days of the co-culture assay. In light of our results, disruption of PFD might lead to a reduction in the parasites biomass *in vivo*.

The presence of PFD confers both advantages and disadvantages to the *P. falciparum* parasites. On the one hand, PFD contributes to the reduced deformability of ring-iRBCs at febrile temperature, suggesting that the protein may support the ring-infected cells during elevated temperature. Since more ring parasites survive at higher temperature, more mature cells are produced and sequester in human organs to avoid the clearance by the spleen. The second advantage is that PFD protein is likely conducive to parasite growth at *in vitro* condition. On the other hand, the PFD containing ring cells can be trapped in the spleen sinus and destroyed by the spleen macrophages due to the mechanically altered membrane properties (Buffet et al, 2011; Safeukui et al, 2008). PFD disrupted iRBCs showed almost no being phagocytosed by the white cells in the spleen compared to the wild-type parasites. The more parasites that are retained in the spleen, the fewer sequestered biomass of mature forms in other organs (Buffet et al, 2011; Safeukui et al, 2008), which is disadvantageous to the parasite survival. However, only a subpopulation of ring cells is retained in the spleen, while a majority of the iRBCs are found in the blood circulation (Safeukui et al, 2008). Alternatively, the disadvantages of having PFD do not outweigh the advantages to the parasites.

The PFD protein may be involved in the mechanism that can regulate the parasite growth to adapt with the changed temperature in human body and maintain their survival in the host for further transmission. The parasites having PFD may start to grow very fast at normal body temperature after their infection to human until the parasite density is high enough in which malaria fever is triggered (Oakley et al,

2011; Oakley et al, 2007). Under the high temperature, the parasite growth slows down since a proportion of the ring-iRBCs could be retained and destroyed by the spleen. It is possible that the parasites still need the host survival in order to gain enough time to produce gametocytes, which is important for their next transmission to mosquito vector and their survival. The down-regulation in multiplication of the parasites is also beneficial to activation of the host immune system. It is conceivable that PFD may play an important role in controlling parasite biomass in the host in order to provide enough time for the parasites to form gametocytes to transmit to the insect vector.

PFD does affect osmotic fragility of iRBCs only slightly. At low tonicity condition, the osmotic fragility of PFD disrupted cells is marginally higher than that of wild-type and tends to be similar to that of uninfected RBCs. It is possible that the disruption of PFD might affect the stability of the iRBCs membrane, resulting in the slight difference in the haemolysis percentage.

Disruption of PFD showed almost no impact on adhesion of the infected cells to CSA-positive placental vesicles. The CSA-containing vesicles in use are derived from the plasma membrane of human placenta (Boeuf et al, 2011). The assay was performed under plate-shaking condition and vesicles are mobilized. In addition, the vesicles are very small (~ 0.15 μm) compared to the size of iRBCs (5 – 7 μm) and only 2 to 4 vesicles are bound to one iRBC (Boeuf et al, 2011), making it hard to see the difference in binding between the iRBCs and the receptors on the small vesicles. The reasons could lead to the 100% normal binding of PFD-knockout iRBCs compared to wild-type, whereas under the physiological flow-condition, disruption of PFD showed 50% reduced adhesion or non-binding of the iRBCs to CSA (Maier et al,

2008). Under the flow condition, the RBCs could have an ellipse shape that could expose more PfEMP1 on the iRBCs surface and hence results in more binding compared to the non-binding of the round shape of the iRBCs under static condition. Disruption of PFD might affect the stability of the parasite-encoded proteins location on the erythrocyte membrane or cytoskeleton although PfEMP1, KAHRP and knobs are expressed normally to some extent (Maier et al, 2008) (see Chapter 3). The physically unstable membrane of the infected cells due to PFD deletion could lead to the reduced adhesion under the force of flow, but no difference under the rotated shaking conditions.

We have conducted a detailed investigation into the physiological role of PFD. The expression of PFD is important for parasite growth and reduces deformability of ring-iRBCs. However, its presence leads to the splenic retention and accelerates parasite clearance and phagocytosis at febrile temperature. The increased clearance by the spleen may diminish the risk of severe malaria complications such as cerebral malaria or multi-organ failure. The present findings also open new avenues for investigation of the mechanism in which the PFD may control the parasite biomass in the host in order to develop their further survival strategy in the insect vector. Being able to interrupt the parasite survival in the human and insect hosts might help to discontinue the spreading of the disease.

Chapter 5

Concluding remarks and future prospects

This thesis has demonstrated the characterization of a *P. falciparum* exported protein encoded by *PFD1170c* gene (referred to here as PFD protein) in order to understand its role in the modifications of the infected erythrocyte membrane. Only a few of parasite-exported proteins have been characterized on the molecular basis. Functional characterization of the proteins may help to understand more about host erythrocyte remodelling by the parasites. PFD is unique to *P. falciparum* and was found to be important for knob formation and adhesion of the iRBCs to CSA (Maier et al, 2008). Hence, we were interested in investigating the molecular interactions and physiological role of the PFD molecule.

In order to explore its molecular interactions, we have investigated the expression of PFD, its location, solubility and interacting partners (chapter 3). We have shown that the protein is expressed in all erythrocytic asexual stages of the parasite with a slight increase in the rings. While fluorescence of PFD-GFP chimera is restricted to the parasite cytoplasm at the early ring stage, rim fluorescence signal of the protein was located to the iRBCs membrane from mid ring to late trophozoite stage. The results are coherent with mRNA levels of PFD peaking at the merozoite stage, suggesting a high level of translation in the early ring stage (Le Roch et al, 2004) when the host cell remodelling starts to occur (Marti et al, 2004). Combining the result with the previous finding that the molecule has influenced knob formation and adhesion of the

iRBCs (Maier et al, 2008), we propose that PFD may play a role in the process of host cell membrane modifications.

The PFD protein is insoluble in TX-100 and TX-114 detergents but soluble in sodium carbonate, indicating that PFD is a peripheral membrane protein. The solubility profile is similar to that of other RBC cytoskeleton-binding proteins (Nilsson et al, 2012; Proellocks et al, 2014), which leads to a speculation that PFD may associate with the RBC cytoskeleton. However, in order to arrive at a definitive conclusion in this regard, confirmation of this interaction using RBC proteins containing insight-out-vesicles, immunoprecipitation (IP) assays and/or mass spectrometry (MS) analysis needs to be performed.

We have also demonstrated that PFD interacts with RESA, a key player in stabilizing the RBC cytoskeleton against febrile temperature (Da Silva et al, 1994). This is based on the fact that the two proteins co-localized in the IFA assays. Moreover, they were co-precipitated by both anti-RESA and anti-PFD antibodies. In addition, the proteins were present in complexes of a similar size at ~ 400 kDa. The data strongly suggest that PFD and RESA are interacting with each other and are likely present in the same complex. In order to clarifying what other proteins are present in the ~ 400 kDa complex in which PFD and RESA are residents, IP assays using anti-PFD antibodies followed by MS analysis could be performed.

The disruption of either PFD or RESA does not affect the localisation of each other: using IFA, we were able to show that the rim fluorescence of RESA or PFD was normal in the PFD disrupted or RESA disrupted cells in comparison to their parental cells. It is possible that they might not transport together therefore their locations are not affected but the two molecules might need to form the complex for their functions

at the ring stage. RESA starts to be degraded at later parasite stages, while PFD remains in / under erythrocyte membrane, suggesting that the protein may be involved in other molecular interactions at the stages.

Disruption of PFD does not affect the localisation of KAHRP and knob formation. The PFD disrupted cells did show the rim fluorescence of KAHRP on the iRBC surface and form knobs as normal as their parental cells. However, we cannot exclude that disruption of PFD may delay the knob formation in the early stages of the asexual parasite lifecycle due to its transient interactions with other unknown knob proteins. In order to answer the question, a quantitative knob analysis in terms of knob number and knob size on tightly synchronised cells might be performed with the service of confocal microscopy, scanning electron microscopy and atomic force microscopy.

In order to further investigate the molecular interactions of PFD and RESA, it is worthwhile to first look at when and where they start to interact with each other. Based on our localisation and expression studies of the PFD protein, it is proposed that the molecule is initially transcribed in late schizonts, merozoites, and translated in very young rings. PFD partner - RESA is secreted from merozoite dense granules (Aikawa et al, 1990). Immunoelectron microscopy and immunoblotting analysis with antibodies against PFD and RESA in the very early stages of the asexual parasites might help to explore this aspect.

In order to explore the biophysical interactions of the PFD and RESA proteins, analysing the structure of the two proteins could be helpful. The recombinant PFD and RESA proteins could be produced in *E. coli* or Yeast and then purified by metal ion-affinity chromatography, ion exchange and size exclusion chromatography. The

Small Angle X-ray Scattering (SAXS) is then performed to identify the position at which the two proteins interact (Mayer et al, 2012).

Regarding the trafficking route of the molecules, double fluorescence tagging of PFD and RESA in the same cells might be generated and imaged with a high-resolution microscopy to see whether these molecules are transported via the same route.

The PFD protein contains a PHISTb domain at the C-terminal that might play a role in protein-protein interactions. At this stage we have not characterized the function of the domain. It could be worthwhile to test whether the PHISTb domain plays a role in interactions between PFD and RESA. PHISTb truncated PFD cell line could be generated. The bindings between the truncated PFD and RESA could be tested via co-IP. Localisation of GFP tagged PFD truncations might be tested to see whether the truncated proteins affect RESA localisation. However it is unlikely given the finding that the PFD disrupted cells did not affect the RESA localisation. To test the function of the PHISTb domain in PFD binding to the iRBC membrane, PFD recombinant proteins could be tested with inside-out-vesicles (IOVs) prepared from normal human RBCs (Waller et al, 2007). The level of the fragmented PFD binding to RESA and/or IOVs will be evaluated by Western blot. The results could reveal the role of PHISTb domain in binding of PFD to the infected erythrocyte membrane and/or RESA.

In chapter 4 we analysed the functions of PFD by investigating how the infected cells with or without PFD behave with regards to osmotic fragility, adhesion, retention and parasite growth. To test the influence of PFD on the iRBCs membrane stability, we performed the osmotic fragility from low to high tonicity of $NaCl/PO_4$ salt concentration. We observed a slight difference in osmotic fragility at low tonicity in

which the haemolysis of the PFD deleted cells is higher than that of wild-type and similar to that of the RBCs.

In order to see how the PFD disrupted cells affect adhesion of the iRBCs to the host receptor, we performed an adhesion assay under plate-shaking condition with CSA-containing vesicles prepared from placental patients. The result did not show significant difference in binding between the wildtype and the disrupted iRBCs, while in previous study the knock-out cells showed a reduced adhesion rate by 50% under physiological flow condition and no adhesion under static condition (Maier et al, 2008). The difference in the adhesion of the PFD disrupted iRBCs and wild-type cells to the CSA-containing vesicles was not observed in the shaking condition.

We have shown that PFD is important for parasite growth during its asexual cycle at body temperature. We compared the growth rate between the disrupted cells and the wild-type cells by co-culturing the two cell lines in the same dish and using quantitative real-time PCR to compare the ratio of parasites genomic DNA between the wild-type and the PFD deleted cells. We observed a 5-time reduction in growth of PFD deleted parasites compared to wild-type after 10 parasite life cycles of the growth competition culture. However, we failed to obtain the competitive growth for the transiently heat-shocked cells since the wild-type parasites seem to be more susceptible to the elevated temperature. It is plausible that disruption of PFD might lead to a reduction in the parasite biomass *in vivo*.

The expression of PFD protein increases the retention rate of the iRBCs at febrile temperature in the human spleen and in its surrogate technique, microsphiltration. We found that filterability of the heat-shocked PFD disrupted ring cells in microsphiltration was significantly reduced by 37% compared to that of wild-type.

Furthermore, we had confirmed the phenotype in the *ex-vivo* perfusion of isolated human spleens in three independent experiments with an average reduced retention of ~ 42% after one hour perfusion. Additionally, the phagocytosis of the PFD disrupted cells by white cells was not observed while the wild-type showed from 35% to 78% of the regard. In order to squeeze through the narrow spaces of the interendothelial slits of the splenic sinus, the iRBCs have to be greatly deformable. It had been found that a proportion of the ring-iRBCs could be retained in the spleen due to its reduced deformability (Deplaine et al, 2011). Our findings suggest that the expression of PFD protein potentially reduces the deformability of the ring-iRBCs and therefore increases the retention and the splenic clearance of the iRBCs, particularly at febrile temperature.

Overall, PFD seems to have two functions: supporting parasite growth at body temperature and facilitating killing of parasites by the spleen at febrile temperature. The PFD might act as a sensor that balances the pace of the parasite growth and the time to form gametocytes for their next transmission. The theory is demonstrated in Figure 5.1 in which the parasites containing the PFD grow faster at body temperature and when the parasite density is high enough to trigger malaria fever, a number of the parasites are retained in the spleen and destroyed by white cells and hence reducing the parasite biomass in the host.

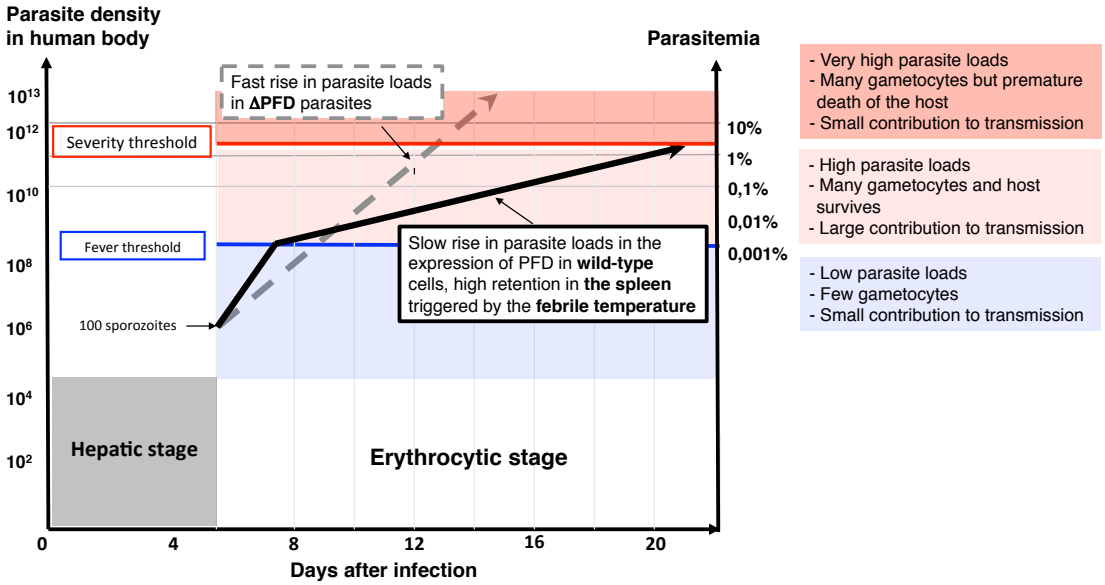

Figure 5.1. A sensor theory for PFD. The presence of PFD is important for the parasite growth at body temperature. A proportion of the iRBCs can be destroyed by the spleen when fever is induced and this leads to the decreased parasitemia in the human body. Continuous line, wild-type; dashed line, PFD disrupted cells.

The wild-type parasites (having PFD) initially multiply at a very fast rate to reach to the pyrogenic threshold (fever threshold), the minimum parasite density in order to trigger malaria fever (see (Oakley et al, 2011; Oakley et al, 2007) for review). Then, the parasites slow their growth in order to prevent death of the host induced by very high parasite loads. The *P. falciparum* parasites do not want to kill their host in order to gain enough time (at least 2 weeks) to produce gametocytes for the continuous parasite transmission to the mosquito vector. The strategy supports the parasite survival in the host. By contrast, the PFD disrupted cells may not have that sensor when the febrile temperature is triggered. Thus, the disrupted parasites can continuously grow very fast and cause premature death of the host when the parasite density reaches to severity threshold. It also means the disrupted cells may not provide the parasite sufficient time to further transmit infection. It is speculated that PFD may be potentially involved in the mechanisms regulating the parasite density in

the human host to adapt to the febrile temperature, which benefits to the long-term parasite existence. However, it is difficult to draw any definite conclusion until experimental evidences *in vivo* are provided, for example the lethality of the infected animals and the gametocyte production in the absence and presence of PFD.

Observations in this study on the molecular interactions and physiological role of PFD are just an initial step in understanding the functions of the protein in the asexual development of the malaria parasites. In order to deepen our understanding of the molecular mechanism of PFD and/or RESA in the *P. falciparum* infected-RBCs, further investigations are needed. We could generate a double knock-out for the two molecules in the same parasites. Simultaneously functional investigations of the three knock-out cell lines ΔPFD, ΔRESA and ΔPFD-ΔRESA could provide additional insights into the role of PFD complexes in host cell modifications by the parasites in terms of parasite growth, the deformability and retention of the iRBCs.

In conclusion, we found that PFD interacts with RESA. The expression of PFD reduces the deformability and increases the retention of the ring-iRBCs at the febrile temperature. The presence of the protein might lead to the reduced parasite loads when fever occurs due to the parasite clearance by the spleen, while the molecule is also important for the parasite growth at body temperature. Our findings raised some new ideas about the mechanism of PFD involved in regulating parasite density when the malaria fever is triggered at the pyrogenic threshold. Exploring the molecular mechanism of PFD might open new avenues in controlling the parasitised-RBC biomass in human body and the parasite transmission to the insect vector, which might diminish the severe complications in the *P. falciparum* infected patients and reduce the spreading of the infectious disease.

Appendix 1: Materials and Methods: General solutions

Complete RPMI

To 1× RPMI (500 mL bottle containing GlutaMAX, HEPES and Phenol Red) (Invitrogen), add under aseptic conditions:		
Per bottle:	**Amount**	**Final Conc.**
45% glucose solution	2 mL	10 mM
200 mM hypoxanthine	1.2 mL	480 µm
10 mg/mL gentamicin solution	1 mL	20 µg/mL
10% ALBUMAX II solution	25 mL	0.5% w/v
Heat inactivated human serum	12.5 mL	2.5% v/v
Store medium at 4ºC for a maximum of one month. If the medium in the bottle is getting low, transfer to a smaller tube to prevent pH change of medium.		
Warm to 37ºC before use.		

TE Buffer, pH 8.0

Per 100 mL	**Amount**	**Final Conc.**
1 M Tris-HCl, pH 7.5	1 mL	10 mM
0.1 M EDTA, pH 8.0	1 mL	1 mM
Dissolve in distilled water	80 mL	-
Adjust to pH 8.0 by dropwise addition of 5 M NaOH		
Make up volume to 100 mL with distilled water		
Sterilise by autoclaving		
Store at RT		

Freezing Solution

Per 50 mL	**Amount**	**Final Conc.**
Glycerol*	14 mL	28% v/v
Sorbitol	1.5 g	3% w/v
NaCl	0.325 g	0.65% w/v
Dissolve in distilled water	30 mL	-
Make up volume to 50 mL with distilled water		
Sterilise using a 0.22 µm filter		
Store at 4ºC		

*Note: Glycerol is viscous and therefore difficult to pipette accurately (1.25 g Glycerol = 1 mL of Glycerol). Weigh glycerol in beaker before adding the other ingredients. It is vital that these are weighed out accurately.

SOC Recovery Medium

Per 1 L	**Amount**	**Final Conc.**
Bacto Tryptone	20 g	2% w/v
Yeast extract	5 g	0.5% w/v
Dissolve in distilled water	900 mL	-
1 M NaCl	10 mL	10 mM
1 M KCl	2.5 mL	2.5 mM
Sterilise by autoclaving (121°C, 20 mins), allow to cool		
2 M Mg^{2+}	10 mL	0.02M
2 M glucose	10 mL	0.02M
Store at 4°C		

Glycerol Broth

Per 100 mL	**Amount**	**Final Conc.**
Brain heart infusion broth powder	3.7 g	3.7% w/v
Dissolve in distilled water	45 mL	-
Make up volume to 50 mL with distilled water		
Glycerol	50 mL	50% v/v
Mix glycerol and broth completely		
Make 10 mL aliquots into 20 mL bottles		
Sterilise by autoclaving (121°C, 20 mins)		
Store at 4°C		

Gel Loading Buffer, 6 x

Per 100 mL	**Amount**	**Final Conc.**
Sucrose	50 g	50% w/v
EDTA disodium salt	3.7 g	0.1 M
Dissolve in distilled water	50 mL	-
Adjust to pH 7.0 by dropwise addition of 10 M NaOH		
Make up volume to 100 mL with distilled water		
Add 50 mg of bromophenol blue to colour the buffer		
Store at RT		

TBE Buffer, 5 x

Per 1 L	**Amount**	**Final Conc.**
Tris base	54 g	445 mM
Boric acid	27.5 g	445 mM
Dissolve in distilled water	800 mL	-
0.5 M EDTA pH 8.0	20 mL	10 mM
Make up volume to 1 L with distilled water		
The final pH of the buffer should be ~ 8.3, store at RT		

GYT Medium

Per 20 mL	**Amount**	**Final Conc.**
Glycerol	2 mL	10% v/v
Yeast extract	25 mg	0.125% w/v
Tryptone	50 mg	0.25% w/v
Make up volume to 20 mL with distilled water		
Sterilise using a 0.22 µm filter		
Store at 4°C		

SSC, 20 x

Per 1 L	**Amount**	**Final Conc.**
NaCL	175.3 g	3 M
Citric acid, trisodium dihydrate	88.2 g	0.3 M
Dissolve in distilled water	700 mL	-
Adjust to pH 7.0 by dropwise addition of concentrated HCl		
Make up volume to 1 L with distilled water, store at RT		

Coomassie Blue Stain Solution

Per 1 L	**Amount**	**Final Conc.**
Coomassie Brilliant Blue R-250	1 g	0.1% w/v
Dissolve in isopropanol	250 mL	25% v/v
Acetic acid, glacial	70 mL	7% v/v
Distilled water	680 mL	-
Filter through Whatman 3MM paper, store at RT		

Coomassie Blue Destain Solution

Per 1 L	**Amount**	**Final Conc.**
Distilled water	500 mL	-
Acetic acid, glacial	100 mL	10% v/v
100% Ethanol	400 mL	40% v/v
Store at RT		

Transfer Buffer, 1 x

Per 1 L	**Amount**	**Final Conc.**
SDS	0.37g	0.037% w/v
Tris	5.8 g	0.58% w/v
Glycine	2.9 g	0.29% w/v
Methanol	200 mL	20% v/v
Distilled water	800 mL	
Store at RT		

Gel Buffer, 3 x

Reagents	**Final Conc.**
ε-amino n-caproic acid	200 mM
Bis-tris pH 7.0	150 mM

Blue Native Loading Dye, 10 x

Reagents	**Final Conc.**
Coomassie blue G	5%
ε-amino n-caproic acid	500 mM
Bis-tris pH 7.0	100 mM

Anode Buffer, 1 x

Reagents	**Final Conc.**
Bis-Tris pH 7.0	50 mM

Cathode Buffer, 1 x

Reagents	**Final Conc.**
Tricine	50 mM
Bis-Tris	15 mM
Coomassie blue G	0.02%

Solubilisation Buffer, 3 x

Reagents	**Final Conc.**
Bis-Tris pH 7.0	60 mM
NaCl	150 mM
Glycerol	30%

Empty Well Buffer

Reagents	**Final Conc.**
Bis-Tris pH 7.0	20 mM
NaCl	50 mM
Glycerol	10%
Coomassie blue G	30%

Acrylamide Solutions

Gel percentage (%)	**4%**	**16%**
3 x gel buffer	33.3 mL	33.3 mL
Acrylamide	8.08 mL	33.3 mL
Glycerol	-	20.0 mL
Distilled water	58.6 mL	13.4 mL
Total	100 mL	100 mL
Store at 4^{o}C in dark		

Denhardts Solution, 100 x

Per 50 mL	**Amount**	**Final Conc.**
Bovine serum albumin (Fraction V)	1 g	2% w/v
Ficoll 400	1 g	2% w/v
Polyvinylpyrrolidone (PVP)	1 g	2% w/v
Sterilise using a 0.22 μm filter		
Store at -20^{o}C		

Maleic Acid Solution, 10 x

Per 1 L	**Amount**	**Final Conc.**
1 M Maleic Acid	116.07 g	1 M
1.5 M NaCl	87.66 g	1.5 M
Adjust to pH 7.5 by adding NaOH		
Store at RT		

Pre-hybridization Solution

Per 100 mL	**Amount**	**Final Conc.**
20 x SSC	30 mL	6 x
100 x Denhardts solution	5 mL	5 x
10% SDS	1 mL	0.1% w/v
10 x Roche blocking solution	10 mL	1 x
10 x Maleic Acid Buffer	10 mL	1 x
Distilled water	Up to 100 mL	
Prepare and use fresh		

PBS, 10 x

Per 1 L	**Amount**	**Final Conc.**
NaCl	80.07 g	1.37 M
KCl	2.01 g	27 mM
Na_2HPO_4	6.1 g	43 mM
KH_2PO_4	1.9 g	14 mM
Dissolve in distilled water	800 mL	-

Adjust to pH 7.4 by dropwise addition of concentrate HCl
Make up volume to 1 L with distilled water
Store at RT

Western Stripping Buffer

Per 1 L	**Amount**	**Final Conc.**
Tris-HCl	7.57 g	62.5 mM
SDS	20 g	2% w/v
Make up volume to 1 L with distilled water, store at RT		

Appendix 2: Supplementary Tables

Table S1. Primers used in the experiments

Primers	5' - 3' sequence (restriction sites underlined)
Al142	gagctcgagTTAATCTCCTTTACAGTATCC
Al143	gatactagtCCACCACTTATACCTCTAATAAATGCATCACC
Al227	acagcggccgcGCCAATTAGCTATTTTTGGTATTTACC
Al228	ccactcgagTTTAAGATAGATTATATCCTACTGAAC
Al166	GATTACGCATACTGCATATATAAAAAGGC
Al167	CCGTTGGAGTTAGAAAAGCTTGATCCG
Aw362	atccgcggAAAATTCGTACAGAAGTCC
Aw364	gatagatctGCTGAGTTCTTAAGATTCTTGCTATCC
Al09	TAAACTAGAAAAGGAATAAC
Al10	TTTGTAATTTCTGTGTTTATG
M13 Forward	GTAAAACGACGGCCAG
M13 Reverse	CAGGAAACAGCTATGAC
Fw156	aaaggatccGGACAATCTACAGATGAA
Fw158	aaaggatccACTATTAAAGCTATGGAA

Underlined lower cases are restriction enzyme sequences. Lower cases are additional nucleotides. Upper cases are coding sequences.

Table S2. Primer and probe sets used in quantitative PCR

Primers and Probes	**5' - 3' sequence**
PFD1170c	
Probe	/56FAM/CGTATGGTT/Zen/ATACCTATGTTGGGTGTTCTCTATGT/3IABkFQ
Forward Primer	CTTTTGATGAAGAGGAAAAGAAAACTGC
Reverse Primer	ATGTAAACATACGTTCTAAAGGGAAAGAGG
hDHFR	
Probe	/5HEX/CAGAACATG/Zen/GGCATCGGCAAGAACG/3IABkFQ/
Forward Primer	CATGGTTCGCTAAACTGCATC
Reverse Primer	GAGGTTGTGGTCATTCTCTGG

Appendix 3: Supplementary Figures

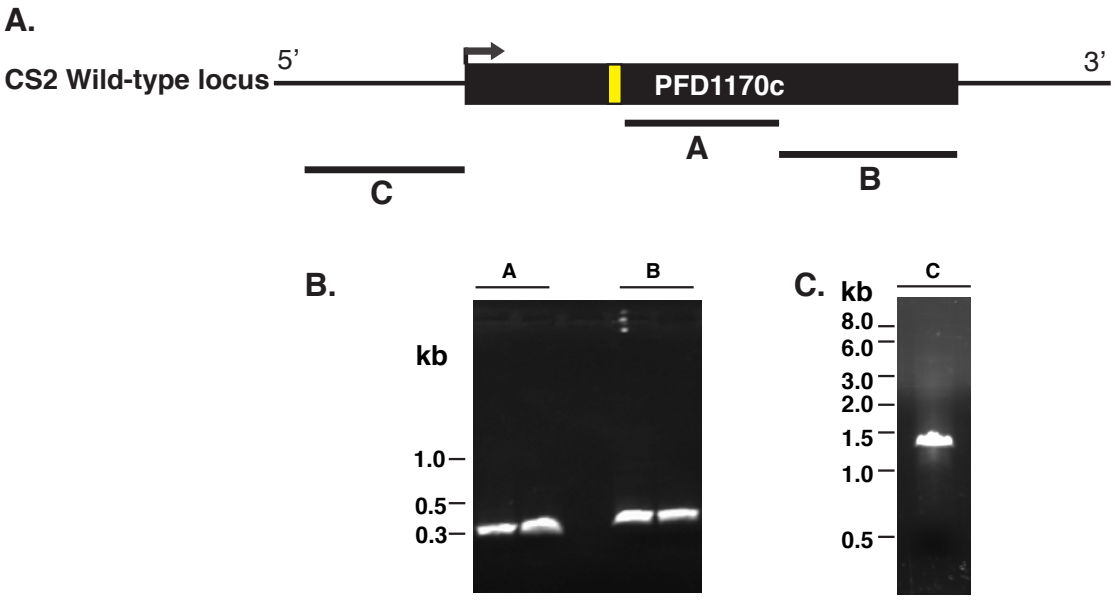

Figure S1. Amplification of *PFD1170c* DNA fragments for antibodies production and endogenous promoter. (**A)** The schematic representation of *PFD1170c* gene locus and selected regions for amplifications. Diagram is not to scale. Yellow bar represents the region encoding PEXEL motif. (**B)** Amplifications of *PFD1170c* DNA regions by Polymerase Chain Reactions (PCR) at different annealing temperatures (52 and 56^{o}C) with CS2 genomic DNA as template**.** Regions A (nucleotides 273 – 573) and B (nucleotides 574 – 927) were amplified using primer sets fw156/al142 and fw158/al143, respectively. Each region was inserted into the plasmid pGEX-4T-1 to generate pGEX-4T-1/*PFD1170c*-A and pGEX-4T-1/*PFD1170c*-B constructs. Region C (*PFD1170c* endogenous promoter, nucleotides (-1,371) – (-1) was amplified using primer set al227/al228 and replaced *CRT* promoter in plasmid pGLUX-6 (with puromycine acetyl transferase drug selection cassette) in order to generate complementation construct pGLUX-6/*PFD1170c* driven by the endogenous promoter. The expected sizes of these fragments were: **A**, 309 bp; **B**, 360 bp and **C**, 1,371 bp. NEB 1 kb and NEB 100 bp markers were used.

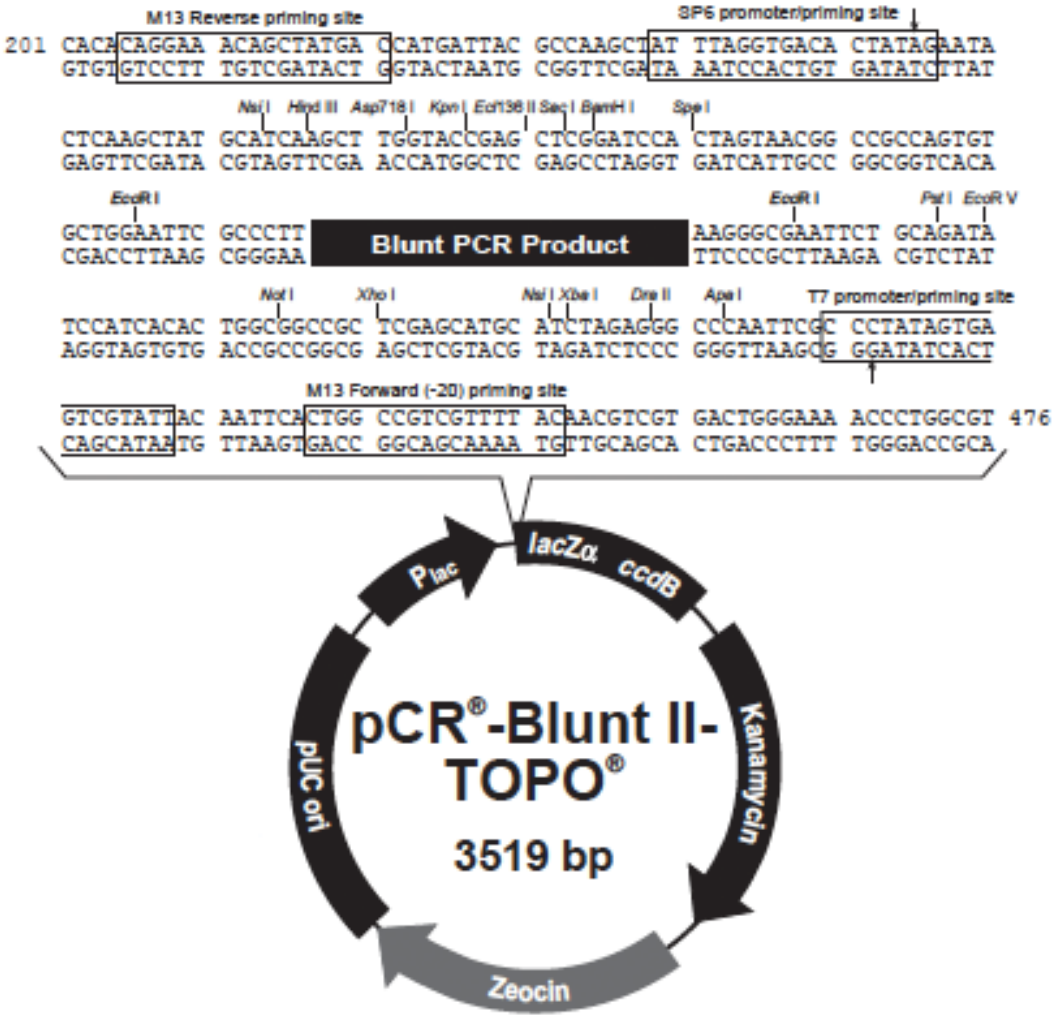

Figure S2. Map of pCR®- Blunt II-TOPO vector (Invitrogen).

The PCR products of *PFD1170c*-A & B were purified and cloned into the pCR®- Blunt II-TOPO at the insertion site (see section 2.2.9) before being transfered into the pGEX-4T-1 vector.

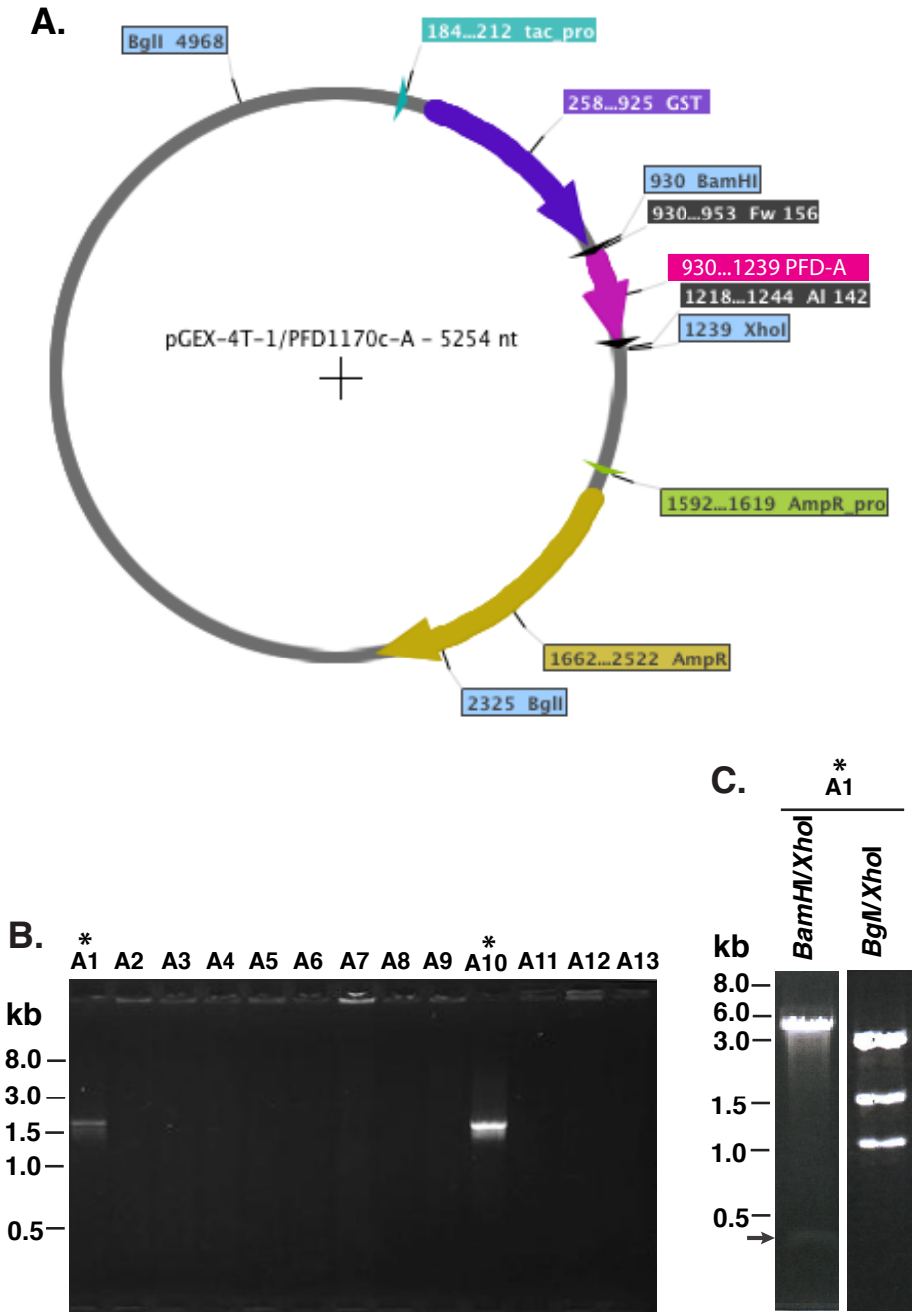

Figure S3. GST tagged *PFD1170c*-A construct. (A) Vector map of pGEX-4T-1 /*PFD1170c*-A construct. **(B)** Screening of bacteria colonies for construct pCR®- Blunt II-TOPO/region A by PCR using primers M13 reverse / al142. The expected size of the product was 1,711 bp. *, positive colonies. **(C)** Confirmation of region A (fragment following PEXEL motif) insertion into pGEX-4T-1 vector by restriction digestions. Positive colonies A1 and A10 were propagated and the plasmids were Miniprep extracted for restriction digestions. Region A was digested by enzymes *BamH*1 and *Xho*I, while internal fragment digestion was performed using *Bgl*I and *Xho*I, respectively. The expected sizes of the products were 309 bp, 4,945 bp for the *BamH*I/*Xho*I digestion; and 1,086 bp, 1,525 bp, 2,643 bp for *Bgl*I/ *Xho*I, respectively. Confirmed positive colony A1 was propagated in LB medium with and without IPTG for testing protein expression**.** NEB 1 kb marker was used.

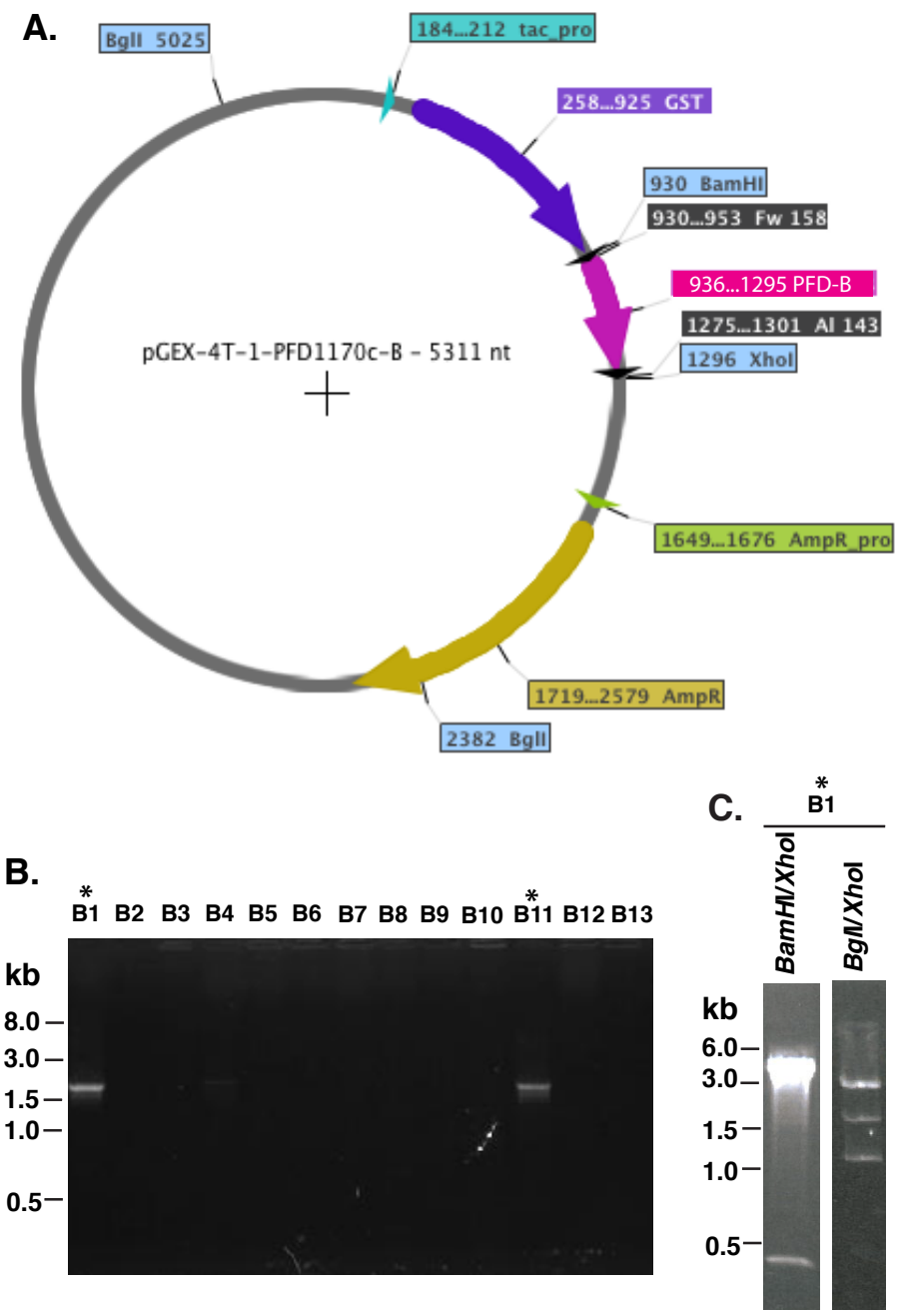

Figure S4. GST tagged *PFD1170c*-B construct. (A) Vector map of pGEX-4T-1 /PFD1170c-B construct. **(B)** Screening of bacteria colonies for construct pCR®- Blunt II-TOPO/region B by PCR using primers M13 reverse /al143. The expected size of the product was 1,751 bp. *, positive colonies. **(C)** Confirmation of region B (3' fragment of *PFD1170c*) insertion into pGEX-4T-1 vector by restriction digestions. Positive colonies B1 and B11 were propagated and the plasmids were Miniprep extracted for restriction digestions. Region B was digested using enzymes *BamH*1 and *Xho*I, while internal fragment digestion was performed using *Bgl*I and *Xho*I, respectively. The expected sizes of the products were 366 bp, 4,945 bp for the *BamH*1/*Xho*I digestion; and 1,086 bp, 1,582 bp, 2,643 bp for *Bgl*I/ *Xho*I, respectively. Confirmed positive colony B1 was inoculated in LB broth with and without IPTG for testing protein expression**.** NEB 1 kb marker was used.

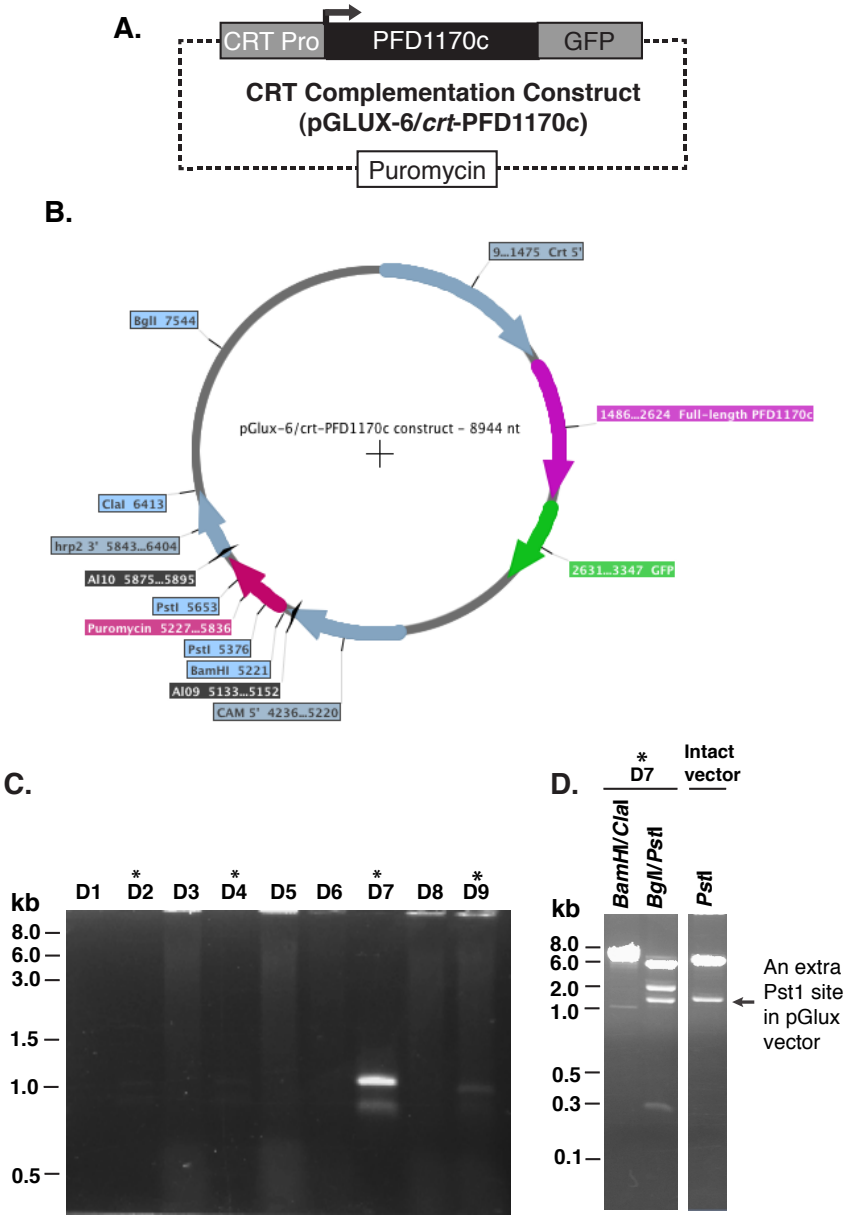

Figure S5. Generation pGLUX-6/crt-*PFD1170c* complementation construct (CRT promoter). (A) Schematic representation of CRT complementation construct. The *hDHFR* selection cassette was replaced by the puromycin selection cassette and the expression of the full-length coding region of *PFD1170c* gene followed by *gfp* gene was driven by the *CRT* promoter. Black box, *PFD1170c* coding region; open box, puromycin selection cassette. **(B)** Vector map of pGLUX-6/crt-*PFD1170c* complementation construct. **(C)** Screening of bacteria colonies for construct pGLUX-6/crt-*PFD1170c* by PCR using primers al09/al10. The expected size of the product was 763 bp. *, positive colonies. **(D)** Confirmation of puromycin selection cassette insertion by restriction digestions. Positive colonies D7 and D9 were propagated and the plasmids were Miniprep extracted for restriction digestions. Puromycin selection cassette was digested using enzymes *BamH*1 and *Cla*I while internal fragment digestion was performed using *Bgl*I and *Pst*I, respectively. The expected sizes of the products were 1,192 bp, 7,752 bp for the *BamH*1/*Cla*I digestion; and 277 bp, 1,891 bp, 6,776 bp for *Bgl*I/ *Pst*I, respectively.

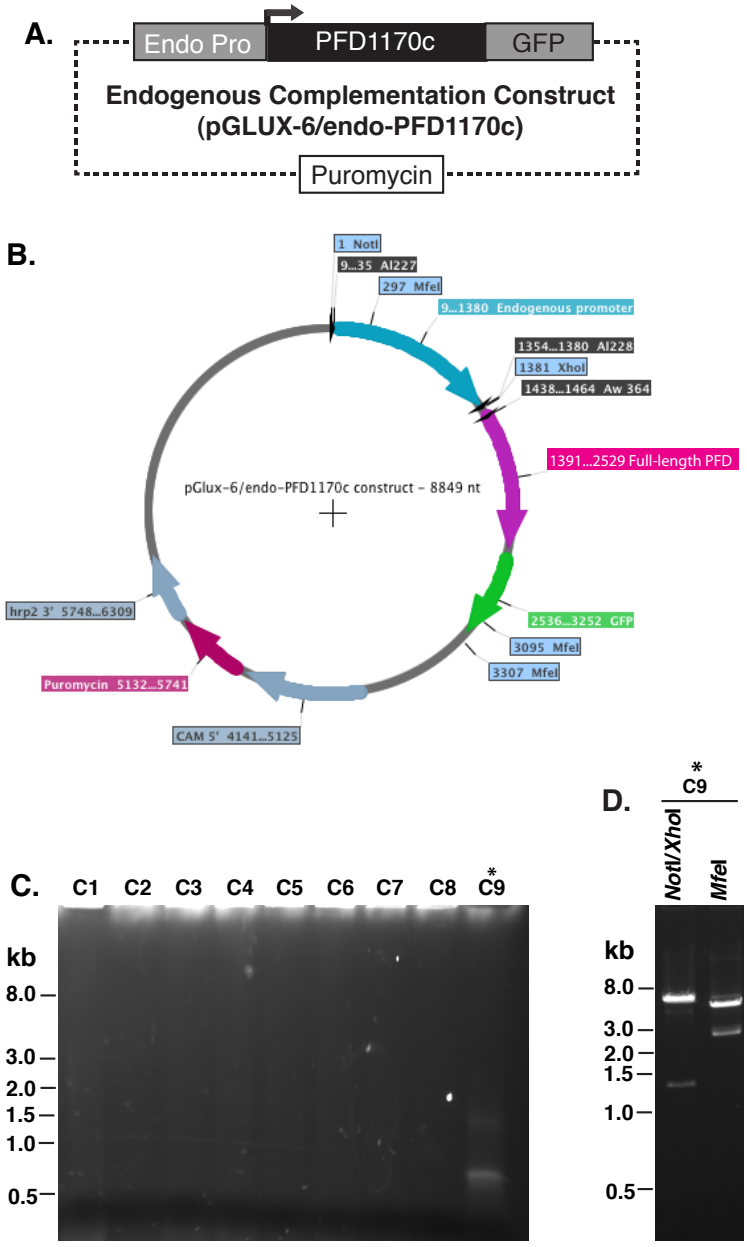

Figure S6. *PFD1170c* endogenous complementation construct (endogenous promoter). (A) Schematic representation of endogenous complementation construct. The *crt* promoter was replaced by endogenous promoter of *PFD1170c* and the expression of the full-length coding region of *PFD1170c* gene followed by *gfp* gene was driven by the endogenous promoter. Black box, *PFD1170c* coding region; open box, puromycin selection cassette. **(B)** Vector map of pGLUX-6/endo-*PFD1170c* complementation construct. **(C)** First screening of bacteria colonies containing construct pGLUX-6/endo-*PFD1170c* by PCR using primers al227/aw364. The expected size of the product was 1,476 bp. *, positive colonies. **(D)** Confirmation of endogenous promoter of *PFD1170c* (region C) insertion by restriction digestions. Positive colonies C9 was propagated and the plasmids were Miniprep extracted for restriction digestions. The promoter was digested using enzymes *Not*I and *Xho*I while internal fragment digestion was performed using *Mfe*I. The expected sizes of the products were 1,380 bp and 7,469 bp for the *Not*I/ *Xho*I digestion; and 212 bp, 2,798 bp, 5,839 bp for *Mfe*I.

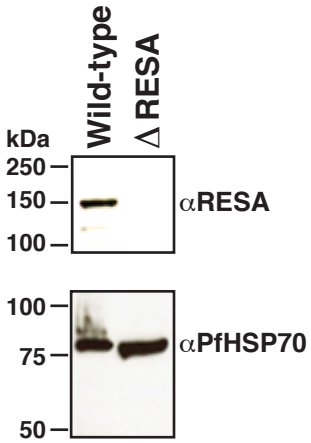

Figure S7. Disruption of RESA protein in CS2 cell line. Mouse anti-RESA (to detect RESA in wild-type) and anti-PfHSP70 (to control loadings) antibodies were used for Western blot analysis.

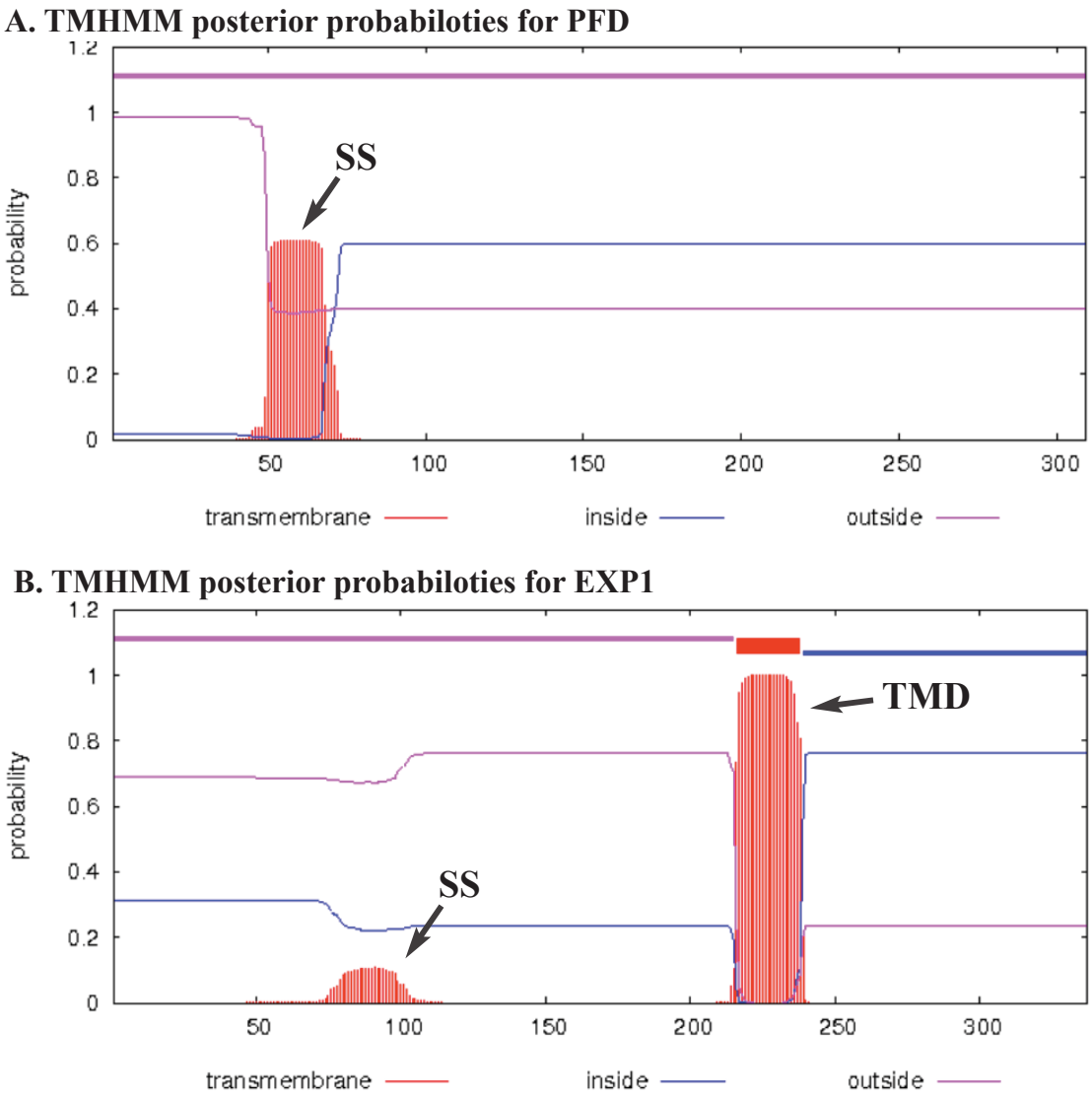

Figure S8. Transmembrane domain (TMD) prediction of PFD (A) and EXP1 (B). PFD contains a signal sequence (SS) at the N-terminal and no transmembrane domain (TMD). As a control, transmembrane protein EXP1 contains a TMD after the SS. The TMD prediction was run by TMHMM program (Sonnhammer et al, 1998).

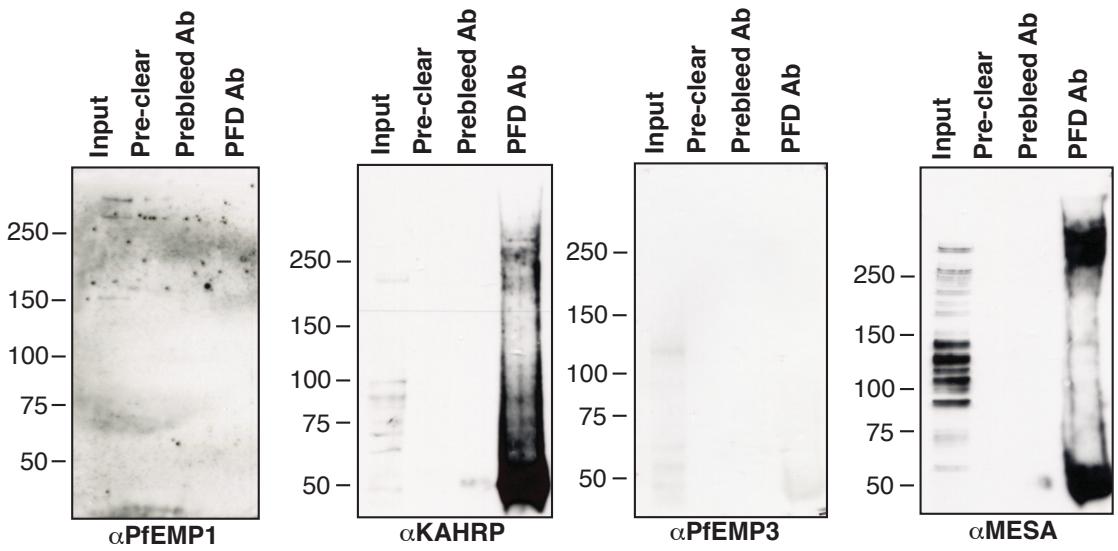

Figure S9. PfEMP1, KAHRP, PfEMP3 and MESA are not found in PFD antibodies precipitated complexes. Immunoprecipitation assays were performed on 1% Zwittergent 3-14 lysed CS2-wildtype cells at trophozoite stage (20 – 28 h). Anti-PFD antibodies were used to precipitate PFD complexes. The immunoblottings of precipitated samples were performed using anti-PfEMP1, KAHRP, PfEMP3 and MESA antibodies. Input, parasite lysate before IP; Pre-clear, precipitation without using antibodies; Pre-bleed Ab, precipitation with pre-bleed antisera (before immunisation); PFD Ab, precipitation with anti-PFD antibodies. Molecular weight of PfEMP1 is ~ 300 - 350 kDa, KAHRP ~ 85 - 110 kDa, PfEMP3 ~ 315 kDa and MESA ~ 250 - 300 kDa.

References

Aikawa M, Torii M, Sjolander A, Berzins K, Perlmann P, Miller LH (1990) Pf155/RESA antigen is localized in dense granules of *Plasmodium falciparum* merozoites. *Experimental Parasitol* **71:** 326-329

Aly ASI, Vaughan AM, Kappe SHI (2009) Malaria parasite development in the mosquito and infection of the mammalian host. *Annual Review of Microbiology* **63:** 195-221

Ansorge I, Benting J, Bhakdi S, Lingelbach K (1996) Protein sorting in *Plasmodium falciparum*-infected red blood cells permeabilized with the pore-forming protein streptolysin O. *Biochemical Journal* **315:** 307-314

Antoine K (2004) Overview of malaria in West Africa. *WHO Newsletter* **5(2)**

Ausubel FM, Brent R, Kingston RE, Moore DD, Seidman JG, Smith JA, Struhl K (2004) *Current Protocols in Molecular Biology*: John Wiley & Sons, Inc. .

Bannister LH, Hopkins JM, Fowler RE, Krishna S, Mitchell GH (2000) A brief illustrated guide to the ultrastructure of *Plasmodium falciparum* asexual blood stages. *Parasitology Today* **16:** 427-433

Barsoum RS (2000) Malarial acute renal failure. *Journal of the American Society of Nephrology* **11:** 2147-2154

Bartoloni A ZL (2012) Clinical aspects of uncomplicated and severe malaria. *Hematology and Infectious Diseases* **4:** e2012026

Baruch DI, Gormely JA, Ma C, Howard RJ, Pasloske BL (1996) *Plasmodium falciparum* erythrocyte membrane protein 1 is a parasitized erythrocyte receptor for adherence to CD36, thrombospondin, and intercellular adhesion molecule 1. *Proceedings of the National Academy of Sciences* **93:** 3497-3502

Beeson JG, Amin N, Kanjala M, Rogerson SJ (2002) Selective accumulation of mature asexual stages of *Plasmodium falciparum*-infected erythrocytes in the placenta. *Infection and Immunity* **70:** 5412-5415

Benting J, Mattei D, Lingelbach K (1994) Brefeldin A inhibits transport of the glycophorin-binding protein from *Plasmodium falciparum* into the host erythrocyte. *Biochemical Journal* **300:** 821-826

Biggs BA, Kemp DJ, Brown GV (1989) Subtelomeric chromosome deletions in field Isolates of *Plasmodium falciparum* and their relationship to loss of cytoadherence invitro. *Proceedings of the National Academy of Sciences* **86:** 2428-2432

Black CG, Proellocks NI, Kats LM, Cooke BM, Mohandas N, Coppel RL (2008) In vivo studies support the role of trafficking and cytoskeletal-binding motifs in the interaction of MESA with the membrane skeleton of *Plasmodium falciparum*-infected red blood cells. *Molecular and Biochemical Parasitology* **160:** 143-147

Boddey JA, Carvalho TG, Hodder AN, Sargeant TJ, Sleebs BE, Marapana D, Lopaticki S, Nebl T, Cowman AF (2013) Role of plasmepsin V in export of diverse protein families from the *Plasmodium falciparum* exportome. *Traffic* **14:** 532-550

Boddey JA, Hodder AN, Gunther S, Gilson PR, Patsiouras H, Kapp EA, Pearce JA, de Koning-Ward TF, Simpson RJ, Crabb BS, Cowman AF (2010) An aspartyl protease directs malaria effector proteins to the host cell. *Nature* **463:** 627-631

Boeuf P, Hasang W, Hanssen E, Glazier JD, Rogerson SJ (2011) Relevant assay to study the adhesion of *Plasmodium falciparum*-Infected erythrocytes to the placental epithelium. *PLoS ONE* **6:** e21126

Bordier C (1981) Phase separation of integral membrane proteins in Triton X-114 solution. *The Journal of Biological Chemistry* **256:** 1604-1607

Buffet PA (1999) Plasmodium falciparum domain mediating adhesion to chondroitin sulfate A: a receptor for human placental infection. *Proceedings of the National Academy of Sciences* **96:** 12743-12748

Buffet PA (2006) Ex vivo perfusion of human spleens maintains clearing and processing functions. *Blood* **107:** 3745-3752

Buffet PA, Safeukui I, Deplaine G, Brousse V, Prendki V, Thellier M, Turner GD, Mercereau-Puijalon O (2011) The pathogenesis of *Plasmodium falciparum* malaria in humans: insights from splenic physiology. *Blood* **117:** 381-392

Buffet PA, Safeukui I, Milon Gv, Mercereau-Puijalon O, David PH (2009) Retention of erythrocytes in the spleen: a double-edged process in human malaria. *Current Opinion in Hematology* **16:** 157-164

Cesta M (2006) Normal structure, function, and histology of the spleen. *Toxicologic Pathology* **34:** 455-465

Chishti AH, Andrabi KI, Derick LH, Palek J, Liu SC (1992) Isolation of skeleton-associated knobs from human red blood cells Infected with malaria parasite *Plasmodium falciparum*. *Molecular and Biochemical Parasitology* **52:** 283-288

Coligan JE, Dunn BM, Speicher DW, Wingfield PT (2009) *Current Protocols in Protein Science*: John Wiley & Sons, Inc.

Collins WE (2012) *Plasmodium knowlesi*: A malaria parasite of monkeys and humans *Annual Review of Entomology* **57:** 107-121

Cooke BM (1994) Rolling and stationary cytoadhesion of red blood cells parasitized by *Plasmodium falciparum* separate roles for ICAM-1, CD36 and thrombospondin. *British Journal of Haematology* **87:** 162-170

Cooke BM, Glenister FK, Mohandas N, Coppel RL (2002) Assignment of functional roles to parasite proteins in malaria-infected red blood cells by competitive flow-based adhesion assay. *British Journal of Haematology* **117:** 203-211

Cooke BM, Mohandas N, Coppel RL (2001) The malaria-infected red blood cell: structural and functional changes. *Advances in Parasitology* **50:** 1-86

Cooke BM, Mohandas N, Coppel RL (2004) Malaria and the red blood cell membrane. *Seminars in Hematology* **41:** 173-188

Coppel RL, Culvenor JG, Bianco AE, Crewther PE, Stahl HD, Brown GV, Anders RF, Kemp DJ (1986) Variable antigen associated with the surface of erythrocytes infected with mature stages of *Plasmodium falciparum*. *Molecular and Biochemical Parasitology* **20:** 265-277

Coppel RL, S. Lustigman, L. Murray, and R.F. Anders. (1988) MESA is a *Plasmodium falciparum* phosphoprotein associated with the erythrocyte membrane skeleton. *Molecular and Biochemical Parasitology* **31:** 223-231

Cowman AF, Crabb BS (2006) Invasion of red blood cells by malaria parasites. *Cell* **124:** 755-766

Crabb BS, Cooke BM, Reeder JC, Waller RF, Caruana SR, Davern KM, Wickham ME, Brown GV, Coppel RL, Cowman AF (1997) Targeted gene disruption shows that knobs enable malaria-infected red cells to cytoadhere under physiological shear stress. *Cell* **89:** 287-296

Crabb BS, Cowman AF (1996) Characterization of promoters and stable transfection by homologous and nonhomologous recombination in *Plasmodium falciparum*. *Proceedings of the National Academy of Sciences* **93:** 7289-7294

Crabb BS, de Koning-Ward TF, Gilson PR (2010) Protein export in *Plasmodium* parasites: from the endoplasmic reticulum to the vacuolar export machine. *International Journal for Parasitology* **40(5):** 509-513

Cranston HA, Boylan CW, Carroll GL, Sutera SP, Williamson JR, Gluzman IY, Krogstad DJ (1984) *Plasmodium falciparum* maturation abolishes physiologic red cell deformability. *Science* **223:** 400-403

Culvenor JG, Day KP, Anders RF (1991) *Plasmodium falciparum* ring-infected erythrocyte surface antigen is released from merozoite dense granules after erythrocyte invasion. *Infection and Immunity* **59:** 1183-1187

Da Silva E, Foley M, Dluzewski AR, Murray LJ, Anders RF, Tilley L (1994) The *Plasmodium falciparum* protein RESA interacts with the erythrocyte cytoskeleton and modifies erythrocyte thermal stability. *Molecular and Biochemical Parasitology* **66:** 59-69

David PH, Hommel M, Miller LH, Udeinya IJ, Oligino LD (1983) Parasite sequestration in *Plasmodium falciparum* malaria: spleen and antibody modulation of

cytoadherence of infected erythrocytes. *Proceedings of the National Academy of Sciences* **80:** 5075-5079

de Koning-Ward TF, Gilson PR, Boddey JA, Rug M, Smith BJ, Papenfuss AT, Sanders PR, Lundie RJ, Maier AG, Cowman AF, Crabb BS (2009) A newly discovered protein export machine in malaria parasites. *Nature* **459:** 945-949

del Portillo HA, Ferrer M, Brugat T, Martin-Jaular L, Langhorne J, Lacerda MVG (2012) The role of the spleen in malaria. *Cellular Microbiology* **14:** 343-355

Deplaine G, Safeukui I, Jeddi F, Lacoste F, Brousse V, Perrot S, Biligui S, Guillotte M, Guitton C, Dokmak S, Aussilhou B, Sauvanet A, Cazals Hatem D, Paye F, Thellier M, Mazier D, Milon G, Mohandas N, Mercereau-Puijalon O, David PH, Buffet PA (2011) The sensing of poorly deformable red blood cells by the human spleen can be mimicked *in vitro*. *Blood* **117:** 88-95

Diez-Silva M, Park Y, Huang S, Bow H, Mercereau-Puijalon O, Deplaine G, Lavazec C, Perrot S, Bonnefoy S, Feld MS, Han J, Dao M, Suresh S (2012) Pf155/RESA protein influences the dynamic microcirculatory behavior of ring-stage *Plasmodium falciparum* infected red blood cells. *Scientific Reports* **2**

Dixon MWA, Hawthorne PL, Spielmann T, Anderson KL, Trenholme KR, Gardiner DL (2008a) Targeting of the ring exported protein 1 to the Maurer's clefts is mediated by a two-phase process. *Traffic* **9:** 1316-1326

Dixon MWA, Thompson J, Gardiner DL, Trenholme KR (2008b) Sex in *Plasmodium*: a sign of commitment. *Trends in Parasitology* **24:** 168-175

Doherty JP, Lindeman R, Trent RJ, Graham MW, Woodcock DM (1993) Escherichia coli host strains SURE(TM) and SRB fail to preserve a palindrome cloned in lambda phage: Improved alternate host strains. *Gene* **124:** 29-35

Duffy MF, Byrne TJ, Elliott SR, Wilson DW, Rogerson SJ, Beeson JG, Noviyanti R, Brown GV (2005) Broad analysis reveals a consistent pattern of var gene transcription in *Plasmodium falciparum* repeatedly selected for a defined adhesion phenotype. *Molecular Microbiology* **56:** 774-788

Duffy MF, Maier AG, Byrne TJ, Marty AJ, Elliott SR, O'Neill MT, Payne PD, Rogerson SJ, Cowman AF, Crabb BS (2006) VAR2CSA is the principal ligand for chondroitin sulfate A in two allogeneic isolates of *Plasmodium falciparum*. *Molecular and Biochemical Parasitology* **148:** 117-124

Dunning CR, McKenzie M, Sugiana C, Lazarou M, Silke J, Connelly A, Fletcher JM, Kirby DM, Thorburn DR, Ryan MT (2007) Human CIA30 is involved in the early assembly of mitochondrial complex I and mutations in its gene cause disease. *The European Molecular Biology Organization Journal* **26:** 3227-3237

Engwerda CR, Beattie L, Amante FH (2005) The importance of the spleen in malaria. *Trends in Parasitology* **21:** 75-80

Fagniez PL, Munoz-Bongrand. N (1999) Vascular control during left splenopancreatectomy in cancer. *Annales de Chirurgie* **52:** 632-634

Fairhurst RM WT (2010) Mandell, Douglas, and Bennett's principles and practice of infectious diseases. In *Plasmodium species (malaria)*, pp 3437-3462.

Favaloro JM, Coppel RL, Corcoran LM, Foote SJ, Brown GV, Anders RF, Kemp DJ (1986) Structure of the RESA gene of *Plasmodium falciparum*. *Nucleic Acids Research* **14:** 8265-8277

Ferri FF (2009) Chapter 332. Protozoal infections. Ferri's color atlas and text of clinical medicine. *Elsevier Health Sciences***:** p1159

Fidock DA, Wellems TE (1997) Transformation with human dihydrofolate reductase renders malaria parasites insensitive to WR99210 but does not affect the intrinsic activity of proguanil. *Proceedings of the National Academy of Sciences* **94:** 10931-10936

Foley M, Murray LJ, Anders RF (1990) The ring-infected erythrocyte surface antigen protein of *Plasmodium falciparum* is phosphorylated upon association with the host cell membrane. *Molecular and Biochemical Parasitology* **38:** 69-75

Foley MM, Tilley LL, Sawyer WHW, Anders RFR (1991) The ring-infected erythrocyte surface antigen of *Plasmodium falciparum* associates with spectrin in the erythrocyte membrane. *Molecular and Biochemical Parasitology* **46:** 137-147

Fujiki Y, Hubbard AL, Fowler S, Lazarow PB (1982) Isolation of intracellular membranes by means of sodium carbonate treatment: application to endoplasmic reticulum. *The Journal of Cell Biology* **93:** 97-102

Gachot B, Wolff M, Nissack G, Veber B, Vachon F (1995) Acute lung injury complicating imported *Plasmodium falciparum* malaria. *Chest* **108:** 746-749

Garcia CRS, de Azevedo MF, Wunderlich G, Budu A, Young JA, Bannister L (2008) *Plasmodium* in the postgenomic era: New insights into the molecular cell biology of malaria parasites. *International Review of Cell and Molecular Biology* **266:** 85-156

Glazier JD, Sibley CP (2006) In vitro methods for studying human placental amino acid transport: placental plasma membrane vesicles. *Methods Molecular Medicine* **122:** 241-252

Glenister FK, Coppel RL, Cowman AF, Mohandas N, Cooke BM (2002) Contribution of parasite proteins to altered mechanical properties of malaria-infected red blood cells. *Blood* **99:** 1060-1063

Goldberg DE, Janse CJ, Cowman AF, Waters AP (2011) Has the time come for us to complement our malaria parasites? *Trends in Parasitology* **27:** 1-2

Goodyer ID, Johnson J, Eisenthal R, Hayes DJ (1994) Purification of mature-stage *Plasmodium falciparum* by gelatine flotation. *Annals of Tropical Medicine and Parasitology* **88:** 209-211

Gravenor MB VHM, Kwiatkowski D (1998) Estimating sequestered parasite population dynamics in cerebral malaria. *Proceedings of the National Academy of Sciences* **95:** 7620-7624

Groom AC, Schmidt EE, MacDonald IC (1991) Microcirculatory pathways and blood flow in spleen: new insights from washout kinetics, corrosion casts, and quantitative intravital videomicroscopy. *Scanning Microscopy* **5:** 159-174

Günther K, Tümmler M, Arnold HH, Ridley R, Goman M, Scaife JG, Lingelbach K (1991) An exported protein of *Plasmodium falciparum* is synthesized as an integral membrane protein. *Molecular and Biochemical Parasitology* **46:** 149-157

Haase S, de Koning-Ward TF (2010) New insights into protein export in malaria parasites. *Cellular Microbiology* **12:** 580-587

Hanssen E, Sougrat R, Frankland S, Deed S, Klonis N, Lippincott-Schwartz J, Tilley L (2008) Electron tomography of the Maurer's cleft organelles of *Plasmodium falciparum*-infected erythrocytes reveals novel structural features. *Molecular Microbiology* **67:** 703-718

Hiller NL, Bhattacharjee S, van Ooij C, Liolios K, Harrison T, Lopez-Estrano C, Haldar K (2004) A host-targeting signal in virulence proteins reveals a secretome in malarial infection. *Science* **306:** 1934-1937

Horrocks P, Pinches RA, Chakravorty SJ, Papakrivos J, Christodoulou Ze, Kyes SA, Urban BC, Ferguson DJP, Newbold CI (2005) PfEMP1 expression is reduced on the surface of knobless *Plasmodium falciparum* infected erythrocytes. *Journal of Cell Science* **118:** 2507-2518

Hortsch M, Meyer DI (1986) Transfer of secretory proteins through the membrane of the endoplasmic-reticulum. *International Review of Cytology-a Survey of Cell Biology* **102:** 215-242

Idro R JN, Newton CR. (2005) Pathogenesis, clinical features, and neurological outcome of cerebral malaria. *Lancet Neurology* **4:** 827-840

Jakeman GN SA, Hogarth WL, Collins WE (1999) Anaemia of acute malaria infections in non-immune patients primarily results from destruction of uninfected erythrocytes. *Parasitology* **119:** 127-133

Jones OT, Earnest JP, McNamee MG (1987) Solubilization and reconstitution of membrane proteins, in Biological membranes: a practical approach. Findlay J, Evans W (eds), 139-177. Oxford, UK: IRL Press

Joshi B, Biswas S, Sharma YD (1992) Effect of heat-shock on *Plasmodium falciparum* viability, growth and expression of the heat-shock protein 'PFHSP70-I' gene. *Federation of European Biochemical Societies Letters* **312:** 91-94

Julianna Schantz-Dunn MaNMN, MD, MPH (2009) Malaria and pregnancy: A global health perspective. *Reviews in Obstetrics and Gynecology* **2(3):** 186-192

Kabilan L, Troye-Blomberg M, Perlmann H, Andersson G, Hogh B, Petersen E, Bjorkman A, Perlmann P (1988) T-cell epitopes in Pf155/RESA, a major candidate for a *Plasmodium falciparum* malaria vaccine. *Proceedings of the National Academy of Sciences* **85:** 5659-5663

Kanodia KV, Shah PR, Vanikar AV, Kasat P, Gumber M, Trivedi HL (2010) Malaria induced acute renal failure: a single center experience. *Saudi Journal of Kidney Diseases and Transplantation, Saudi Arabia* **21:** 1088-1091

Kappes B, Suetterlin BW, Hofer-Warbinek R, Humar R, Franklin RM (1993) Two major phosphoproteins of *Plasmodium falciparum* are heat shock proteins. *Molecular and Biochemical Parasitology* **59:** 83-94

Keller BO, Suj J, Young AB, Whittal RM (2008) Interferences and contaminants encountered in modern mass spectrometry. *Analytica Chimica Acta* **627:** 71-81

Kilejian A (1979) Characterization of a protein correlated with the production of knob-like protrusions on membranes of erythrocytes Infected with *Plasmodium-falciparum*. *Proceedings of the National Academy of Sciences* **76:** 4650-4653

Kilejian A, Rashid MA, Aikawa M, Aji T, Yang YF (1991) Selective association of a fragment of the knob protein with spectrin, actin and the red cell membrane. *Molecular and Biochemical Parasitology* **44:** 175-182

Kjellen L, Lindahl U (1991) Proteoglycans - Structures and Interactions. *Annual Review of Biochemistry* **60:** 443-475

Knell AJ. (1991) MALARIA: A publication of the tropical programme of The Wellcome Trust. *Oxford University Press*, New York.

Kwiatkowski D (1989) Febrile temperatures can synchronize the growth of *Plasmodium falciparum* in vitro. *Journal of Experimental Medicine* **169:** 357-361

Lambros C, Vanderberg JP (1979) Synchronization of *Plasmodium falciparum* erythrocytic stages in culture. *The Journal of Parasitology* **65:** 418-420

Langreth SG, Peterson E (1985) Pathogenicity, stability, and immunogenicity of a knobless clone of *Plasmodium falciparum* in Colombian owl monkeys. *Infection and Immunity* **47:** 760-766

Lanzer M, Wickert H, Krohne G, Vincensini L, Breton CB (2005) Maurer's clefts: A novel multi-functional organelle in the cytoplasm of *Plasmodium falciparum*-infected erythrocytes. *International Journal for Parasitology* **36:** 23-36

Le Roch KG, Johnson JR, Florens L, Zhou Y, Santrosyan A, Grainger M, Yan SF, Williamson KC, Holder AA, Carucci DJ, Yates JR, Winzeler EA (2004) Global analysis of transcript and protein levels across the *Plasmodium falciparum* life cycle. *Genome Research* **14:** 2308-2318

Lensen JFM, Rops ALWMM, Wijnhoven TJM, Hafmans T, Feitz WFJ, Oosterwijk E, Banas B, Bindels RJM, van den Heuvel LPWJ, van der Vlag J, Berden JHM, van Kuppevelt TH (2005) Localization and functional characterization of glycosaminoglycan domains in the normal human kidney as revealed by phage display-derived single chain antibodies. *Journal of the American Society of Nephrology* **16:** 1279-1288

Li X, Chen H, Oo TH, Daly TM, Bergman LW, Liu S-C, Chishti AH, Oh SS (2004) A co-ligand complex anchors *Plasmodium falciparum* merozoites to the erythrocyte invasion receptor band 3. *The Journal of Biological Chemistry* **279:** 5765-5771

Link AJ, LaBaer J (2011) Trichloroacetic acid (TCA) precipitation of proteins. In *Cold Spring Harbor protocols*, pp 993-994.

Lopaticki S, Maier AG, Thompson J, Wilson DW, Tham W-H, Triglia T, Gout A, Speed TP, Beeson JG, Healer J, Cowman AF (2011) Reticulocyte and erythrocyte binding-like proteins function cooperatively in invasion of human erythrocytes by malaria parasites. *Infection and Immunity* **79:** 1107-1117

Luche S, Santoni Vr, Rabilloud T (2003) Evaluation of nonionic and zwitterionic detergents as membrane protein solubilizers in two-dimensional electrophoresis. *Proteomics* **3:** 249-253

Luse SA, Miller LH (1971) Plasmodium falciparum malaria: Ultrastructure of parasitized erythrocytes in cardiac vessels. *American Journal of Tropical Medicine and Hygiene* **20:** 655-660

Lustigman S, Anders RF, Brown GV (1990) The mature-parasite-infected erythrocyte surface antigen (MESA) of *Plasmodium falciparum* associates with the erythrocyte membrane skeletal protein, band 4.1. *Molecular and Biochemical Parasitology* **38:** 261-270

Macpherson GG, Warrell MJ, White NJ, Looareesuwan S, Warrell DA (1985) Human cerebral malaria. A quantitative ultrastructural analysis of parasitized erythrocyte sequestration. *American Journal of Pathology* **119:** 385-401

Magowan C, Wollish W, Anderson L, Leech J (1988) Cytoadherence by *Plasmodium falciparum*-infected erythrocytes is correlated with the expression of a family of variable proteins on infected erythrocytes. *Journal of Experimental Medicine* **168:** 1307-1320

Maier AG, Braks JAM, Waters AP, Cowman AF (2006) Negative selection using yeast cytosine deaminase/uracil phosphoribosyl transferase in *Plasmodium falciparum*

for targeted gene deletion by double crossover recombination. *Molecular and Biochemical Parasitology* **150:** 118-121

Maier AG, Cooke BM, Cowman AF, Tilley L (2009) Malaria parasite proteins that remodel the host erythrocyte. *Nature Review Microbiology* **7:** 341-354

Maier AG, Rug M (2013) *In vitro* culturing *Plasmodium falciparum* erythrocytic stages. In *Malaria : Methods and Protocols*, Ménard R (ed), Vol. 923, 2nd edn, pp 3-15. Humana Press

Maier AG, Rug M, O'Neill MT, Brown M, Chakravorty S, Szestak T, Chesson J, Wu Y, Hughes K, Coppel RL, Newbold C, Beeson JG, Craig A, Crabb BS, Cowman AF (2008) Exported proteins required for virulence and rigidity of *Plasmodium falciparum*-Infected human erythrocytes. *Cell* **134:** 48-61

Marti M, Baum J, Rug M, Tilley L, Cowman AF (2005) Signal-mediated export of proteins from the malaria parasite to the host erythrocyte. *The Journal of Cell Biology* **171:** 587-592

Marti M, Good RT, Rug M, Knuepfer E, Cowman AF (2004) Targeting malaria virulence and remodeling proteins to the host erythrocyte. *Science* **306:** 1930-1933

Mattow J, Siejak F, Hagens K, Schmidt F, Koehler C, Treumann A, Schaible UE, Kaufmann SHE (2007) An improved strategy for selective and efficient enrichment of integral plasma membrane proteins of mycobacteria. *Proteomics* **7:** 1687-1701

Mayer C, Slater L, Erat MC, Konrat R, Vakonakis I (2012) Structural analysis of the *Plasmodium falciparum* erythrocyte membrane protein 1 (PfEMP1) intracellular domain reveals a conserved interaction epitope. *Journal of Biological Chemistry* **287:** 7182-7189

Miller LH, Baruch DI, Marsh K, Doumbo OK (2002) The pathogenic basis of malaria. *Nature* **415:** 673-679

Miller LH, Good MF, Milon G (1994) Malaria pathogenesis. *Science* **264:** 1878-1883

Mills JP, Diez-Silva M, Quinn DJ, Dao M, Lang MJ, Tan KSW, Lim CT, Milon G, David PH, Mercereau-Puijalon O (2007) Effect of plasmodial RESA protein on deformability of human red blood cells harboring *Plasmodium falciparum*. *Proceedings of the National Academy of Sciences* **104:** 9213-9217

Mohandas N, Gallagher PG (2008) Red cell membrane: past, present, and future. *Blood* **112:** 3939-3948

Murphy SC, Hiller NL, Harrison T, Lomasney JW, Mohandas N, Haldar K (2006) Lipid rafts and malaria parasite infection of erythrocytes (Review). *Molecular Membrane Biology* **23:** 81-88

Murray CJL, Rosenfeld LC, Lim SS, Andrews KG, Foreman KJ, Haring D, Fullman N, Naghavi M, Lozano R, Lopez AD (2012) Global malaria mortality between 1980 and 2010: a systematic analysis. *Lancet* **379:** 413-431

Newbold C (1999) Cytoadherence, pathogenesis and the infected red cell surface in *Plasmodium falciparum*. *International Journal for Parasitology* **29:** 927-937

Nilsson S, Angeletti D, Wahlgren M, Chen Q, Moll K (2012) *Plasmodium falciparum* antigen 332 is a resident peripheral membrane protein of Maurer's clefts. *PLoS ONE* **7:** e46980

Oakley MS, Gerald N, McCutchan TF, Aravind L, Kumar S (2011) Clinical and molecular aspects of malaria fever. *Trends in Parasitology* **27:** 442-449

Oakley MSM, Kumar S, Anantharaman V, Zheng H, Mahajan B, Haynes JD, Moch JK, Fairhurst R, McCutchan TF, Aravind L (2007) Molecular factors and biochemical pathways induced by febrile temperature in intraerythrocytic *Plasmodium falciparum* parasites. *Infection and Immunity* **75:** 2012-2025

Oakley. MSM, Kumar. S, Anantharaman. V, Zheng. H, Haynes. BMJD, Moch. JK, Fairhurst. R, McCutchan. TF, Aravind. L (2007) Molecular factors and biochemical pathways induced by febrile temperature in intraerythrocytic *Plasmodium falciparum* parasites. *Infection and Immunity* **75:** 2012-2025

Oh SS, Voigt S, Fisher D, Yi SJ, LeRoy PJ, Derick LH, Liu SC, Chishti AH (2000) *Plasmodium falciparum* erythrocyte membrane protein 1 is anchored to the actin-spectrin junction and knob-associated histidine-rich protein in the erythrocyte skeleton. *Molecular and Biochemical Parasitology* **108:** 237-247

Parker PD, Tilley L, Klonis N (2004) *Plasmodium falciparum* induces reorganization of host membrane proteins during intraerythrocytic growth. *Blood* **103:** 2404-2406

Parpart AK, Lorenz PB, Parpart ER, Gregg JR, Chase AM (1947) The osmotic resistance (fragility) of human red cells. *Journal of Clinical Investigation* **26:** 636-640

Pasloske BL, Baruch DI, Howard RJ (1993) Cloning and characterization of a *Plasmodium falciparum* gene encoding a novel high-molecular weight host membrane-associated protein, PfEMP3. *Molecular and Biochemical Parasitology* **59:** 59-72

Pasternack. GR, Racusen RH (1989) Erythrocyte protein 4.1 binds and regulates myosin. *Proceedings of the National Academy of Sciences* **86:** 9712-9716

Pei X, Guo X, Coppel R, Bhattacharjee S, Haldar K, Gratzer W, Mohandas N, An X (2007) The ring-infected erythrocyte surface antigen (RESA) of *Plasmodium falciparum* stabilizes spectrin tetramers and suppresses further invasion. *Blood* **110:** 1036-1042

Perlmann HK, Berzins K, Wahlin B, Udomsangpetch R, Ruangjirachuporn W, Wahlgren M, Perlmann PH (1987) Absence of antigenic diversity in Pf155, a major

parasite antigen in membranes of erythrocytes infected with *Plasmodium falciparum*. *Journal of Clinical Microbiology* **25:** 2347-2354

Petersen C, Nelson R, Magowan C, Wollish W (1989) The mature erythrocyte surface antigen of *Plasmodium falciparum* is not required for knobs or cytoadherence. *Molecular and Biochemical Parasitology* **36:** 61-65

Pologe LG, Pavlovec A, Shio H, Ravetch JV (1987) Primary structure and subcellular localization of the knob-associated histidine-rich protein of *Plasmodium falciparum*. *Proceedings of the National Academy of Sciences* **84:** 7139-7143

Pongponratn E, Riganti M, Punpoowong B, Aikawa M (1991) Microvascular sequestration of parasitised erythrocytes in human *falciparum* malaria: a pathological study. *The America Journal of Tropical Medicine and Hygiene* **44:** 168-175

Pouvelle B, Buffet PA, Lepolard C, Scherf A, Gysin J (2000) Cytoadhesion of *Plasmodium falciparum* ring-stage-infected erythrocytes. *Nature Medicine* **6:** 1264-1268

Proellocks NI, Herrmann S, Buckingham DW, Hanssen E, Hodges EK, Elsworth B, Morahan BJ, Coppel RL, Cooke BM (2014) A lysine-rich membrane-associated PHISTb protein involved in alteration of the cytoadhesive properties of *Plasmodium falciparum*-infected red blood cells. *The Federation of American Societies for Experimental Biology* **28:** 000-000

Prommano O, Chaisri U, Turner GD (2005) A quantitative ultrastructural study of the liver and the spleen in fatal *falciparum* malaria. *The Southeast Asian Journal of Tropical Medicine and Public Health* **36:** 1359-1370

Prudêncio M, Rodriguez A, Mota MM (2006) The silent path to thousands of merozoites: the *Plasmodium* liver stage. *Nature Reviews Microbiology* **4:** 849-856

Punjabi A, Traktman P (2005) Cell biological and functional characterization of the vaccinia virus F10 kinase: implications for the mechanism of virion morphogenesis. *Journal of Virology* **79:** 2171-2190

Rogerson SJ, Chaiyaroj SC, Ng K, Reeder JC, Brown GV (1995) Chondroitin sulfate a is a cell surface receptor for *Plasmodium falciparum*-infected erythrocytes. *Journal of Experimental Medicine* **182:** 15-20

Rug M (2006) The role of KAHRP domains in knob formation and cytoadherence of *P falciparum*-infected human erythrocytes. *Blood* **108:** 370-378

Rug M, Maier AG (2013) Transfection of *Plasmodium falciparum*. In *Malaria : Methods and Protocols*, Ménard R (ed), Vol. 923, 2nd edn, pp 75-98. Humana Press

Rug M, Wickham ME, Foley M, Cowman AF, Tilley L (2004) Correct promoter control is needed for trafficking of the ring-infected erythrocyte surface antigen to the host cytosol in transfected malaria parasites. *Infection and Immunity* **72:** 6095-6105

Russo I, Babbitt S, Muralidharan V, Butler T, Oksman A, Goldberg DE (2010) Plasmepsin V licenses *Plasmodium* proteins for export into the host erythrocyte. *Nature* **463:** 632-636

Safeukui I, Correas JM, Brousse V, Hirt D, Deplaine G, Mule S, Lesurtel M, Goasguen N, Sauvanet A, Couvelard A, Kerneis S, Khun H, Vigan-Womas I, Ottone C, Molina TJ, Treluyer JM, Mercereau-Puijalon O, Milon G, David PH, Buffet PA (2008) Retention of *Plasmodium falciparum* ring-infected erythrocytes in the slow, open microcirculation of the human spleen. *Blood* **112:** 2520-2528

Salanti A, Dahlb√§ck M, Turner L, Nielsen MA, Barfod L, Magistrado P, Jensen ATR, Lavstsen T, Ofori MF, Marsh K, Hviid L, Theander TG (2004) Evidence for the involvement of VAR2CSA in pregnancy-associated malaria. *Journal of Experimental Medicine* **200:** 1197-1203

Salzer U, Prohaska R (2001) Stomatin, flotillin-1, and flotillin-2 are major integral proteins of erythrocyte lipid rafts. *Blood* **97:** 1141-1143

Sambrook J, Fritsch EF, Maniatis T (1989) *Molecular Cloning: A Laboratory Manual*, second edn. Cold Spring Harbor, NY: Cold Spring Harbor Laboratory Press.

Sargeant T, Marti M, Caler E, Carlton J, Simpson K, Speed T, Cowman A (2006) Lineage-specific expansion of proteins exported to erythrocytes in malaria parasites. *Genome Biology* **7:** R12

Schägger H, von Jagow G (1991) Blue native electrophoresis for isolation of membrane protein complexes in enzymatically active form. *Analytical Biochemistry* **199:** 223-231

Scherf A, Lopez-Rubio JJ, Riviere L (2008) Antigenic variation in *Plasmodium falciparum*. *Annual Review of Microbiology* **62:** 445-470

Schmidt EE, MacDonald IC, Groom AC (1993) Comparative aspects of splenic microcirculatory pathways in mammals: the region bordering the white pulp. *Scanning Microscopy* **7:** 613-628

Shonhai A, Boshoff A, Blatch GL (2007) The structural and functional diversity of Hsp70 proteins from *Plasmodium falciparum*. *Protein Science* **16:** 1803-1818

Siddiqui WA, Kan SC, Kramer K, Richmond-Crum SM (1979) In vitro production and partial purification of *Plasmodium falciparum* antigen. *Bulletin of the World Health Organization* **57:** 75-82

Silamut K, Phu NH, Whitty C, Turner GDH, Louwrier K, Mai NTH, Simpson JA, Hien TT, White NJ (1999) A quantitative analysis of the microvascular sequestration of malaria parasites in the human brain. *American Journal of Pathology* **155:** 395-410

Silva MD, Cooke BM, Guillotte M, Buckingham DW, Sauzet J-P, Scanf CL, Contamin H, David P, Mercereau-Puijalon O, Bonnefoy S (2005) A role for the

Plasmodium falciparum RESA protein in resistance against heat shock demonstrated using gene disruption. *Molecular Microbiology* **56:** 990-1003

Simonetti AB (1996) The biology of malarial parasite in the mosquito: A review. *Memorias do Instituto Oswaldo Cruz* **91:** 519-541

Sonnhammer EL, von Heijne G, Krogh A (1998) A hidden Markov model for predicting transmembrane helices in protein sequences. *Proceedings / International Conference on Intelligent Systems for Molecular Biology* **6:** 175-182

Spielmann T, Hawthorne PL, Dixon MWA, Hannemann M, Klotz K, Kemp DJ, Klonis N, Tilley L, Trenholme KR, Gardiner DL (2006) A cluster of ring stage-specific genes linked to a locus implicated in cytoadherence in *Plasmodium falciparum* codes for PEXEL-negative and PEXEL-positive proteins exported into the host cell. *Molecular Biology of the Cell* **17:** 3613-3624

Takakuwa Y (2000) Protein 4.1, a multifunctional protein of the erythrocyte membrane skeleton: structure and functions in erythrocytes and nonerythroid cells. *International Journal of Hematology* **72:** 298-309

Trager W, Jensen JB (1976) Human malaria parasites in continuous culture. *Science* **193:** 673-675

Trampuz A, Jereb M, Muzlovic I, Prabhu RM (2003) Clinical review: Severe malaria. *Critical Care* **7:** 315-323

Tran PN (2014) A female-gametocyte-specific transporter plays a role in lipid metabolism in the malaria parasites. Doctor of Philosophy Thesis, Biochemistry, La Trobe University, Melbourne

Udeinya IJ, Schmidt JA, Aikawa M, Miller LH, Green I (1981) *Falciparum* malaria-infected erythrocytes specifically bind to cultured human-endothelial cells. *Science (New York, NY)* **213:** 555-557

Udomsangpetch R, Aikawa M, Berzins K, Wahlgren M, Perlmann P (1989) Cytoadherence of knobless *Plasmodium falciparum*-infected erythrocytes and its inhibition by a human monoclonal antibody. *Nature* **338:** 763-765

Veale MF, Healey G, Sparrow RL (2011) Effect of additive solutions on red blood cell (RBC) membrane properties of stored RBCs prepared from whole blood held for 24 hours at room temperature. *Transfusion* **51 Suppl 1:** 25S-33S

Vincensini L, Richert S, Blisnick T, Van Dorsselaer A, Leize-Wagner E, Rabilloud T, Braun Breton C (2005) Proteomic analysis identifies novel proteins of the Maurer's clefts, a secretory compartment delivering *Plasmodium falciparum* proteins to the surface of its host cell. *Molecular & Cellular Proteomics* **4:** 582-593

Waller KL (2003) Mature parasite-infected erythrocyte surface antigen (MESA) of *Plasmodium falciparum* binds to the 30-kDa domain of protein 4.1 in malaria-infected red blood cells. *Blood* **102:** 1911-1914

Waller KL, Cooke BM, Nunomura W, Mohandas N, Coppel RL (1999) Mapping the Binding Domains Involved in the Interaction between the *Plasmodium falciparum* knob-associated histidine-rich protein (KAHRP) and the cytoadherence ligand *P.falciparum* erythrocyte membrane protein 1 (PfEMP1). *The Journal of Biological Chemistry* **274:** 23808-23813

Waller KL, Stubberfield LM, Dubljevic V, Nunomura W, An X, Mason AJ, Mohandas N, Cooke BM, Coppel RL (2007) Interactions of *Plasmodium falciparum* erythrocyte membrane protein 3 with the red blood cell membrane skeleton. *Biochimica Et Biophysica Acta-Biomembranes* **1768:** 2145-2156

Walter P, Lingappa V (1986) Mechanisms of protein translocation across the endoplasmic reticulum membrane. *Annual Review of Cell Biology* **2:** 499-516

Waterkeyn JG, Wickham ME, Davern KM, Cooke BM, Coppel RL, Reeder JC, Culvenor JG, Waller RF, Cowman AF (2000) Targeted mutagenesis of *Plasmodium falciparum* erythrocyte membrane protein 3 (PfEMP3) disrupts cytoadherence of malaria-infected red blood cells. *The European Molecular Biology Organization Journal* **19:** 2813-2823

Weatherall DJ (2002) Malaria and the red cell. *Hematology* **2002:** 35-57

White NJ (2008) *Plasmodium knowlesi*: the fifth human malaria parasite. *Clinical Infectious Diseases* **46:** 172-173

White NJ, Chapman D, Watt G (1992) The effects of multiplication and synchronicity on the vascular distribution of parasites in *falciparum* malaria. *Transactions of the Royal Society of Tropical Medicine and Hygiene* **86:** 590-597

WHO (2013) World malaria report. pp ix-xiii

Wickert H, Krohne G (2007) The complex morphology of Maurer's clefts: from discovery to three-dimensional reconstructions. *Trends in Parasitology* **23:** 502-509

Wu Y, Craig A (2006) Comparative proteomic analysis of metabolically labelled proteins from *Plasmodium falciparum* isolates with different adhesion properties. *Malaria Journal* **5:** 67

Yosaatmadja F, Andrews KT, Duffy MF, Brown GV, Beeson JG, Rogerson SJ (2008) Characterization of VAR2CSA-deficient *Plasmodium falciparum*-infected erythrocytes selected for adhesion to the BeWo placental cell line. *Malaria Journal* **7:51**

Zehnder L, Schulzki T, Goede JS, Hayes J, Reinhart WH (2008) Erythrocyte storage in hypertonic (SAGM) or isotonic (PAGGSM) conservation medium: influence on cell properties. *Vox Sanguinis* **95:** 280-287